Coral Reef Ecosystem Monitoring Report For The Pacific Remote Islands Marine National Monument

2000–2017

Chapter 4
Jarvis Island

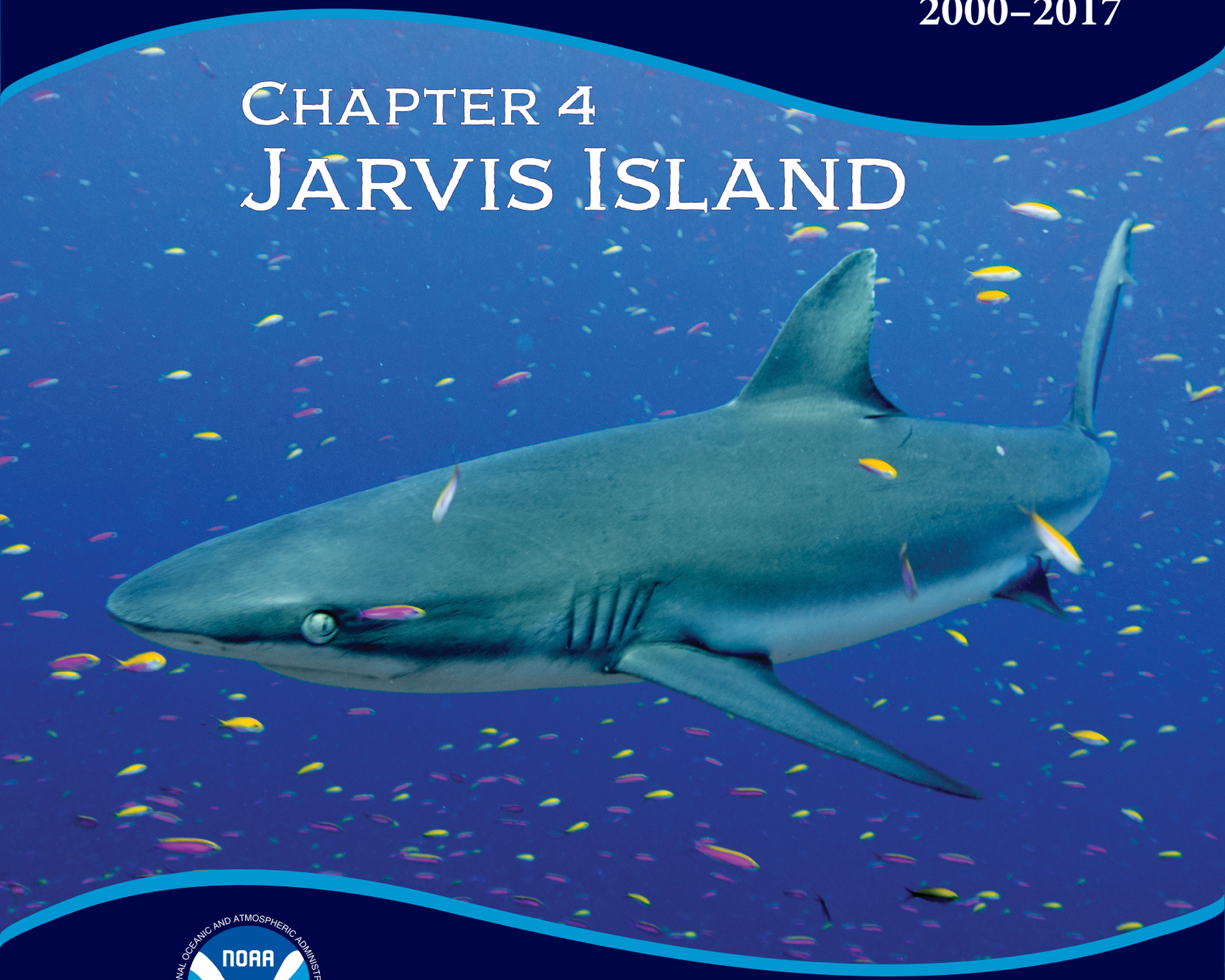

NOAA FISHERIES

Ecosystem Sciences Division

Pacific Islands Fisheries Science Center

Coral Reef Ecosystem Monitoring Report for the Pacific Remote Islands Marine National Monument 2000–2017

Chapter 4: Jarvis Island

Authors

Brainard, Russell E.[1]; Acoba, Tomoko[2]; Asher, Megan A.M.[2]; Asher, Jacob M.[2]; Ayotte, Paula M.[2]; Barkley, Hannah C.[2]; DesRochers, Annette[2]; Dove, Dayton[2]; Halperin, Ariel A.[2]; Huntington, Brittany[2]; Kindinger, Tye L.[2]; Lichowski, Frances[2]; Lino, Kevin C.[2]; McCoy, Kaylyn S.[2]; Oliver, Thomas[1]; Pomeroy, Noah[2]; Suka, Rhonda[2]; Timmers, Molly[2]; Vargas-Ángel, Bernardo[2]; Venegas, Roberto M.[2]; Wegley Kelly, Linda[3]; Williams, Ivor D.[1]; Winston, Morgan[2]; Young, Charles W.[2]; Zamzow, Jill[2]

[1]National Oceanic and Atmospheric Administration, Pacific Islands Fisheries Science Center
[2]University of Hawaii, Joint Institute for Marine and Atmospheric Research
[3]San Diego State University

PIFSC Special Publication SP-19-006d
2019

United States Department of Commerce, National Oceanic and Atmospheric Administration, National Marine Fisheries Service, Pacific Islands Fisheries Science Center

NOAA Inouye Regional Center
Attn: NMFS/PIFSC/Ecosystem Sciences Division
1845 Wasp Boulevard, Building 176
Honolulu, Hawaii 96818 U.S.A.

This report is a deliverable for the NOAA Coral Reef Conservation Program's National Coral Reef Monitoring Program (NCRMP) Data, Reports, and Information Products for Management, Project ID 31186. It also contributed to the NOAA Pacific Islands Fisheries Science Center (PIFSC) Milestone P19-ESD-05 and PIFSC Accomplishment P19-ESD-36. The data used to generate this report are described in the NOAA Fisheries Enterprise Data Management tool, InPort, at the following link: https://inport.nmfs.noaa.gov/inport/item/53206. In addition, all monitoring data are archived with the NOAA National Centers for Environmental Information and most benthic habitat mapping data and products are available on the PIFSC Ecosystem Sciences Division's Pacific Islands Benthic Habitat Mapping Center website, unless otherwise specified in the InPort record.

Citations

This report as a whole may be referenced in the following manner:

Brainard RE, Acoba T, Asher MAM, Asher JM, Ayotte PM, Barkley HC, DesRochers A, Dove D, Halperin AA, Huntington B, Kindinger TL, Lichowski F, Lino KC, McCoy KS, Oliver T, Pomeroy N, Suka R, Timmers M, Vargas-Ángel B, Venegas RM, Wegley Kelly L, Williams ID, Winston M, Young CW, Zamzow J (2019) Coral Reef Ecosystem Monitoring Report for the Pacific Remote Islands Marine National Monument 2000–2017. Pacific Islands Fisheries Science Center, PIFSC Special Publication, SP-19-006. 820 p.

This chapter may be referenced in the following manner:

Brainard RE, Acoba T, Asher MAM, Asher JM, Ayotte PM, Barkley HC, DesRochers A, Dove D, Halperin AA, Huntington B, Kindinger TL, Lichowski F, Lino KC, McCoy KS, Oliver T, Pomeroy N, Suka R, Timmers M, Vargas-Ángel B, Venegas RM, Wegley Kelly L, Williams ID, Winston M, Young CW, Zamzow J (2019) Chapter 4: Jarvis Island. In: Coral Reef Ecosystem Monitoring Report for the Pacific Remote Islands Marine National Monument 2000–2017. Pacific Islands Fisheries Science Center, PIFSC Special Publication, SP-19-006d. 94 p. doi:10.25923/t645-dk90

For more information or to download a copy of this publication:

http://go.usa.gov/xpRRx

Front Cover: Grey reef shark (*Carcharhinus amblyrhynchos*) and anthias. Photo: Andrew E. Gray, NOAA Fisheries.

Back Cover: Grey reef shark (*Carcharhinus amblyrhynchos*) among blackfin barracuda (*Sphyraena qenie*) at Jarvis Island. Photo: James Morioka, NOAA Fisheries.

Table of Contents

Executive Summary

The work presented within the *Coral Reef Ecosystem Monitoring Report for the Pacific Remote Islands Marine National Monument 2000–2017* is a direct result of nearly 20 years of research in the U.S. Pacific Remote Islands Marine National Monument (PRIMNM) conducted over hundreds of field days aboard National Oceanic and Atmospheric Administration (NOAA) ships by dozens of contributors from NOAA, University of Hawaii–Joint Institute for Marine and Atmospheric Research, and partner scientists. For their efforts, we are eternally grateful and appreciative of their work.

Here, we examine seven islands and atolls within the PRIMNM, using a variety of methods across multiple disciplines in order to gauge how these unique ecosystems have fared through time. In brief, this report describes and highlights the spatial patterns and temporal trends of marine ecosystems associated with Johnston Atoll, Howland Island, Baker Island, Jarvis Island, Palmyra Atoll, Kingman Atoll, and Wake Atoll, along with cross-comparative assessments among the islands, reefs, and atolls of the PRIMNM and other island areas of the U.S. Pacific Islands region in "Chapter 9: Pacific Remote Islands Marine National Monument in the Pacific-wide Context."

Each island, reef, and atoll chapter, along with the Pacific-wide chapter, is constructed as follows: Introduction, Benthic Characterization, Ocean and Climate Variability, Coral Reef Benthic Communities, Cryptofauna Biodiversity (in the Pacific-wide chapter only), Microbiota, Reef Fishes, Marine Debris, and Ecosystem Integration.

Key Findings

- Given the wide geographic extent and large variance in oceanographic conditions experienced across the PRIMNM, it is more informative to consider the PRIMNM as three groupings: the northernmost oligotrophic islands of Johnston and Wake Atolls, the central transition islands of Kingman Reef and Palmyra Atoll, and the equatorial upwelling islands of Howland, Baker, and Jarvis Islands.
- Due to the combined effects of equatorial and locally-intense topographic upwelling of the eastward-flowing subsurface Equatorial Undercurrent, Jarvis Island, and to a lesser extent Howland and Baker Islands, are subject to noticeably cooler mean sea surface temperatures (SSTs) than their nearest neighbors (Palmyra Atoll and Kingman Reef). The upwelling routinely experienced by these islands further results in the highest chlorophyll *a* (chl-*a*) concentrations and associated biological productivity measured across the PRIMNM. In contrast, the lower chl-*a* concentrations observed at Wake and Johnston Atolls are similar to concentrations within the Mariana Archipelago and American Samoa, which are located in the oligotrophic gyres of the North Pacific and South Pacific.
- Higher aragonite saturation values correspond to the greater availability of carbonate ions, and thus favor the growth of corals, crustose coralline algae, and other marine calcifiers. The PRIMNM's northernmost oligotrophic islands (Johnston and Wake Atolls) retained two of the lowest average carbonate accretion rates in the U.S. Pacific Islands, indicating low reef growth over time.

- Jarvis Island experienced a massive decline in coral cover in response to acute thermal stress associated with the 2015–2016 El Niño warming event; Jarvis has shown no substantial recovery in coral cover since. Coral cover at Baker Island and Kingman Reef also declined from 2015 to 2018, reflecting a 13% decline over 3 years at both islands.
- Calcifiers comprised approximately half of the benthic communities at Howland Island, Kingman Reef, and Baker Island. Despite Jarvis's catastrophic decline in coral cover in 2016, the recent proportion of calcifiers at Jarvis Island remains high, likely due to a marked increase in cover of crustose coralline algae (CCA) observed in 2018.
- Across the PRIMNM, the crown-of-thorns sea star (*Acanthaster planci*, COTS) was consistently observed only at Kingman Reef and Johnston Atoll, though densities at these islands fluctuated across survey years. Localized outbreaks that were synchronized in timing across central Pacific reefs appeared to be genetically independent, rather than spread via the planktonic larvae released from a primary outbreak source.
- Mean reef fish biomass varied by a factor of >15 among all U.S. Pacific islands surveyed. The equatorial upwelling and central transition islands of the PRIMNM were among the islands that retained the highest biomass, especially of piscivores and planktivores, although Wake Atoll was an exception to this trend.
- The PRIMNM has also been notable for supporting larger abundances of species listed by the Endangered Species Act (ESA), including the greatest densities of the green sea turtle (*Chelonia mydas*) observed in the U.S. Pacific.

Scientists are increasingly recognizing the magnitude of ongoing and projected effects from global warming and ocean acidification on coral reef ecosystems. As such, this report provides an essential scientific foundation for informed decision making for the long-term conservation and management of the coral reef ecosystems within the PRIMNM. By summarizing trends in ecosystem response across space and time, this report is the first step towards assessing ecosystem resilience and identifying potential underlying drivers that impede or promote such resilience. Understanding these trends can inform the prioritization among candidate areas for management, as well as among the various types of policies and management actions themselves. In conclusion, the individual island, reef, atoll, and Pacific-wide comparison chapters give resource managers and policymakers an unprecedented scale of spatial status and temporal trends to examine each ecosystem throughout the PRIMNM, with the hope of protecting and conserving these unique resources for generations to come.

Acknowledgements

We would like to give credit to all National Oceanic and Atmospheric Administration (NOAA) Pacific Islands Fisheries Science Center (PIFSC) and Research Corporation of the University of Hawaii/Joint Institute for Marine and Atmospheric Research (JIMAR) scientists and staff, and the numerous partners who provided support to the Pacific Reef Assessment and Monitoring Program (Pacific RAMP) during 2000–2017, and contributed to the development of this report. We extend a special thanks to the officers and crews from the NOAA Ships *Townsend Cromwell*, *Oscar Elton Sette*, and *Hi'ialakai* who provided field support for the Pacific RAMP surveys. We further express our sincere appreciation to PIFSC, JIMAR, the NOAA Coral Reef Conservation Program (CRCP), and Pacific Islands Regional Office (PIRO) for funding and providing collaborative resources throughout these efforts.

We specifically acknowledge Malia Chow as PIRO branch chief for the Essential Fish Habitat-Pacific Marine National Monuments, along with PIRO's Heidi Hirsh and Richard Hall for their collaboration, reviews, and inputs throughout this report's genesis, along with their participation in associated workshops. We would like to recognize the United States Fish and Wildlife Service Pacific Islands Refuges and Monuments Office for their partnership throughout Pacific RAMP history and their participation in the workshops associated with the report. In addition, we appreciate their reviews and those of PIRO interns, Jesi Bautista and Savannah Smith of Kupu Hawaii, who collectively provided valuable inputs toward the "History and Human Influences" sections for each island, reef, and atoll chapter. We further extend our thanks to the United States Air Force, 611th CES/CEIE, Joint Base Pearl Harbor, Hawaii for their collaborative efforts at Wake Atoll and inputs toward the report and at workshops.

We would like to recognize PIFSC Editorial Services, in particular, Jill Coyle, Katie Davis, and Hoku Johnson for their inputs throughout the editorial process, Donald Kobayashi, PIFSC, for his extensive time and insights in conducting chapter technical reviews, and PIFSC Director Michael Seki and PIFSC ESD Director Frank Parrish for their support and reviews. In addition, we wish to express our gratitude to the CRCP Coral Reef Information System and JIMAR data managers for their efforts to manage and make Pacific RAMP data publicly accessible and compliant with the Public Access to Research Results requirements.

Lastly, we are appreciative of Tom Hourigan and Dale Brown of NOAA Fisheries, two of the earliest visionaries in the establishment of the first Pacific long-term, integrated ecosystem-based monitoring program.

PIFSC has been fortunate to work with many partners who contributed to Pacific RAMP and associated efforts, and while this list is by no means comprehensive, we sincerely thank each and every one of you. Your contributions helped make this report possible, and as a result, we have collectively provided valuable inputs to the management and conservation of the coral reef ecosystems of the Pacific Remote Islands Marine National Monument.

Coral Reef Ecosystem Monitoring Report for the Pacific Remote Islands Marine National Monument 2000–2017

Chapter 4: Jarvis Island

Jarvis Island National Wildlife Refuge, U.S. Fish and Wildlife Service sign.
Photo: LTJG Laura Rock, NOAA Fisheries.

4.1 Introduction

Report Overview

The *Coral Reef Ecosystem Monitoring Report for the Pacific Remote Islands Marine National Monument 2000–2017* provides an overview of key spatial patterns and temporal trends of the environmental and oceanographic conditions, biological resources, and composition of coral reef ecosystems across the seven islands, atolls, and reefs of the Pacific Remote Islands Marine National Monument (PRIMNM). The data compiled for this report are from Pacific Reef Assessment and Monitoring Program (Pacific RAMP) research surveys conducted over the period from 2000 through 2017 by the National Oceanic and Atmospheric Administration (NOAA) Pacific Islands Fisheries Science Center (PIFSC) Ecosystem Sciences Division (ESD) and external collaborating scientists.

This report represents one of many installments of ESD's ongoing efforts to bring resource managers and interested stakeholders the best available, ecosystem-based data to help them make informed decisions about the sustainable use and conservation of the resources they manage, in this case, coral reef ecosystem in the PRIMNM. The information herein serves three main purposes:

- Provide snapshots of the status and condition of coral reef resources around each of the islands, atolls, and reefs in the PRIMNM over the course of the survey periods.
- Provide a foundation of knowledge regarding ecosystem conditions in the PRIMNM for ongoing monitoring of temporal changes to the ecosystem.
- Serve as a resource for stakeholders and resource managers for understanding marine areas of interest and formulating evolving management questions about how to best manage and conserve marine resources in the face of climate and ocean changes.

The report consists of nine chapters. In addition, attached to "Chapter 9: Pacific Remote Islands Marine National Monument in the Pacific-wide Context" are Appendix A, "Total Generic Richness of Hard Corals in the PRIMNM," and Appendix B, "Reef Fish Encounter Frequency in the PRIMNM." For more background information on the report as a whole, operational background, Pacific RAMP methods, and Public Access to Research Results, refer to "Chapter 1: Overview."

Chapter Overview

Jarvis Island, located only 40 km (25 mi) south of the equator in the central equatorial Pacific Ocean at 0°22′S 160°01′W, is a small (4.5 km^2 or 91.75 mi^2), uninhabited coral island of the central Line Islands, also known as the Teraina Islands. Jarvis is the crest of an ancient coral reef cap and massive underlying extinct volcano. The center of Jarvis is a dried former lagoon where deep guano deposits have accumulated (Figure 1). The marine ecosystem surrounding Jarvis is exceptionally productive due to the combined effects of wind-driven equatorial upwelling and topographic upwelling of the eastward-flowing Equatorial Undercurrent (EUC) as it encounters the western submerged flanks of the island. Both forms of upwelling introduce cool, nutrient-rich waters to the relatively shallow euphotic (sunlit) zone where photosynthesis drives high levels of biological productivity for the coral reef ecosystem.

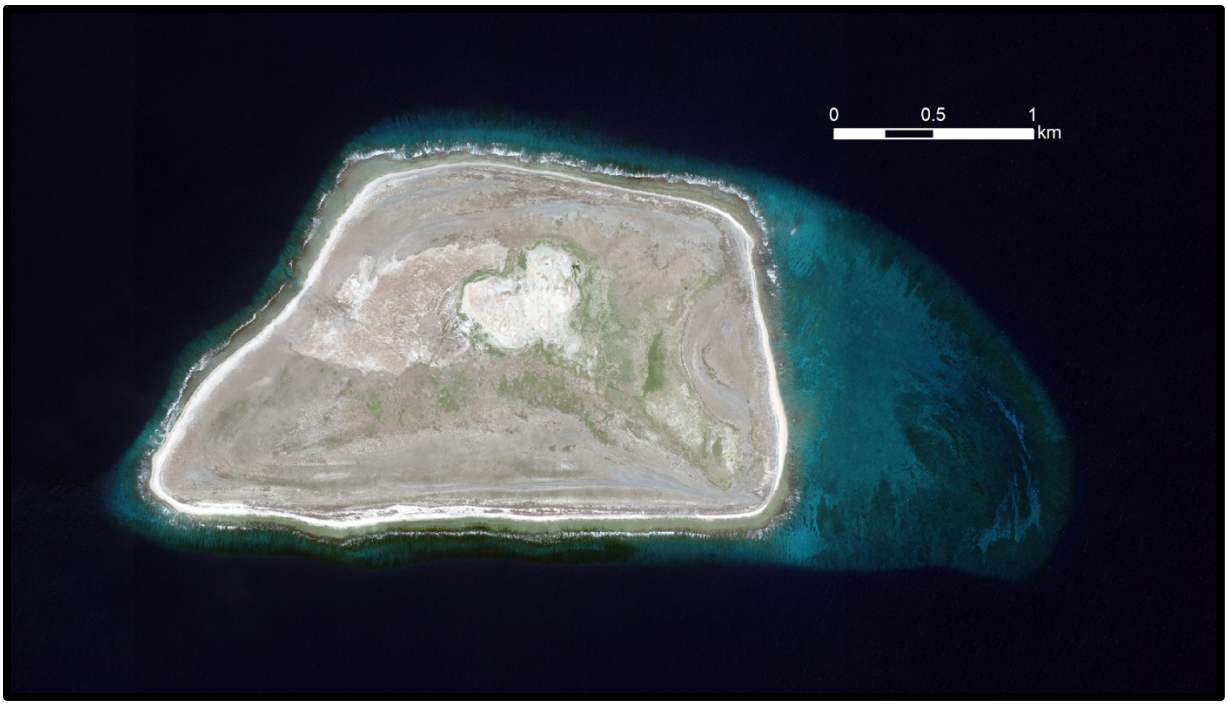

Figure 1. Satellite image of Jarvis Island, December 15, 2016. (© DigitalGlobe Inc. All rights reserved.)

This chapter consists of sections on "Benthic Characterization," "Ocean and Climate Variability," "Coral Reef Benthic Communities," "Microbiota," "Reef Fishes," and "Marine Debris" to assist managers in making informed decisions relating to Jarvis Island and its coral reef ecosystems. Information from these sections is then tied together in the "Ecosystem Integration" section at the end of the chapter to provide a better understanding of the interactions and relationships among the various ecosystem components at Jarvis.

To facilitate discussions about the spatial patterns of ecological and oceanographic observations that appear throughout this chapter, six geographic regions, hereafter referred to as georegions, were defined for Jarvis (Figure 2). Most map-based figures throughout this chapter use the basemap template as shown in Figure 2, which includes georegions, land, and the 30 m and 100 m depth contours (isobaths).

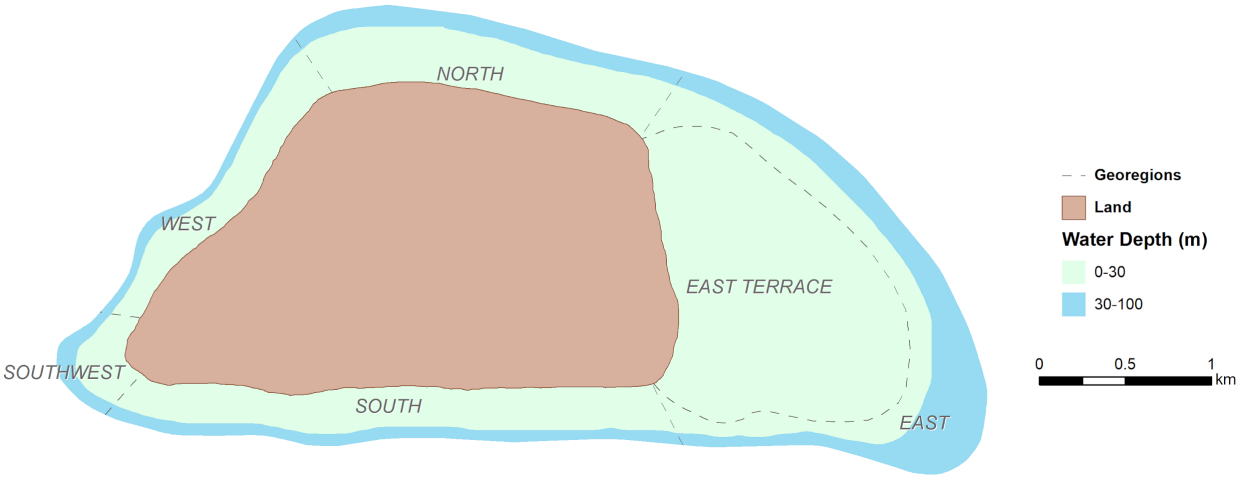

Figure 2. The six geographic regions, or georegions, for Jarvis Island: North, West, Southwest, South, East Terrace, and East.

History and Human Influences

The first known sighting of Jarvis Island by Europeans was on August 21, 1821, by the British ship *Eliza Francis* owned by Edward, Thomas, and William Jarvis, for whom the island was named. American whalers and other seafarers exploring the central Pacific discovered guano resulting in the United States Exploring Expedition to survey Jarvis in 1840 (Stanton 1975). In 1857, Arthur Benson and Charles Judd, aboard the Hawaiian schooner *Liholiho,* took possession of Jarvis and claimed it for the American Guano Company under the Guano Islands Act of 1856. Later that same year, Charles Henry Davis, aboard the U.S.S. *St. Mary's,* surveyed and made formal claim of the island in the name of the United States. The island was formally annexed in 1858, quickly becoming one of the most extensively exploited of the guano islands. Since the island is surrounded by coral reef, the guano workers had to blast away portions of it to create a channel allowing the guano to be transported to vessels anchored offshore. After the American guano diggers withdrew in 1879, several other companies attempted to stake their claim, with Great Britain annexing the island in 1889 and erecting dwellings, mining infrastructure, and a day beacon.

Several shipwrecks were documented in the late 19th and early 20th centuries at Jarvis, including the barquentine *Amaranth* that struck the southwest reef of Jarvis in 1913. The ship was quickly broken apart, its cargo of coal washed ashore. The ship's crew documented the ruins of ten wooden guano-mining buildings, including a two-story house. In 1924, the U.S.S. *Whippoorwill* Expedition, which was sponsored by Bishop Museum, surveyed the island. This expedition found a white beacon structure, a few graves, rusty rails and boilers, and coral boulders that marked the sites of former buildings.

Jarvis was reclaimed by the United States government and colonized from 1935 to 1942, under the American Equatorial Islands Colonization Project, also called the Hui Panala'au project, which required Hawaiian students to occupy the island. The Millersville settlement arose on the island's western shore and evolved from simple tents and shacks built from wreckage of the *Amaranth* to later become a community consisting of stone and wood dwellings equipped with

refrigeration, radio equipment, and a weather station. The men cleared an aircraft landing area on the northeast side of the island with a T-shaped marker from gathered stones, but no airplane is known to have ever landed there. At the beginning of World War II, four young colonists were fired upon by an Imperial Japanese Navy submarine that surfaced off the west coast. In 1942, the United States Coast Guard cutter *Taney* shelled and burned the dwellings after evacuating the colonists. The roughly cleared landing area on the island's northeast end was later shelled by the Japanese, leaving crater holes (Bryan 1974).

Jarvis was visited by scientists representing the Scripps Institution of Oceanography during the International Geophysical Year from 1957 to 1958. During a severe storm, building ruins from both the guano diggers and the 1935–1942 colonization were swept away without a trace leaving the day beacon and the 19th century tram track remains in the dried lagoon bed as the lone surviving man-made structures on the island (Jewell 1961). Cat, rats, goats, and mice brought by human settlers modified the habitat for terrestrial wildlife at Jarvis.

In 1974, Jarvis Island National Wildlife Refuge was established and included the land, waters, as well as submerged and emergent lands, from the mean low tide water lines out to 3 nm. In 2009, President George W. Bush established the Pacific Remote Islands Marine National Monument (PRIMNM) to protect and preserve the marine environment from 0 to 50 nm around Baker, Howland, and Jarvis Islands, Wake, Johnston, and Palmyra Atolls, and Kingman Reef, for the proper care and management of the historic and scientific objects therein (National Oceanic and Atmospheric Administration 2009). As part of the PRIMNM designation, the Refuge boundaries were extended to include the waters and submerged lands from 0–3 nm to 12 nm. In 2014, President Barack Obama issued Executive Order 9173 to expand the area of the PRIMNM out to the 200 nautical mile U.S. Exclusive Economic Zone boundary for Wake, Johnston, and Jarvis islands, which are cooperatively managed by the National Oceanic and Atmospheric Administration (NOAA Fisheries) and the U.S. Fish and Wildlife Service (Executive Office of the President 2014).

During the extreme 2015–2016 El Niño, prolonged anomalously warm sea surface temperatures (SSTs) caused mass coral bleaching and mortality on many Pacific reefs, including those at Jarvis. However, signatures of community-wide bleaching preserved in skeletons of surviving corals indicate this was not the first severe event at Jarvis (Barkley et al. 2018). Despite a history of repetitive bleaching, Jarvis maintained relatively high calcifier cover—in the form of crustose coralline algae (CCA)—and abundant fish biomass, likely sustained by exceptional productivity associated with strong equatorial and topographic upwelling. While the magnitude and duration of the 2015–2016 El Niño was unprecedented, Jarvis' history of weathering extreme conditions combined with its protected status and few local stressors maximizes the rebound potential of this coral reef ecosystem.

Geology and Environmental Influences

Jarvis Island is included in the Central Pacific subregion of the Polynesian Region of the Pacific Basin. This subregion is the most remote part of the tropical Pacific and includes only low-lying reef islands, atolls, and submerged reefs (Palawski 2007). The island has a tropical desert climate, with high daytime temperatures, relatively steady easterly trade winds, and intense equatorial sun throughout the year. The land is mostly sandy and reaches 7 m (23 ft) at its

highest point. Jarvis has no known natural freshwater lens and scant rainfall (less than 1 m [40 inches] per year) with no plants larger than shrubs. Its sparse bunch grass, vines, and low-growing shrubs are primarily nesting, roosting, and sheltering habitats for seabirds, shorebirds, and numerous land hermit crabs. Jarvis Island has more nesting seabirds than any other island in the U.S. tropical Pacific Islands. The shallow marine benthic habitats around Jarvis consist of a fringing reef with shallow back reefs, a steep forereef, and moderate-sized reef terrace on the eastern windward side of the island.

Loading the Research Vessel AHI *onto the NOAA Ship* Oscar Elton Sette*. Photograph: NOAA Fisheries.*

Benthic Characterization

4.2 Benthic Characterization

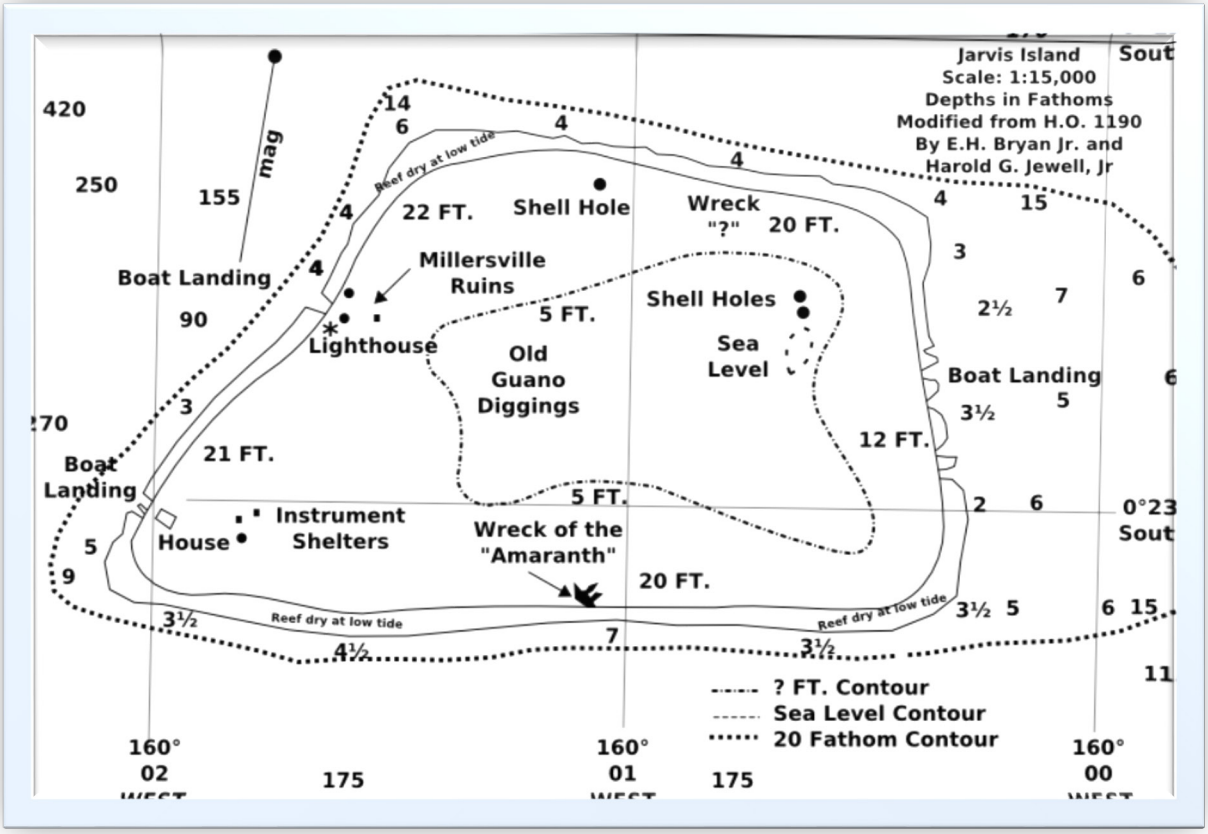

Map of Jarvis Island. This map is based on the original drawing from Bryan (1942).
Source: Jarvis Island website

In this section, the benthic habitats of Jarvis Island are characterized for the depth range from 0 to 1,000 m, using integrated and synthesized data from numerous sources.

Survey Effort

NOAA has been collecting benthic habitat mapping data for the nearshore areas around Jarvis Island since 2006, using a variety of methods as described in the "Benthic Characterization Methods" section of "Chapter 1: Overview." These methods include multibeam bathymetric and backscatter surveys, and single-beam surveys for depth validation.

Multibeam Surveys

Mapping surveys were conducted around Jarvis Island during the 2006 Pacific Reef Assessment and Monitoring Program (RAMP) research cruise using multibeam sonar systems aboard the NOAA Ship *Hi'ialakai* (Simrad EM 300 and EM 3002D) and R/V *AHI* (Reson 8101-ER). Bathymetric and backscatter data were collected for depths between approximately 10 and

3,500 m and used to derive mapping products covering a total of approximately 316 km^2. Approximately 2.1 km^2 of the area remained unmapped, because the shallower areas were inaccessible to survey with vessel-mounted multibeam systems.

Two of the resulting gridded bathymetric products are a 5 m high-resolution grid of the reefs, banks, shelf, and slope habitats to allow for the identification of fine-scale features to a depth of 300 m and a coarser 20 m mid-resolution grid that includes the full extent of the multibeam bathymetric data collected (Figure 3). The data and supporting documentation are available on the Jarvis Bathymetry page of the Pacific Island Benthic Habitat Mapping Center (PIBHMC) website.

Figure 3. Bathymetric coverage map for Jarvis Island showing extent of high- (5 m) and mid-resolution (20 m) gridded multibeam data acquired by the Ecosystem Sciences Division (ESD) in 2006 (lighter blues), and estimated bathymetry derived by ESD from satellite imagery (dark blue). The dotted dark blue line represents the 1,000 m depth contour. Gaps in bathymetric coverage are shown in white and land features in black. Satellite-derived bathymetry is discussed later in this section.

The backscatter data from the shallower surveys conducted from the R/V *AHI* were gridded at 1 m resolution, while the data from the deeper surveys conducted from the *Hi'ialakai* were gridded at 5 m resolution. Acoustic backscatter intensities indicate characteristics of the seabed around Jarvis that can be related to topography and slope. While these data are useful for geomorphology and habitat interpretation, both the shallow and deeper backscatter data have quality issues, including high noise levels and patchiness in the coverage. The data and supporting documentation are available on the Jarvis Backscatter page of the PIBHMC website.

Single-beam Surveys

Single-beam sonar data were acquired around Jarvis Island from depths between 1 and 380 m in 2012, between 1 and 223 m in 2015, and between 3 and 1254 m in 2017 (Figure 4). As ocean conditions varied each year and new survey equipment was introduced in 2017, the errors associated with the three years of data also varied. Soundings error was found to be significantly greater in 2017 (0.82 m compared with 0.14 m in 2015). Therefore, the data collected in 2017 were filtered to exclude depths deeper than 100 m in Figure 4. The 2012 data were not included in the error analysis; however, upon visual inspection the data correlated well with the existing bathymetric data.

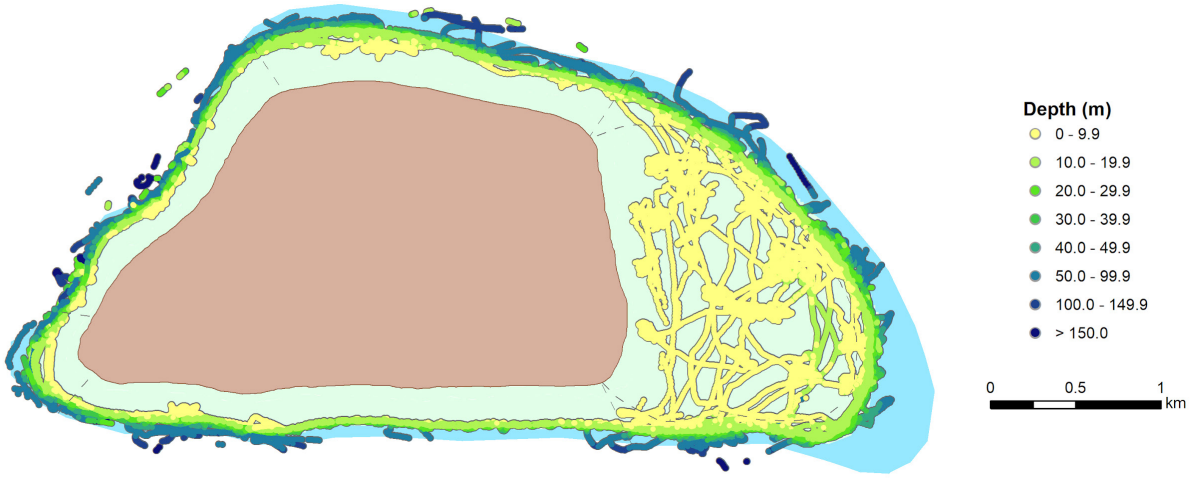

Figure 4. Depth validation data for Jarvis Island collected by the Ecosystem Sciences Division in 2012, 2015, and 2017. Soundings deeper than 100 m have been excluded from the 2017 surveys due to data quality concerns.

Towed-camera Surveys

No habitat validation data for habitat mapping purposes were collected at Jarvis Island.

Habitat characterization

Satellite-derived Bathymetry

The Ecosystem Sciences Division (ESD) derived estimated depths between 0 and 13 m around Jarvis Island from WorldView-2 satellite imagery acquired in 2016 to fill gaps in the nearshore shallow-water bathymetric coverage. Depth soundings collected in 2015 (Figure 4) were used to validate the satellite-derived depths, resulting in 55% agreement between the overlapping soundings and estimated depths. The data and supporting documentation are available on the Jarvis Bathymetry page of the PIBHMC website. Though these estimated depths provide useful information for areas with little or no bathymetric measurements, the low depth accuracy limits the use of these data. See Figure 3 for the extent of satellite-derived depths generated by ESD that partially filled the bathymetric coverage gap around Jarvis.

Integrated Bathymetry

ESD's multibeam bathymetry and satellite-derived depths were combined to produce an integrated bathymetric map for Jarvis Island (Figure 5).

Bathymetric data around Jarvis indicate a small, isolated island elongated in an east-west direction that rises from the deep seafloor with no underlying ridge structures (Keating 1992). It is characterized as a low-lying, coral island surrounded by narrow and occasionally emergent fringing reefs with a broad forereef terrace (East Terrace georegion) that extends 1.5 km to the east to depths of approximately 20 m, after which it drops off steeply. The reef slopes are steep in the North, West, Southwest, and South georegions, ranging from 30–40° (Maragos et al. 2008). Remnants of short channels blasted through the shallow fringing reefs to facilitate small boat access to the island for historical mining and military activities are evident in the West and East Terrace georegions (Figure 5).

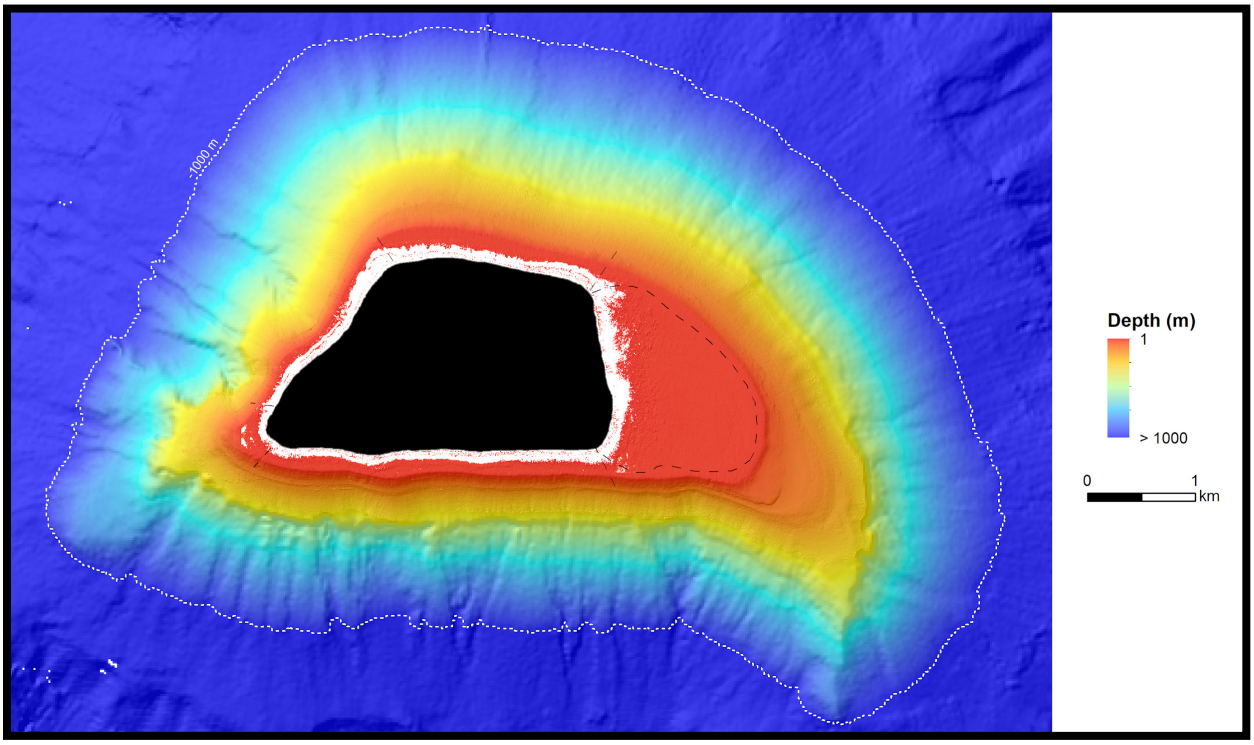

Figure 5. Integrated bathymetric map focusing on depths from 0 m to ~1,000 m for Jarvis Island, with gaps in bathymetric coverage shown in white and land features in black. The dotted white line represents the 1,000 m depth contour.

Bathymetric Derivatives

No bathymetric derivatives (e.g., slope, rugosity, or bathymetric position index layers) are currently available for Jarvis Island.

Seafloor Substrate

ESD generated predicted seafloor substrates (i.e., hard or soft bottom) for Jarvis Island in 2018 (Figure 6). The source data used to produce the substrate map for Jarvis for water depths to 1,000 m include multibeam bathymetric and backscatter data from the *Hi'ialakai* surveys and satellite imagery acquired in 2016. The data and supporting documentation are available on the Jarvis Seafloor Characterization page of the PIBHMC website.

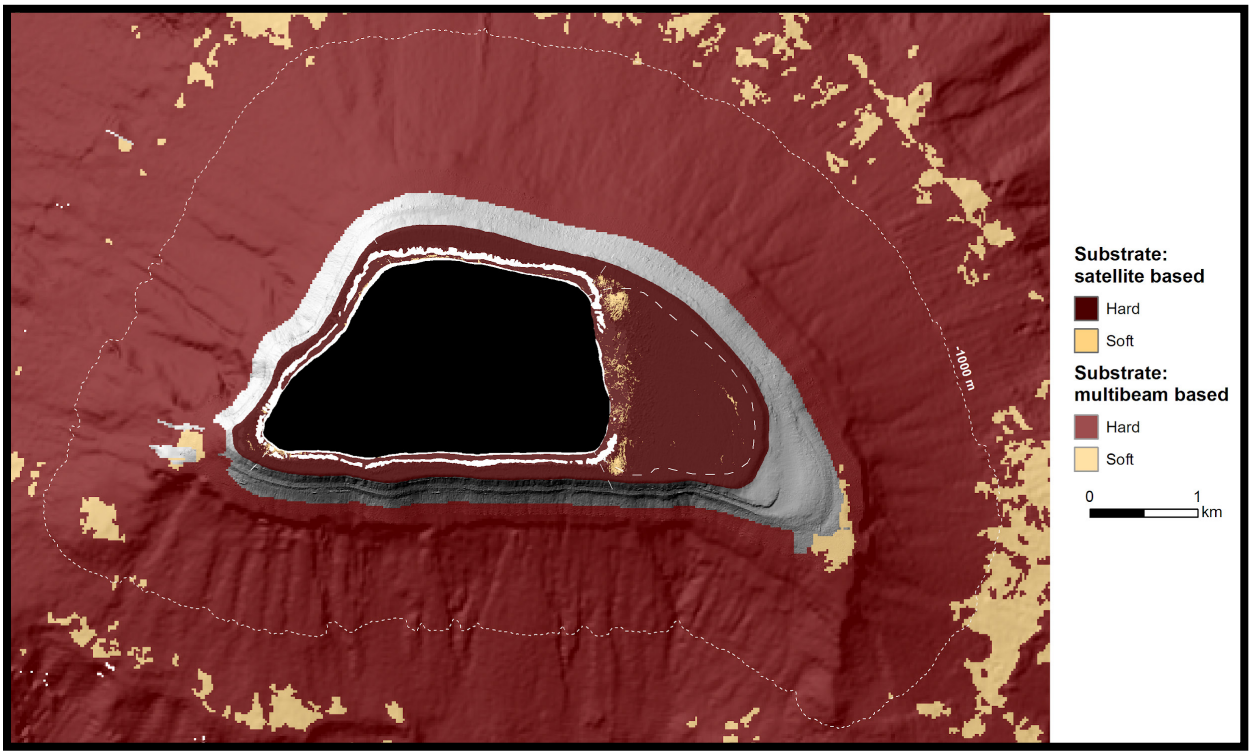

Figure 6. Seafloor substrate map of Jarvis Island showing hard- and soft-bottom habitats. Depths from ~0 m to 30 m were derived from WorldView-2 satellite imagery, and depths >30 m were based on gridded multibeam bathymetric and backscatter data (20 m and 5 m resolution, respectively). The dotted white line represents the 1,000 m isobath. Gaps in substrate coverage are shown in grey and land features in black.

An approximately 200–800 m wide gap exists between the deepest extent (~30 m) of the shallow substrate map and the shallowest extent (~230 m) of the deeper substrate map (Figure 6). Though the multibeam data acquired from the *AHI* surveys overlap this gap, these data were not used to derive substrates because the backscatter data produced erroneous results.

The seafloor surrounding Jarvis (from the shoreline to 1,000 m depths) is predominantly hard substrate with small patches of soft-bottom habitat primarily in depths below 30 m and along the shoreline of the East Terrace georegion. An area-specific classification was applied in the Southwest georegion where the original satellite-derived predictions underestimated soft substrate.

Maps to Inform the Coral Reef Fish and Benthic Monitoring Survey Design

Many biological communities are structured by depth and habitat (i.e., reef zone), often due to differences in associated environmental parameters, such as light, temperature, salinity, and wave energy. The current Pacific RAMP stratified-random survey design restricts monitoring surveys to hard-bottom habitats in the 0–30 m depth range, stratified by both depth and reef zone.

Depth Strata

The integrated bathymetry shown in Figure 5 has been used to classify depth bins (Figure 7) from 0 to 1,000 m. For the Pacific RAMP surveys, depth strata have been defined as shallow (>0–6 m), mid (>6–18 m), and deep (>18–30 m). Estimated seafloor areas for each of the depth strata are included in Table 1.

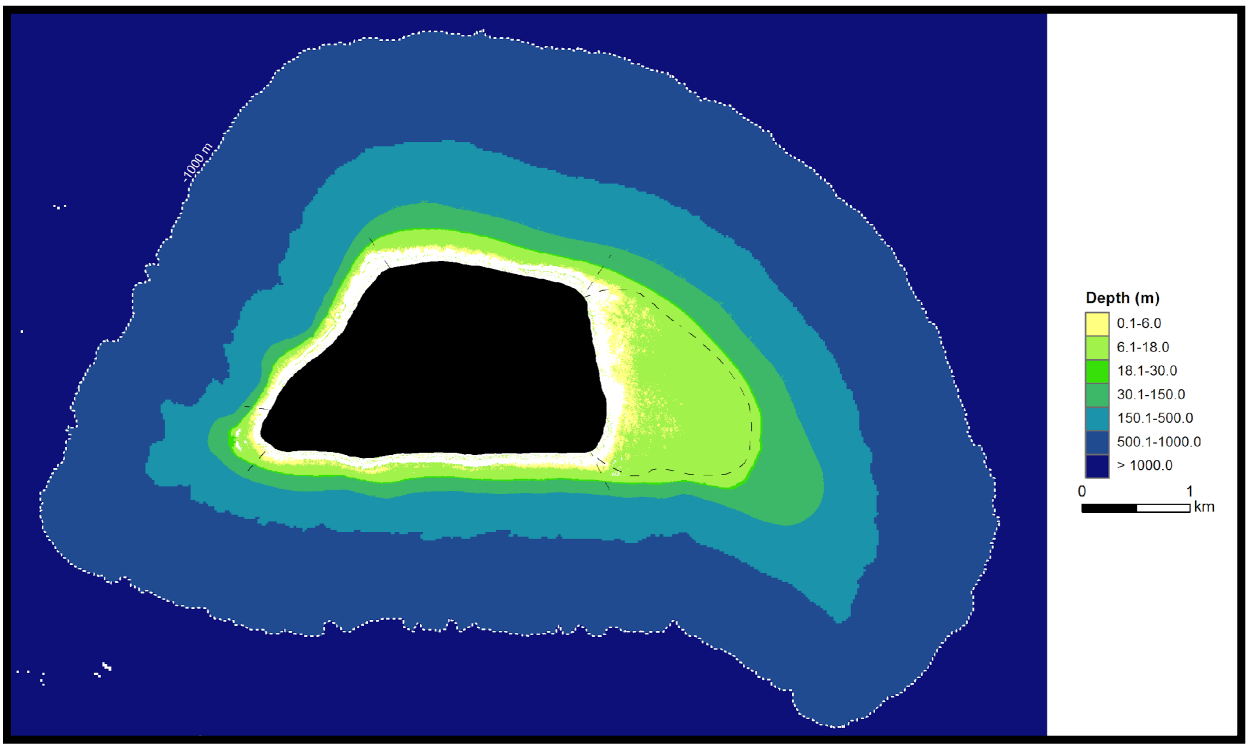

Figure 7. Depth strata map for Jarvis Island from 0 m to 1,000 m. The dotted white line represents the 1,000 m depth contour. Gaps in bathymetric coverage are shown in white and land features in black.

The shallow-water bathymetry gap at Jarvis Island precluded derivation of a 6 m isobath; therefore, the two shallowest depth strata (>0–6 m and >6–18 m) have been combined in Table 1. The actual mapped seafloor area for the combined depth strata differs from the estimated seafloor area. At Jarvis, 75% of the seafloor between 0 and 18 m depths was mapped, leaving a gap of approximately 1 km^2. The map of the seafloor from 18 to 1,000 m depths was spatially complete.

Table 1. Land and seafloor area by depth strata from 0 to 1,000 m depths for Jarvis Island. Seafloor area statistics include actual mapped area (km^2) and estimated seafloor area (km^2) based on the integrated bathymetric map for Jarvis. Land area is 4.5 km^2.

Depth (m)	Estimated Seafloor (km^2)	Mapped Seafloor (km^2)
>0–18	4.0	3.0
>18–30	0.2	0.2
Subtotal: >0–30	**4.2**	**3.2**
>30–150	2.5	2.5
>150–500	7.6	7.6
>500–1,000	20.4	20.4
Total: >0–1,000	**34.7**	**33.7**

Reef Zones

To support the stratified-random design for Pacific RAMP monitoring surveys, reef zones have been delineated for Jarvis Island, including forereef, reef crest/reef flat, channel, and land (Figure 8). Satellite imagery was primarily used to manually digitize the zones. Reef crests/reef flat areas include the shoreline out to and including breaking waves; however, the date of the satellite image may influence the accurate delineation of the reef crest (i.e., due to seasonal changes in wave action).

Only forereef habitats have been surveyed around the island, because these habitats most commonly occur in coral reef areas. Therefore, results from surveys at Jarvis can be compared with results from surveys across all coral reefs of the U.S. Pacific Islands. Moreover, hazards from emergent reef in the shallow reef crest/reef flat areas precluded surveys in these habitats at Jarvis.

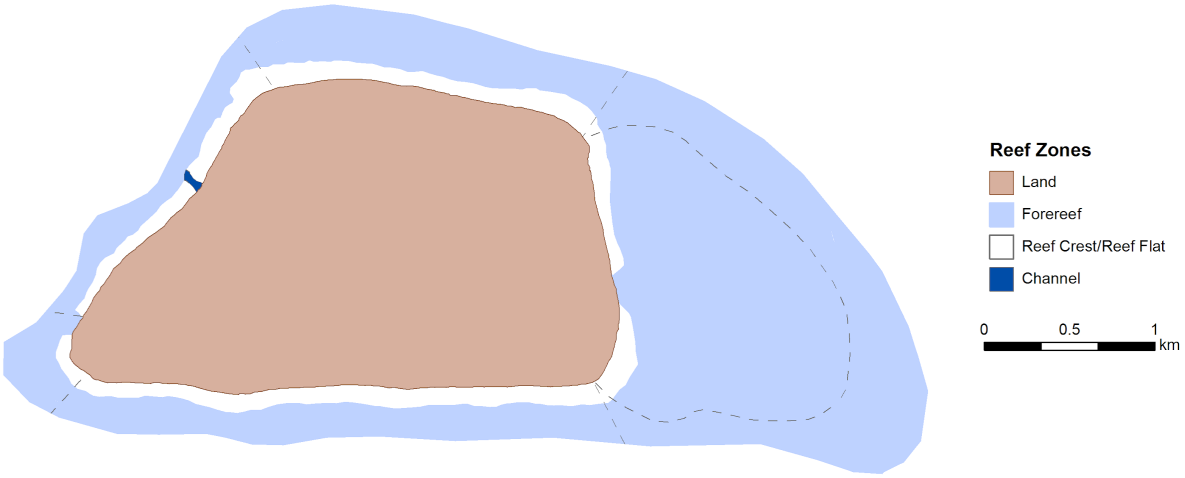

Figure 8. Reef zones for Jarvis Island digitized from WorldView-2 satellite imagery.

Substrate

Only hard-bottom substrates were targeted for stratified-random reef fish and benthic monitoring surveys of Pacific RAMP. However, at the time the survey strata were established for Jarvis Island, no substrate information existed. As previously discussed, predicted seafloor substrates have since been developed for Jarvis and will be incorporated into the survey strata in advance of the Pacific RAMP surveys at Jarvis scheduled for 2021. In general, hard-bottom substrates comprise the majority of the seafloor area around Jarvis with relatively small patches of soft-bottom substrates around the island (Figure 6).

Survey Strata

To date, the survey strata used for the stratified-random fish and benthic surveys were based on depth only (Figure 7). A cursory assessment of the new substrate and reef zone data together with the depth strata indicate approximately 3.2 km^2 of surveyable seafloor is available within forereef, hard-bottom habitats in the 0–30 m depth range at Jarvis Island.

Field team on small boat with booby in the foreground. Photo: NOAA Fisheries.

Ocean and Climate Variability

4.3 Ocean and Climate Variability

Coring coral at Jarvis Island
Photo: Frances Lichowski, NOAA Fisheries

Survey Effort and Site Information

The coral reef ecosystems at Jarvis Island experience complex and extremely variable oceanographic and ecological dynamics. Located just 40 km south of the equator in the central Pacific, Jarvis is positioned in the equatorial cold tongue characterized by cool, nutrient-rich waters due to equatorial upwelling, a process caused by the divergence of easterly trade wind-driven surface waters away from equator. These surface waters are replaced by cooler, nutrient-rich subsurface waters. Jarvis also sits directly in the path of both the westward-flowing South Equatorial Current at the surface and the eastward-flowing subsurface EUC. Intense, localized topographic upwelling occurs as the subsurface EUC encounters the steep western slope of the island. The combined equatorial and topographic upwelling bathe the coral reefs of Jarvis in unusually cool, low-pH, and nutrient-rich waters that elevate local biological productivity (Gove et al. 2006). The strength of the EUC and the intensity of upwelling at Jarvis vary dramatically with interannual variability in the El Niño Southern Oscillation (ENSO). During La Niña years, a strong EUC drives intense upwelling, cool temperatures, and high productivity. During El Niño

events, anomalously weak trade winds reduce equatorial upwelling, and an anomalously weak EUC reduces topographic upwelling, with the combined effects resulting in elevated temperatures and reduced productivity.

ENSO-driven fluctuations in nearshore ocean conditions affect the health of coral reef ecosystems at Jarvis. These environmental oscillations are occurring on a backdrop of global climate change, as concentrations of carbon dioxide in the atmosphere are altering the temperature and chemistry of the seawater in these coral reef habitats. Episodic high temperatures, largely driven by El Niño events, have led to increases in the frequency and intensity of coral bleaching in the past few decades. In addition, the dissolution of carbon dioxide in ocean surface waters sets off a chain of chemical reactions in seawater that decreases pH impeding the growth of corals and calcifying reef organisms. Understanding the shifts in ocean conditions that are occurring and the sensitivity of coral reef ecosystems to these changes is critical for projecting their survival under 21st century climate change.

Since 2000, Pacific RAMP efforts have monitored the oceanographic environments of coral reef ecosystems in the PRIMNM. These efforts have collected data on key parameters using: (1) a diverse suite of moored instruments; (2) nearshore conductivity, temperature, and depth (CTD) vertical profiles of water column structure; (3) discrete water samples to assess dissolved nutrients, chlorophyll-*a*, and carbonate chemistry; and (4) estimates of calcium carbonate accretion, bioerosion rates, and coral growth and skeletal density to examine the balance between production and removal of calcium carbonate on the reef (Figure 9, Figure 10, Figure 11, Figure 12, and Figure 13). A summary of the environmental survey efforts around Jarvis from 2000 to 2017 is shown in Table 2. Refer to the Overview chapter for oceanographic instrumentation specifics and water sample collection methodologies.

We complemented field data collections with satellite remote sensing data sets and model products to provide the large-scale climate and oceanographic context for our in situ observations. Specifically, we used the Oceanic Niño Index (ONI, the standard index of ENSO activity), sea surface temperature (SST) anomalies from the Optimum Interpolation SST data set, the Degree Heating Week (DHW) index from Coral Reef Watch, chlorophyll-*a* (chl-*a*, a proxy for primary productivity) anomalies from the Sea-Viewing Wide Field-of-View Sensor, and Moderate Resolution Imaging Spectroradiometer Aqua, and global WaveWatch III model output to explore multi-decadal variability in ocean wave conditions.

Table 2. Summary of the oceanographic and environmental data collection efforts at Jarvis Island by year over the period 2000 through 2017. The following instruments were deployed: sea surface temperature (SST) buoy, subsurface temperature recorder (STR), Seabird Electronics MicroCAT (SBE-37), ecological acoustic recorder (EAR), SoundTrap acoustic recorders, ocean data platform (ODP), acoustic Doppler current profiler (ADCP), Satlantic SeaFET pH sensor (SeaFET), calcification accretion unit (CAU), bioerosion monitoring unit (BMU), and autonomous reef monitoring structures (ARMS). Diel suite sampling included moored conductivity-temperature-depth (CTD) and discrete water samples. CTD casts, shallow (near reef) and deep (offshore), had corresponding discrete water samples, shallow (near reef) and deep (offshore). Coral cores were collected from *Porites* spp. Numbers indicate the quantity of instruments deployed (D) and retrieved (R) as D/R, water samples and diel suite collections, CTD casts, and coral cores per year.

												Diel Suite		CTD Casts		Water Samples		Coral Cores
Year	SST	STR	SBE-37	EAR	SoundTrap	ODP	ADCP	SeaFET	CAU	BMU	ARMS	Moored CTD	Water Samples	Shallow	Deep	Shallow	Deep	*Porites* spp.
2000	–	–	–	–	–	–	–	–	–	–	–	–	–	21	–	–	–	–
2001	–	–	–	–	–	–	–	–	–	–	–	–	–	19	–	–	–	–
2002	1/-	–	–	–	–	1/-	–	–	–	–	–	–	–	15	–	–	–	–
2004	1/-	4/-	–	–	–	1/1	–	–	–	–	–	–	–	33	–	–	–	–
2006	1/-	8/4	–	–	–	1/1	–	–	–	–	–	–	–	54	–	72	–	–
2008	1/-	9/8	–	1/-	–	1/1	–	–	–	–	9/-	–	–	31	21	49	78	–
2010	1/1	15/10	3/2	1/1	–	-/1	3/3	–	25/-	–	9/9	–	–	19	18	12	87	6
2012	–	7/13	1/2	1/1	–	–	1/1	–	25/24	–	9/9	–	–	16	24	21	120	9
2015	–	17/12	–	-/1	–	–	2/2	2/2	25/12	15/-	9/9	2	14	15	–	22	–	–
2016	–	5/5	–	–	–	–	2/2	2/2	–	–	–	2	41	12	–	14	–	–
2017	–	3/3	–	2/-	2/-	–	2/2	2/2	–	–	–	2	22	8	–	13	–	–
Total	5/1	68/55	4/4	5/3	2/-	4/4	10/10	6/6	75/36	15/-	36/27	6	77	95	59	203	285	15

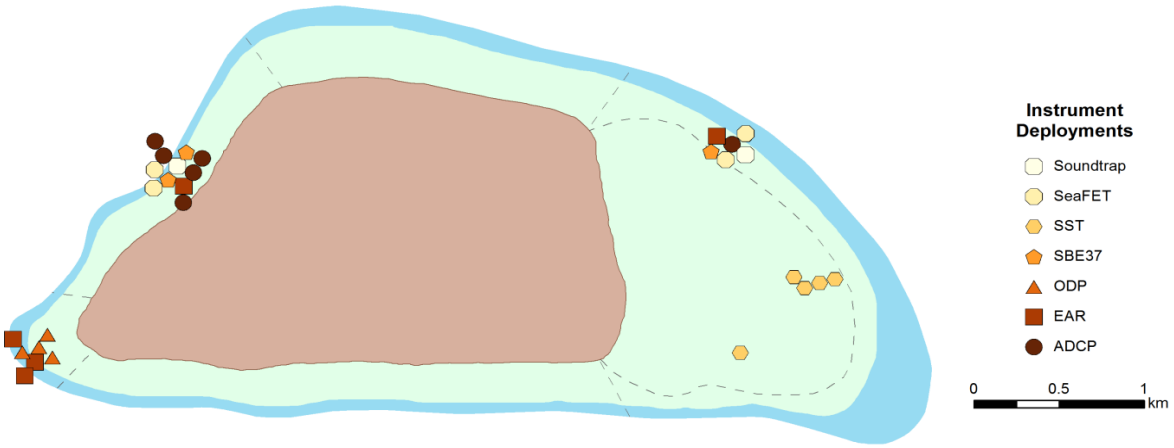

Figure 9. Deployment locations of SoundTrap acoustic recorders, Satlantic SeaFET pH sensor (SeaFET), sea surface temperature (SST) buoys, Seabird Electronics MicroCATs (SBE37), ocean data platforms (ODP), ecological acoustic recorders (EAR), and Nortek acoustic Doppler current profilers (ADCP) around Jarvis Island. Instrument deployments at the same location over multiple years have been plotted adjacent to one another and organized around their shared location on the map.

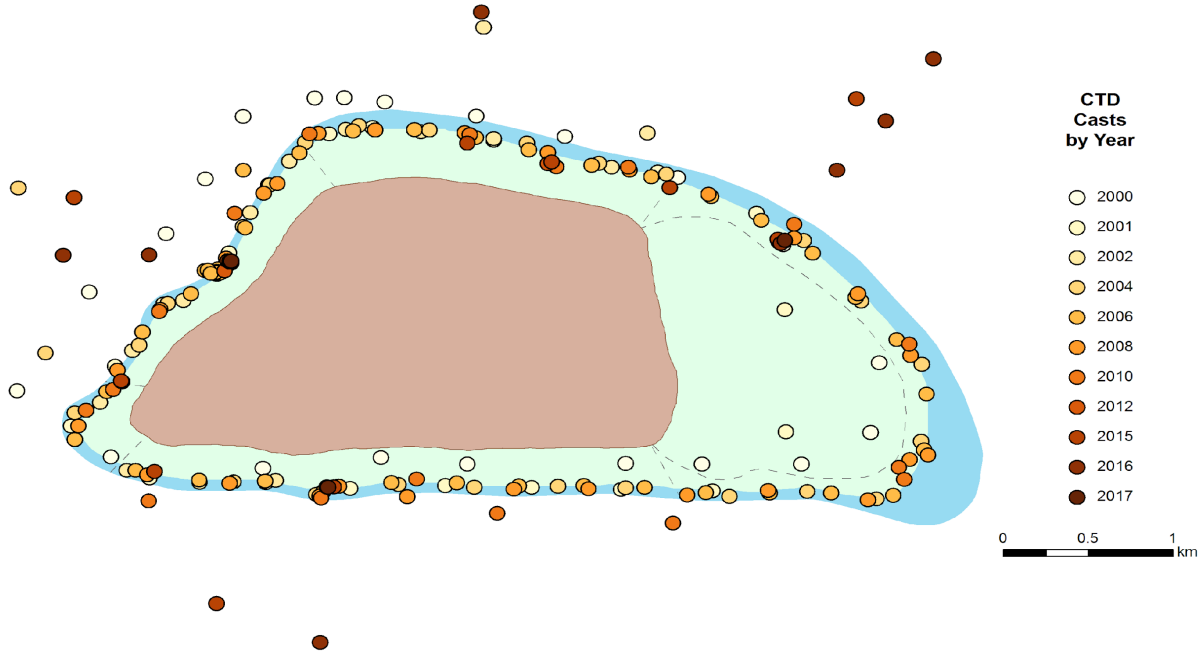

Figure 10. Locations of nearshore conductivity-temperature-depth (CTD) hydrocasts, measuring water column salinity and temperature from the ocean surface to a depth of ~30 m around Jarvis Island. Casts in earlier years (2000–2010) prioritized sampling the entire perimeter of the forereef, while later efforts (2012–2015) focused on permanent instrumentation sites (sites with subsurface temperature recorders, autonomous reef monitoring structures, and/or calcification accretion units).

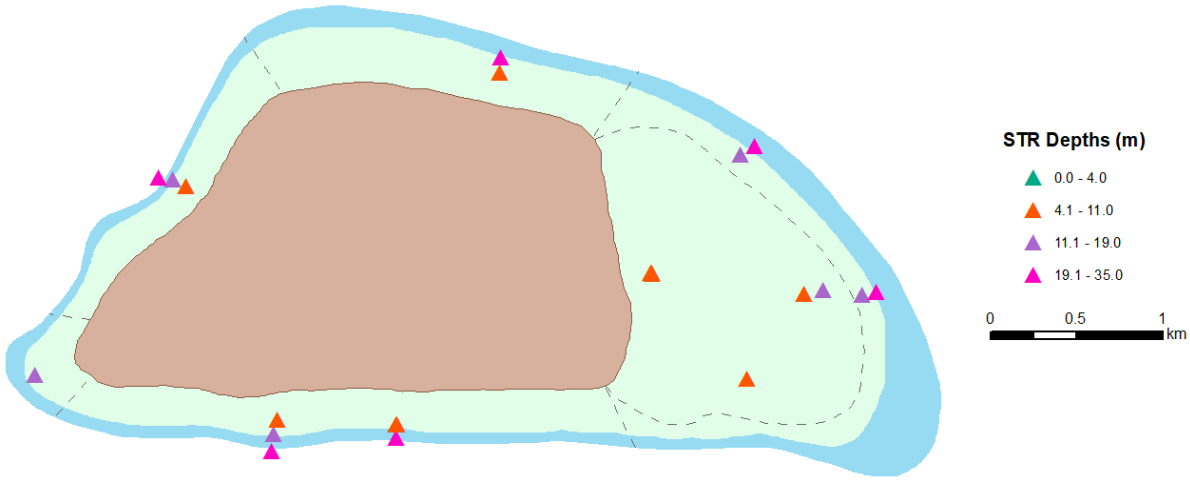

Figure 11. Locations of subsurface temperature recorders (STRs), deployed on the reef substrate in depths ranging from 1 to 32 m around Jarvis Island. Multiple STRs may have been collected at the same location over multiple years; however, they are represented by a single marker on the map.

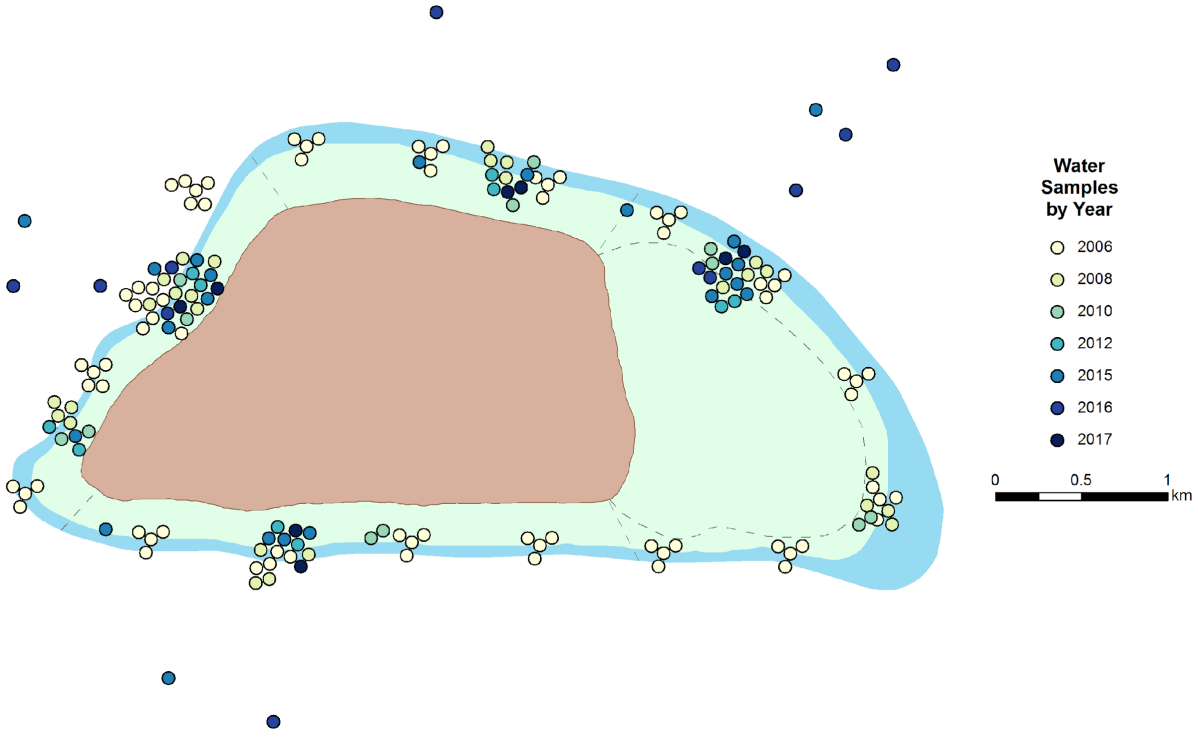

Figure 12. Locations of discrete seawater sample collections from 1 to 32 m depths around Jarvis Island. Samples evaluated for various analytes: dissolved inorganic carbon, total alkalinity, chlorophyll-*a*, and dissolved inorganic nutrients. Water samples collected at the same location over multiple years have been plotted adjacent to one another and organized around their shared location on the map.

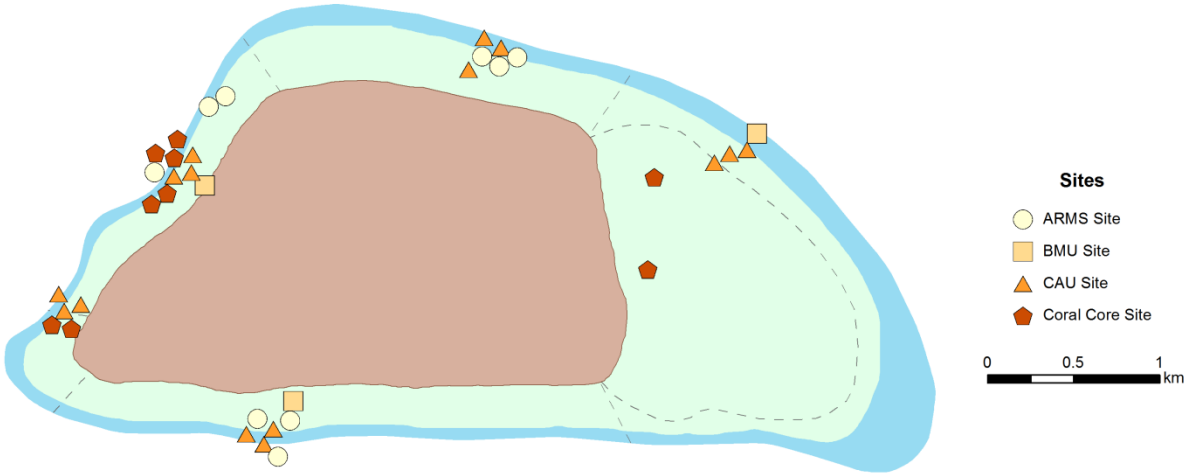

Figure 13. Locations of autonomous reef monitoring structures (ARMS), bioerosion monitoring units (BMU), calcification accretion units (CAU), deployed on the reef at ~15 m depths around Jarvis Island. Coral cores of *Porites* spp. collected opportunistically at depths from 5 to 15 m. Instrument deployments at the same location over multiple years have been plotted adjacent to one another and organized around their shared location on the map.

Oceanographic Observations

Oceanographic conditions around Jarvis Island show a strong relationship with ENSO variability. The ONI, SST anomalies, DHWs, and chl-*a* anomalies in recent decades are presented in Figure 14. The ONI shows the variability and frequency of warm (positive) and cool (negative) thermal anomalies (i.e., El Niño and La Niña, respectively) over the period 1981–2017 based on a threshold of ±0.5 °C [3-month running mean of SST anomalies in the El Niño 3.4 region (5°N–5°S, 120°W–170°W)]. The SST anomalies for the small area immediately surrounding Jarvis closely track the magnitude and direction of the ONI, with positive SST anomalies persisting during El Niño events and negative SST anomalies persisting during La Niña events (Figure 14a and b).

The coral reefs at Jarvis have experienced frequent and severe episodes of ENSO-driven high temperatures over the past four decades, visualized as SST anomalies over the period 1981–2017 in Figure 6b and as DHW over the period 1985–2017 in Figure 6c. DHWs estimate the amount of thermal stress that has accumulated in an area over a 12-week period by summing and integrating the magnitude and duration of temperatures exceeding the local coral bleaching threshold defined as 1 °C above the maximum monthly mean. SST anomalies above this threshold can drive significant coral bleaching when sustained for several weeks to months, with moderate bleaching predicted when DHW >4 °C-weeks and severe bleaching expected when DHW >8 °C-weeks. The cumulative DHWs during this period related directly to strong warm events observed in the ONI (Figure 14a). DHWs >10 °C-weeks were accumulated at Jarvis in response to El Niño events in 1982–1983, 1987–1988, 1991–1992, 1995–1996, 1997–1998, 2002–2003, 2009–2010, and 2015–2016. The most severe warming occurred during the extreme 2015–2016 El Niño, during which DHW in excess of 30 °C-weeks were observed in the waters influencing the coral reefs at Jarvis.

An inverse relationship exists between ENSO-driven variability in SST and phytoplankton chl-*a* pigment concentration, where increased temperatures were associated with decreased concentrations of chl-*a* (Figure 14d, Figure 15b). During La Niña, enhanced equatorial and topographic upwelling of cool, nutrient-rich deeper waters drives high chl-*a* concentrations and greater primary productivity. During El Niño conditions, anomalously weak easterly trade winds decrease equatorial upwelling, and an anomalously weak EUC suppresses topographic upwelling. The combined effects of decreased equatorial and topographic upwelling results in decreased chl-*a* concentrations and productivity during El Niños. Chl-*a* anomalies were negative during the severe 1997–1998 and 2015–2016 El Niño events, and spikes in chl-*a* were observed during the transitions from El Niño to La Niña in 1997–1998 and 2009–2010. However, because a strong La Niña did not follow the El Niño in 2016, there was no subsequent pulse in chl-*a* or primary productivity.

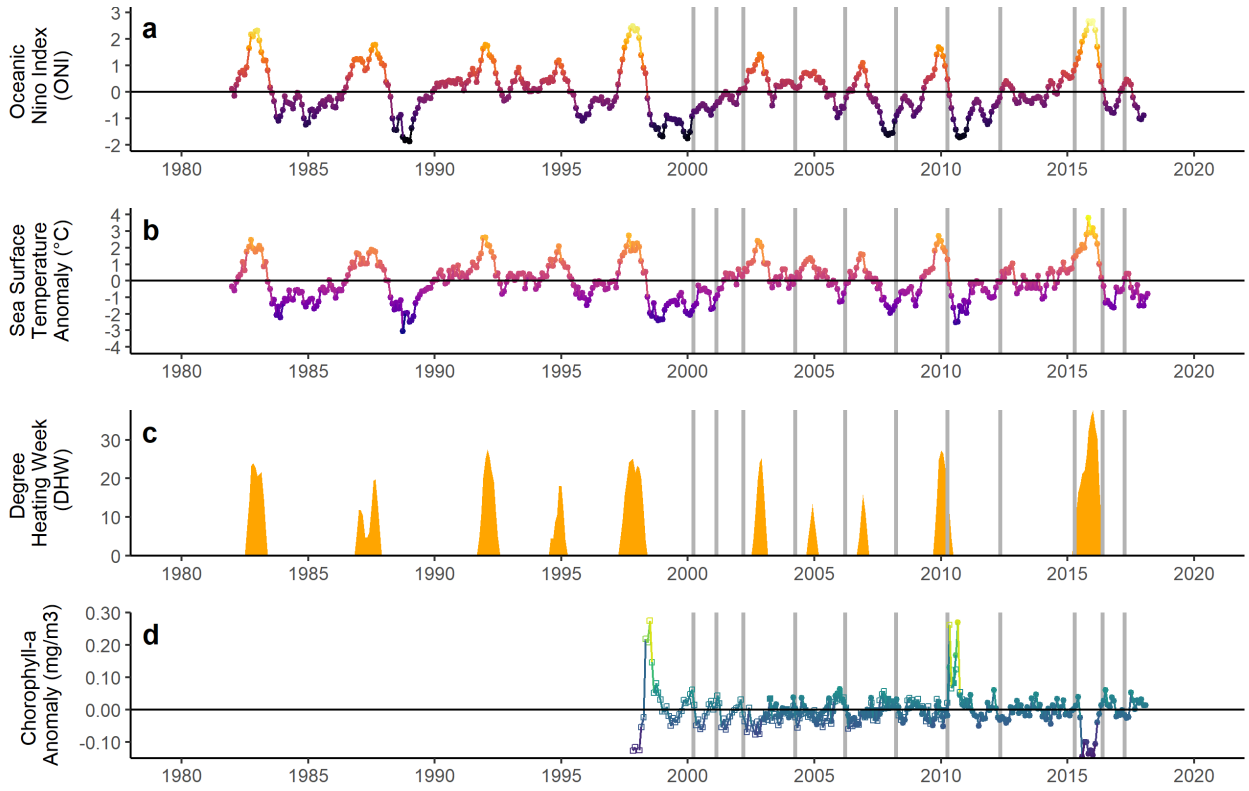

Figure 14. Time series of oceanographic conditions at Jarvis Island: (a) a 3-month rolling mean of Oceanic Niño Index (ONI) from September 1981 to April 2018 in the El Niño 3.4 region (5° N–5° S, 120–170° W), (b) sea surface temperature (SST) anomalies from September 1981 to April 2018, (c) Cumulative Degree Heating Week (DHW) from 1985 to 2017, and (d) phytoplankton chlorophyll-*a* pigment (chl-*a*) concentrations from 1997 to 2017. Available data for ONI, SST, DHW, and chl-*a* were extracted for a box around Jarvis Island (Latitude North: -0.26907 to -0.47354 and Longitude West: -160.106 to -159.881). Shading for SST and chl-*a* data indicates the magnitude of the anomaly, and vertical bars show the dates of field data collections.

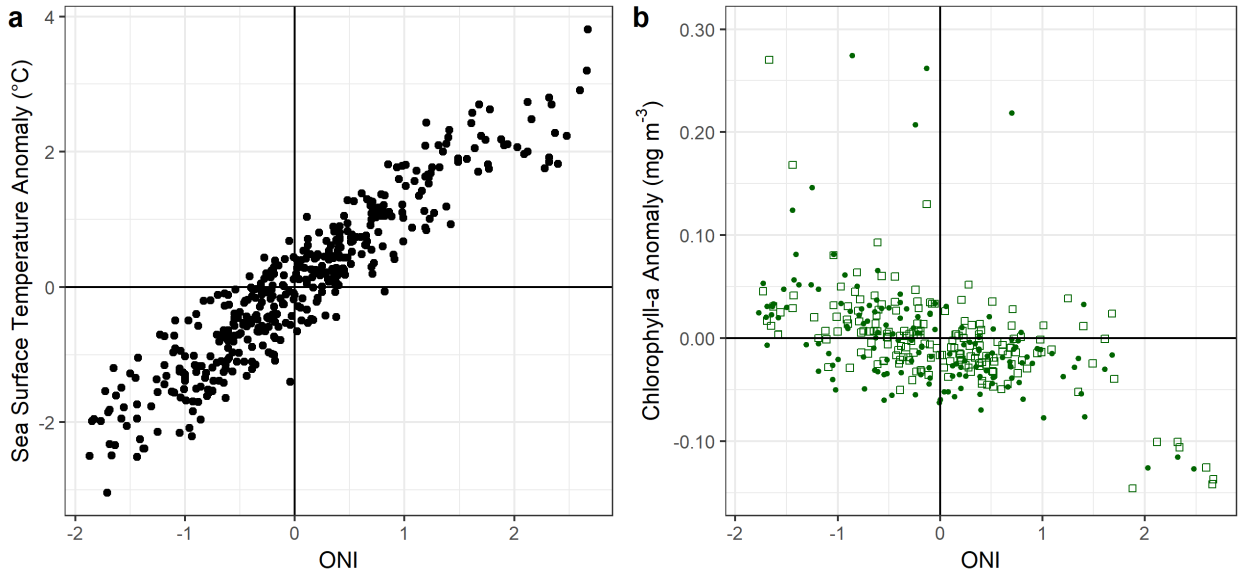

Figure 15. Relationship between monthly-averaged oceanographic conditions at Jarvis Island: (a) Oceanic Niño Index (ONI) vs. sea surface temperature (SST) anomaly, and (b) ONI vs. satellite-derived chlorophyll-*a* (chl-*a*, Sea-Viewing Wide Field-of-View Sensor in boxes and Moderate Resolution Imaging Spectroradiometer in circles) anomaly data. Available data for ONI, SST anomaly, and chl-*a* were extracted for a box around Jarvis Island (Latitude North: -0.26907 to -0.47354 and Longitude West: -160.106 to -159.881).

Water Column Observations

The physical properties and stratification of Jarvis Island's water column varied both temporally, with phases of ENSO, and spatially, around the exposed forereef. Figure 16 shows the location of shallow-water CTD casts conducted in the nearshore waters around Jarvis in 2000 (21 casts) and 2008 (24 casts). Cast data document measurable differences in temperature, salinity, and density profiles between weak (2000) and moderate (2008) La Niña years. Island-mean temperatures in 2000 were about 1.1 °C warmer, and salinity and density were slightly higher relative to 2008 (Figure 17). In both 2000 and 2008, there was little vertical stratification on the forereef, suggesting that the water column around Jarvis is well-mixed (Figure 17). However, profiles from 2000 capture localized topographic upwelling of the eastward-flowing EUC as it interacted with the western flanks of the island, resulting in lower temperatures, higher salinities, and associated higher seawater densities in the West and Southwest georegions as compared with the other reef areas around Jarvis. This localized signature of upwelling on the western side of the island was less apparent in 2008 even though moderate La Niña conditions generally favor increased upwelling intensity. The anomalous results may be due to either the timing of the casts during a transient period of reduced upwelling strength or the location of casts closer to shore.

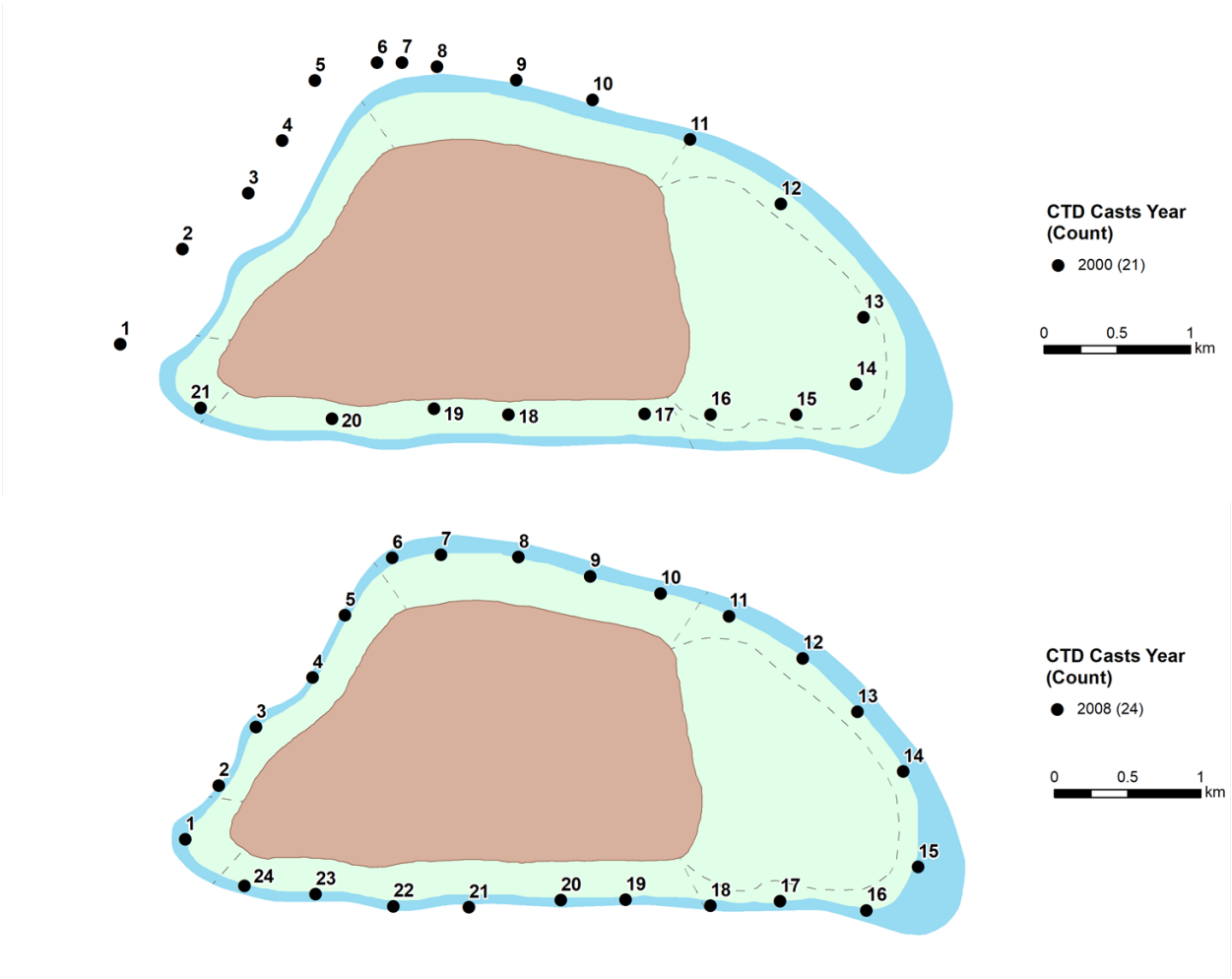

Figure 16. Shallow-water conductivity-temperature-depth (CTD) sampling locations around Jarvis Island. CTDs were conducted during March of 2000 (21 casts) and March of 2008 (24 casts). The casts are numbered sequentially in a clockwise direction around the island from left to right.

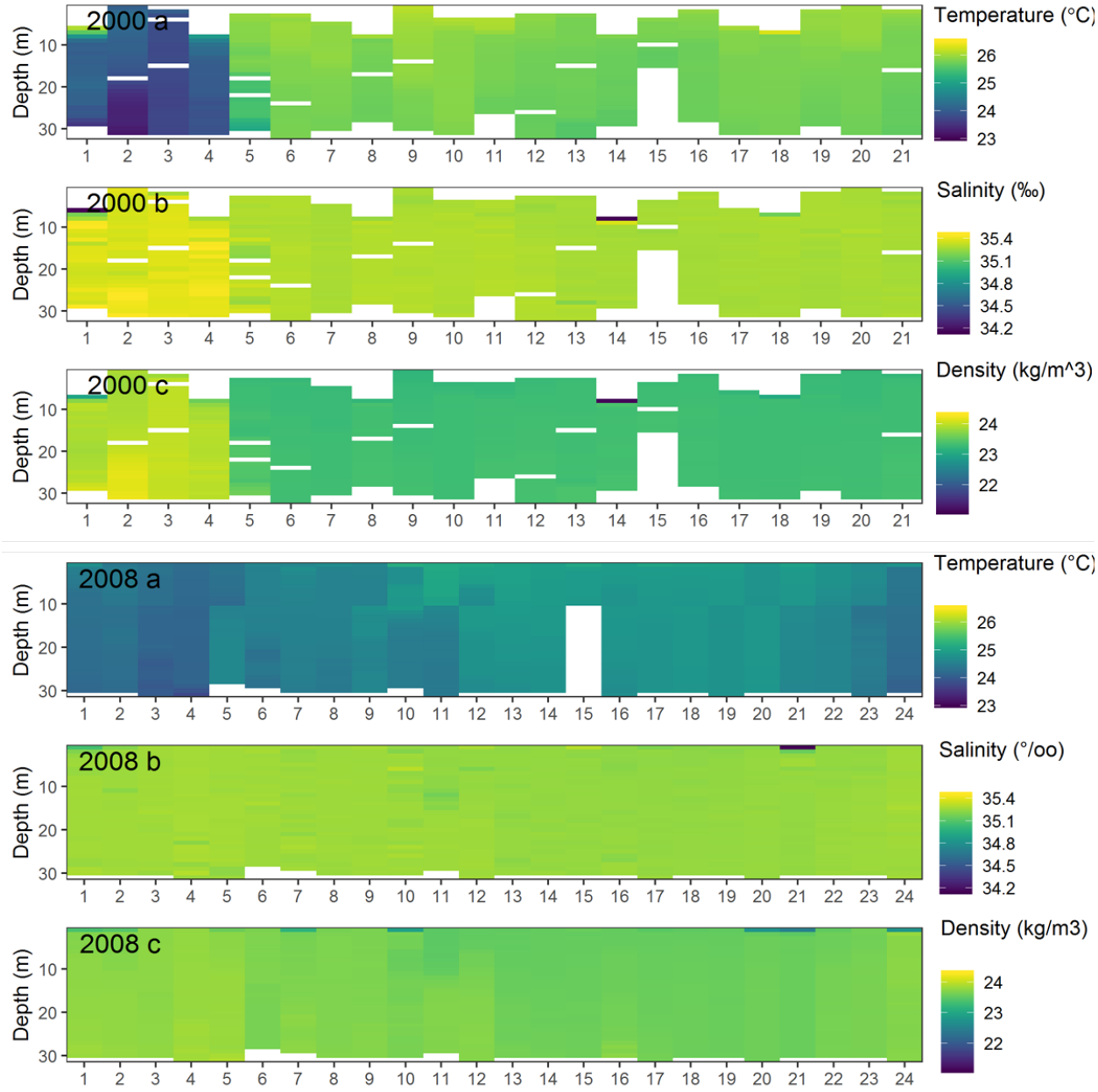

Figure 17. Profiles from shallow-water conductivity-temperature-depth casts around Jarvis Island in 2000 (top three panels) and 2008 (bottom three panels) for (a) temperature (°C), (b) salinity (psu), and (c) sigma-t density (density of seawater at atmospheric pressure in kg m^{-3}-1,000) from the surface to depths of 32 m. The casts are numbered sequentially in a clockwise direction around the island. The top three panels show March of 2000 profiles 1–21 and the bottom three panels show March of 2008 profiles 1–24.

Between 2004 and 2017, a total of 68 moored subsurface temperature recorders (STRs) collected temperature time series at depths between 1 and 32 m (Figure 18). This suite of STRs provides in situ vertical thermal structure observations to characterize the temperature regimes experienced by Jarvis's coral reefs at smaller spatial scales and greater depths than possible using only satellite SST observations at the surface. Interannual variability in temperature was large,

particularly on the western (upwelling) side of the island, where temperatures ranged from above 30 °C during El Niño years to temperatures as low as 21 °C during La Niña years. Temperatures in the North, East, and South georegions were generally homogenous with depth, suggesting that they were well mixed vertically. The West and Southwest georegions showed higher variability in vertical thermal structure, presumably due to internal waves and topographic upwelling that caused periods of vertical stratification of temperature. Notably, the vertical structure in temperatures present on the west side of the island disappeared between late 2015 and early 2016, as upwelling shut down during El Niño and then reappeared in mid-2016 once upwelling resumed.

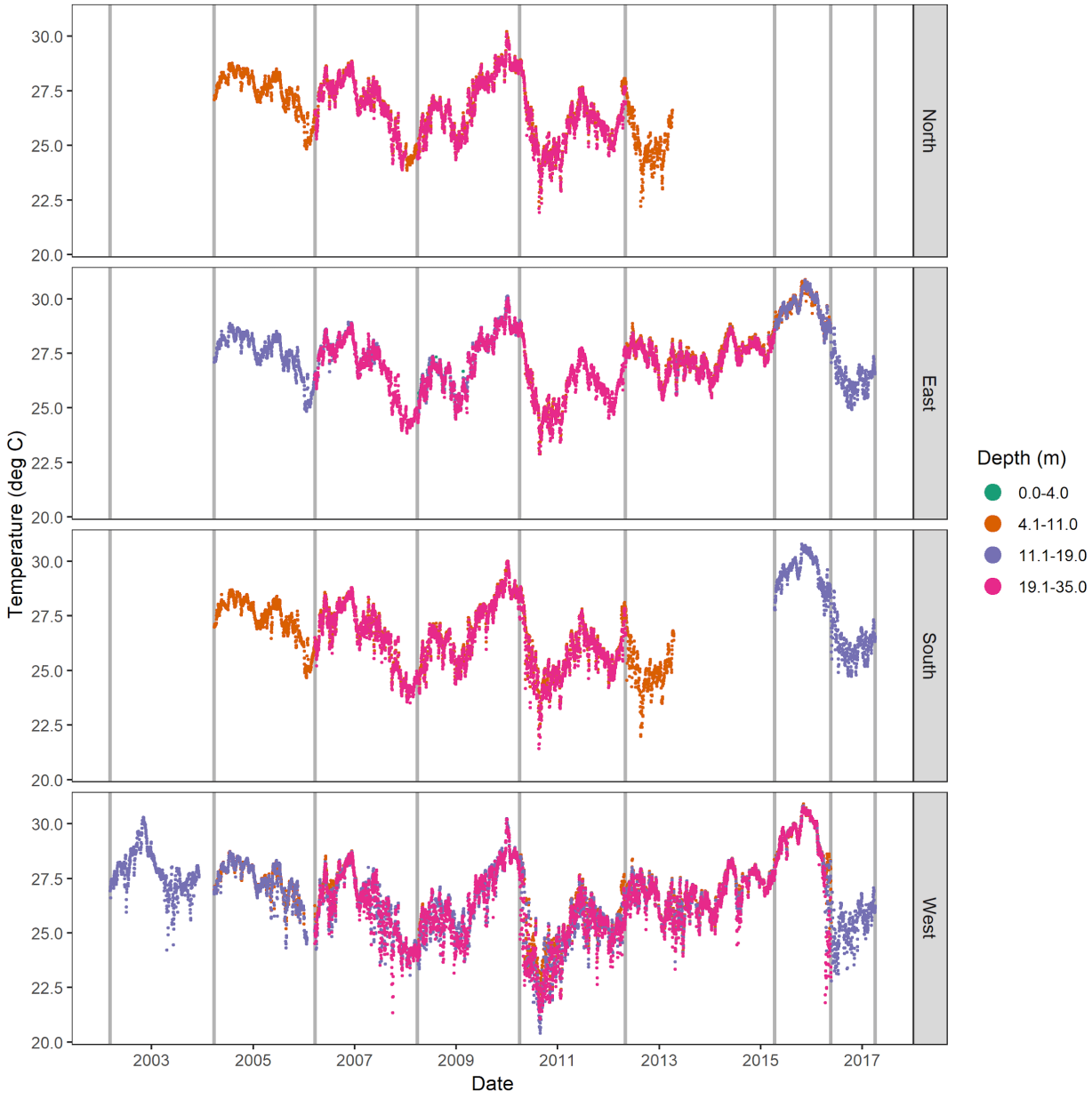

Figure 18. Daily subsurface temperature recorder time-series observations of temperature over the period between 2004 and 2017, collected around Jarvis Island (North, South, West, and East). Four different depth ranges were defined at each of these locations: green (0–4.0 m), red (4.1–11.0 m), blue (11.1–19.0 m), and magenta (19.1–35.0 m). Vertical bars show the dates of field data collection.

Wave Energy

Ocean wave dynamics strongly influence the environmental conditions of coastal habitats. The energy generated by ocean waves varies on seasonal and interannual time scales, and spatial differences in the direction, magnitude, and frequency of waves around an island or atoll can have significant impacts on the sub-island distribution of coral reef communities. Hourly data from 2010 to 2016 are shown in Figure 19 and Figure 20. The North and West georegions of

Jarvis Island experienced more waves that had a longer period (the length of time between crests) and height (the distance from trough to crest) from December through February (Figure 19, left panels). The South and East georegions were exposed to more waves with both a higher period and height in July through September (Figure 19, right panels). The mean annual integrated wave power was greatest in the East georegion of Jarvis, likely reflecting the influence of strong and steady easterly trade wind swells that affect the coral reefs in the East Terrace georegion (Figure 20).

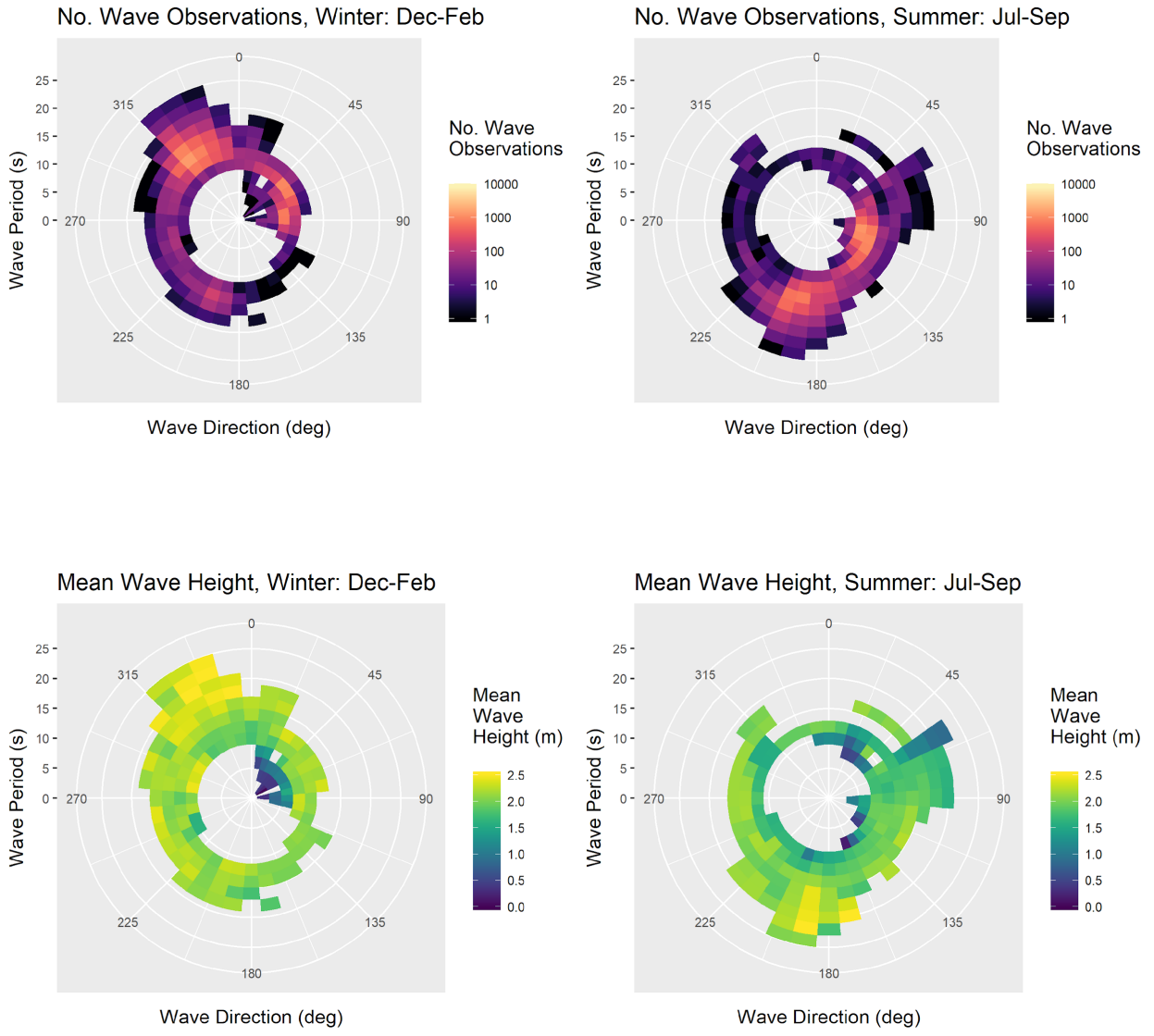

Figure 19. WaveWatch III data from 2010–2016 for the region around Jarvis Island. Top panels: Polar plot of hourly wave data from December–February (left panel) and July–September (right panel). Bottom panels: Polar plot of derived mean wave height between December–February (left panel), and between July–September (right panel). The position of wave data around the 360 degree circle (in 10-degree bins) displays the direction from which the waves hitting Jarvis travel, where 0 degrees indicates that waves arrive from due north and 180 degrees from due south. The height of directional bin radiating from the center is a histogram of wave period (greater distances from center represent longer wave periods), and the shading shows the number of hourly observations (top) and mean wave height (bottom) for each direction and period.

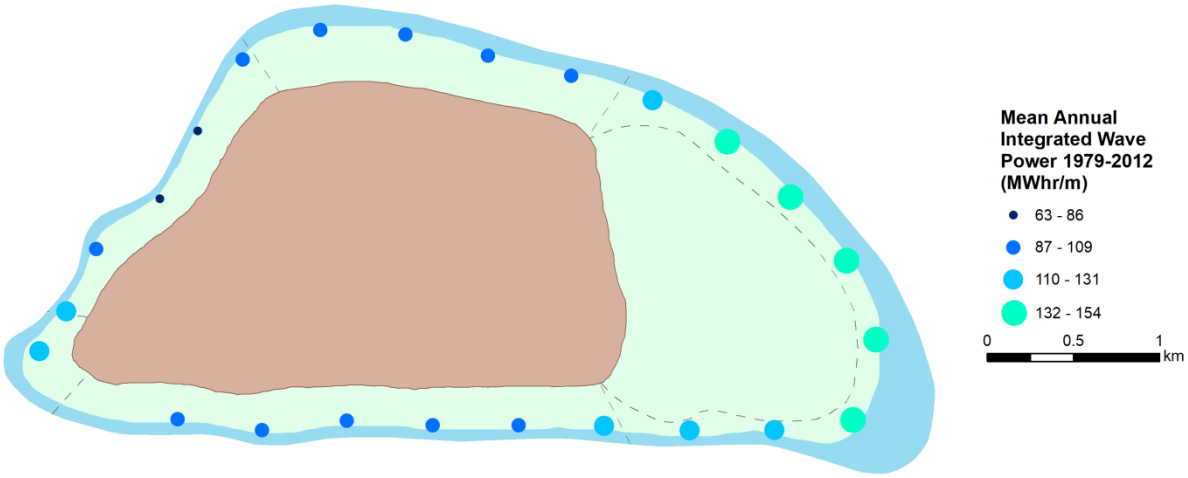

Figure 20. Mean annual integrated wave power (MWhr/m) at Jarvis Island. Data from 1979 to 2012 correspond to modified WaveWatch III by coastline shadowing using the incident wave swath method (Clark and Oliver, In prep).

Carbonate chemistry

Aragonite saturation state (Ω_A) is a measure of the degree to which seawater is saturated with respect to the carbonate mineral aragonite, where Ω_A values above 1 indicate supersaturated conditions. Ω_A is often used as a more biologically-relevant alternative to pH because it reflects the availability of the carbonate ion (CO_3^{2-}) building blocks which calcifying organisms need in order to construct their calcium carbonate ($CaCO_3$) shells and skeletons. Greater values of Ω_A correspond to higher CO_3^{2-} concentrations and thus favor the growth of corals, CCA, and other reef calcifiers. However, under the process of ocean acidification, with increased dissolution of carbon dioxide in seawater, the seawater pH, Ω_A, and concentrations of CO_3^{2-} all decrease. This makes it more difficult for corals and calcifying reef organisms to grow.

Due to the effects of upwelling, Ω_A values at Jarvis Island are relatively low, especially on the western side of the island, which experiences both topographic and equatorial upwelling. There is also strong interannual variability in Ω_A related to ENSO (Figure 21). The highest Ω_A values were measured during El Niño in 2010, driven by decreased equatorial and topographic upwelling that brings deep, lower-Ω_A water to the surface and possibly also driven by coral bleaching, which decreases the biological drawdown of Ω_A present on a healthy reef, causing Ω_A to rise. Ω_A decreased during more ENSO-neutral periods in 2012 and 2015 (2015 data were collected prior to the onset of warming late in the year), and the lowest Ω_A values were observed in 2016 once El Niño conditions had subsided and upwelling resumed. Ω_A and pH values for the reef waters around Jarvis have been consistently at or below the median of values observed by ESD across the U.S. Pacific Island region since 2010 (Figure 22).

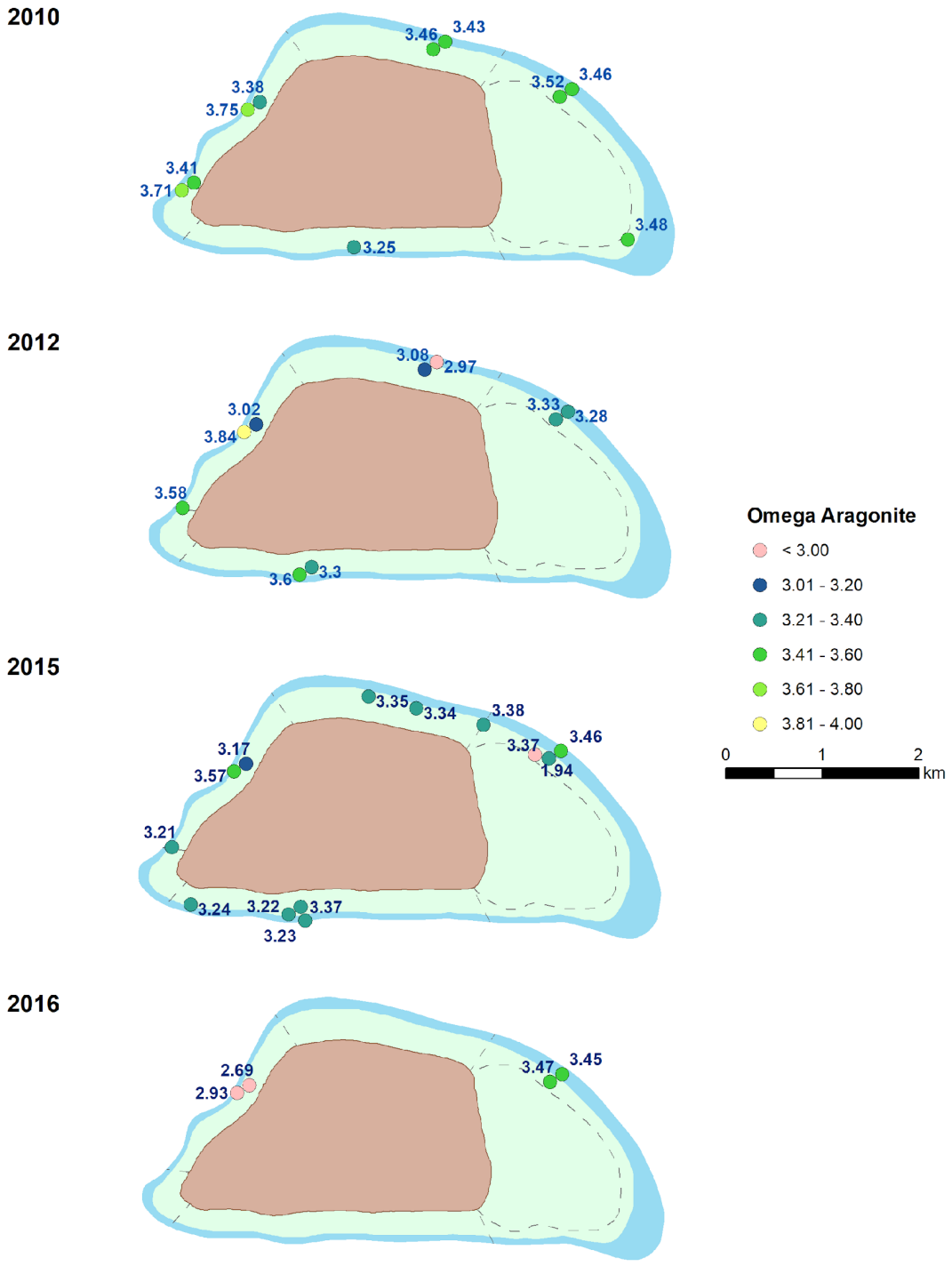

Figure 21. Spatial distribution of aragonite saturation state (Ω_A) from observations made in 2010, 2012, 2015, and 2016 around Jarvis Island.

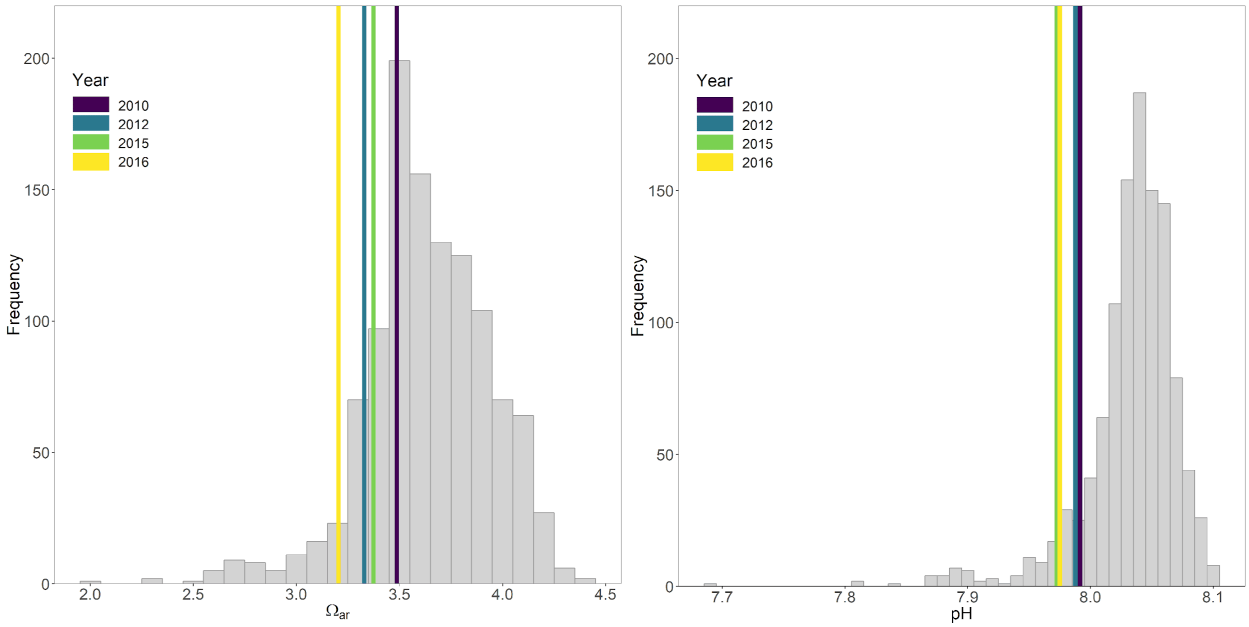

Figure 22. Histogram of all aragonite saturation state (Ω_A; left panel) and pH (right panel) values measured from discrete seawater samples across the U.S. Pacific Islands region from 2010 to 2017 (gray). The medians of Jarvis data in 2010 (purple), 2012 (blue), 2015 (green), and 2016 (yellow) are denoted as overlaid vertical bars.

Diel Variation

The spatial and temporal patterns in carbonate chemistry observed on a coral reef are a direct result of the dynamic interplay between nearshore environmental conditions and biological processes occurring both day and night. Abiotic factors (e.g., variation in light levels, transport of water across the reef with waves, tides, currents, and oceanographic activities, such as upwelling and internal wave action) interact with and influence the rate of metabolic processes (e.g., photosynthesis, respiration, calcification, and dissolution) and together alter the chemistry of the seawater that interacts with the benthic communities. Some of the most dramatic changes in reef chemistry occur over the diel cycle as the result of day-to-night changes in the reef environment and shifts in biological activity. Recently, the opportunistic collection of 24-hour data through remotely deployed instrumentation has allowed us to contextualize our traditional discrete water sampling (which occurs only during daylight) with measured ranges of diel variation. These combined data sets allow for the inference of metabolic processes affecting the coral reef ecosystem.

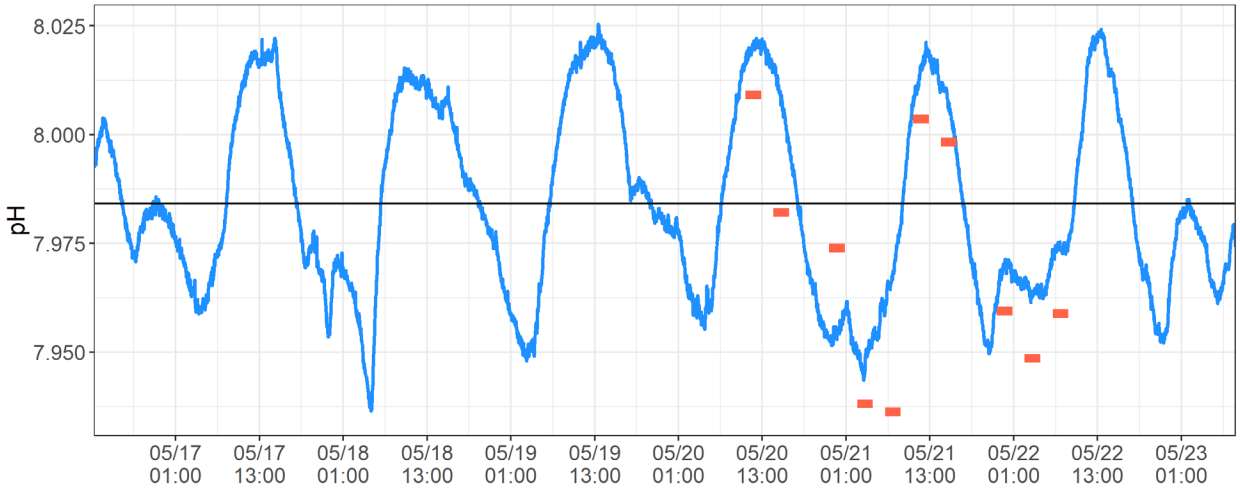

Figure 23. Diel variability in pH over the period May 17–23, 2015. Red points represent pH observations from discrete water samples collected every 4 hours using portable underwater collectors. The blue line represents a continuous observation of pH collected using an ocean pH sensor, and the black line shows the mean of the continuous pH measurements.

Temporal changes in seawater pH, driven by variability in reef metabolic processes, were measured using a continuously monitoring pH sensor and discrete seawater pH samples collected every 4 hours by portable underwater collectors (PUCs) over the period May 17–23, 2015, in the East Terrace georegion of Jarvis Island (Figure 15). Discrete carbonate chemistry samples generally produce more reliable estimates of pH than those measured by instruments, and data from water samples can be used to calculate other carbonate parameters that paint a more complete picture of the nearshore environment and coral reef health (e.g., Ω_A, pCO_2). However, instruments are able to sample much more frequently than discrete samplers. Therefore, discrete PUC samples can be used to calibrate the continuous time series captured by a pH sensor and calculate the full carbonate system chemistry. Values of pH from the continuous instrument time series and those calculated from discrete PUC water samples captured the same overall patterns in the diel cycle. However, the instrument time series consistently overestimated pH relative to discrete samples.

The diel pH time series shows that photosynthesis was the dominant process occurring during daylight hours, raising pH by removing CO_2 from the seawater. Respiration dominated at night and into the early morning, leading to a temporary decrease in pH as CO_2 was added back into the water.

Net Carbonate Accretion

Calcification accretion units (CAUs) are simple, two-plate fouling structures that are staked to the reef substrate for 2-3 years and then analyzed for the total weight of $CaCO_3$ accreted by the calcareous organisms that recruit to the plates (largely, CCA and hard corals). CAUs provide a proxy for the net rate of $CaCO_3$ accretion that results from the competing processes of carbonate precipitation by calcifying organisms and the removal of material by physical (e.g., strong waves) and/or biological (e.g., parrotfish, burrowing bivalves) erosion. $CaCO_3$ accretion is essential for reefs because it builds the structural framework for coral reef ecosystems and

provides essential habitat for reef organisms. However, accretion rates are strongly influenced by dynamic nearshore environmental conditions. In particular, calcification rates of corals and CCA are sensitive to changes in carbonate chemistry and decrease with decreasing pH and Ω_A (Pandolfi et al. 2011). Refer to the Overview chapter for CAU-design specifics and deployment methodologies.

CAUs were deployed from 2010 to 2012, and from 2012 to 2015, around Jarvis Island to assess spatial and temporal variability in accretion (75 CAUs deployed, 36 recovered). Significant spatial differences in carbonate accretion rates were observed during the 2012–2015 deployment (samples were only collected from one site for the 2010–2012 deployment). Higher accretion rates typically occurred in the West and East georegions (Figure 24) where higher nutrient concentrations (west) or higher Ω_A levels and wave energy (east) favor calcification (Figure 21). Compared to the rest of the Pacific, accretion rates at Jarvis were higher than most surveyed sites (Figure 25). Because pH and Ω_A are relatively low at Jarvis, it is likely that high accretion rates observed are driven primarily by high nutrient concentrations and primary productivity, as well as other environmental variables.

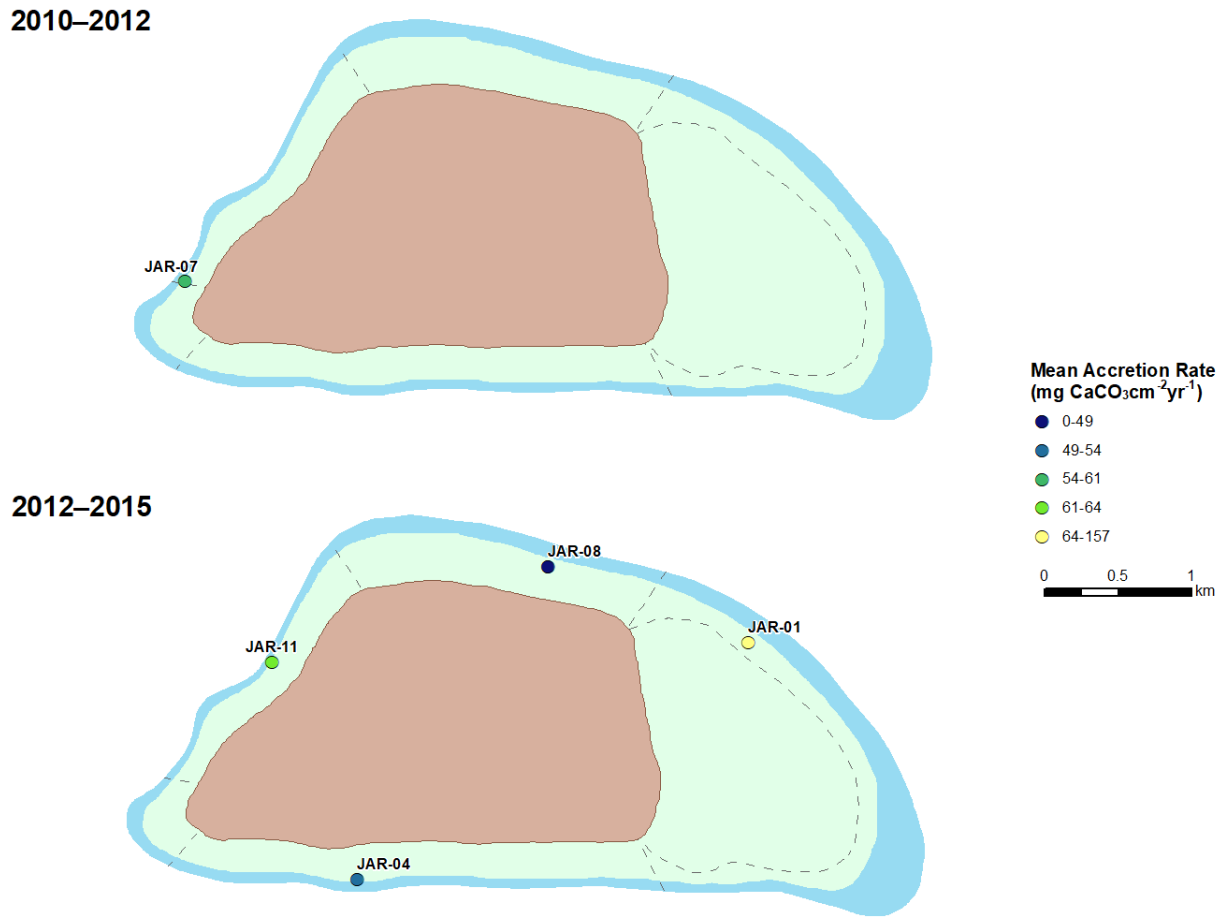

Figure 24. Spatial distribution of mean carbonate accretion rate (mg $CaCO_3$ cm^{-2} yr^{-1}) at Jarvis Island during 2010–2012 (top map) and 2012–2015 (bottom map). The calcification accretion unit sites are shown by location code of JAR and the site number.

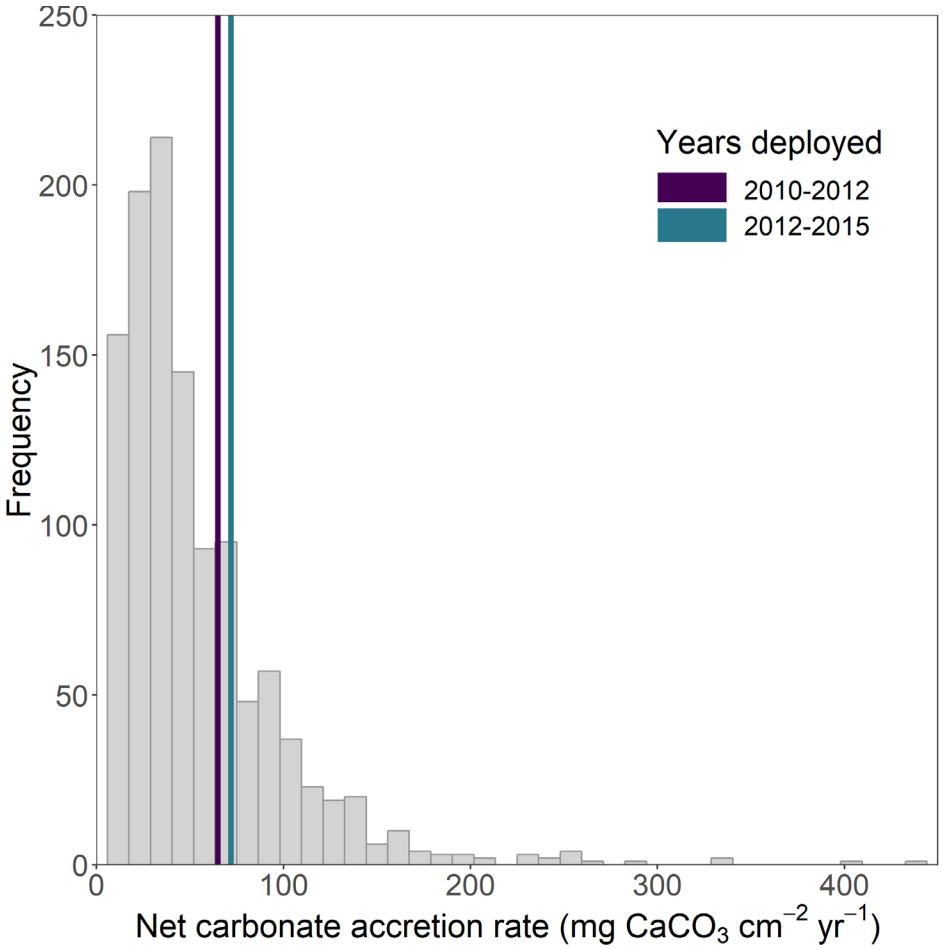

Figure 25. Histogram of all net carbonate accretion rates (m $CaCO_3$ cm^{-2} yr^{-1}) measured by all calcification accretion units during the period 2010–2017 across the U.S. Pacific Islands region (gray), and median values for 2010–2012 (purple) and 2012–2015 (blue) samples for Jarvis Island.

Benthic diver at Jarvis Island, April 2017. Photo: Kevin Lino, NOAA Fisheries.

4.4 Coral Reef Benthic Communities

NOAA divers conducting benthic surveys at Jarvis Island.
Photo: Hatsue Bailey, NOAA Fisheries.

Survey Effort and Site Information

Data to characterize benthic habitats and the coral populations around Jarvis Island were collected using Rapid Ecological Assessment (REA) surveys and towed-diver surveys (TDS) during ten survey efforts conducted between 2001 and 2017 (Table 3). REA surveys at Jarvis were primarily performed at repeat sites at mid-depth (>6–18 m) until 2015, when a stratified-random sampling (StRS) survey design was adopted to generate more statistically-robust island-scale estimates of coral reef benthic communities. The use of a StRS study design allowed for an increased number of survey sites across multiple depth strata (shallow: >0–6 m; mid: >6–18 m; and deep: >18–30 m). The stratified-random sites were more widely and evenly distributed around the island than the former repeat sites (Figure 26). Benthic REA surveys implemented the line-point-intercept (LPI) method from 2006 through 2012 and the photoquadrat method from 2015 through 2017, to estimate percent cover of benthic communities. Photoquadrat surveys

were also conducted at fish REA sites in 2015, yielding a significantly greater sample size to determine benthic cover. The belt-transect (BLT) method was used from 2004 through 2015 to estimate the abundance, distribution, condition, and diversity of the coral populations (with progressive updates to the methods detailed in the Overview chapter). Benthic TDS were conducted primarily around the island perimeter at predominantly mid-depth forereef habitats to estimate the percent cover of benthic functional groups, the density of ecologically- or economically-important macroinvertebrates, and occurrences of potentially significant ecological events, such as widespread bleaching, outbreaks of disease, and abundance of invasive or nuisance species.

Opportunistic benthic surveys between the normal Pacific RAMP survey years (2015 and 2018) were conducted in 2016 and 2017, specifically to monitor the aftermath of the extreme 2015–2016 El Niño-induced coral bleaching event (Brainard et al. 2018).

Table 3. **The total number of Rapid Ecological Assessment (REA) survey sites and towed-diver survey (TDS) segments completed by year and strata (if applicable) at Jarvis Island. Numbers in parentheses (bold) indicate the number of surveys conducted at mid-depths (>6–18 m). *Note: In 2015, REA survey methodology changed from repeat sites to stratified-random sampling (StRS). StRS sites were located across three depth strata: shallow (S), mid (M), and deep (D).**

Year	TDS	REA	
		Coral Populations	Benthic Communities
2001	39 (**38**)	–	–
2002	40 (**40**)	–	–
2004	98 (**82**)	6	–
2006	110 (**94**)	9	10 (**9**)
2008	154 (**112**)	9	10 (**9**)
2010	117 (**88**)	10	10 (**9**)
2012	92 (**89**)	10	10 (**9**)
2015*	60 (**56**)	14 (S) 21 (M) 6 (D)	32 (S) 52 (M) 19 (D)
2016*	–	9 (S) 17 (M) 4 (D)	19 (S) 32 (M) 9 (D)
2017*	60 (**56**)	11 (S) 12 (M) 9 (D)	22 (S) 25(M) 13 (D)

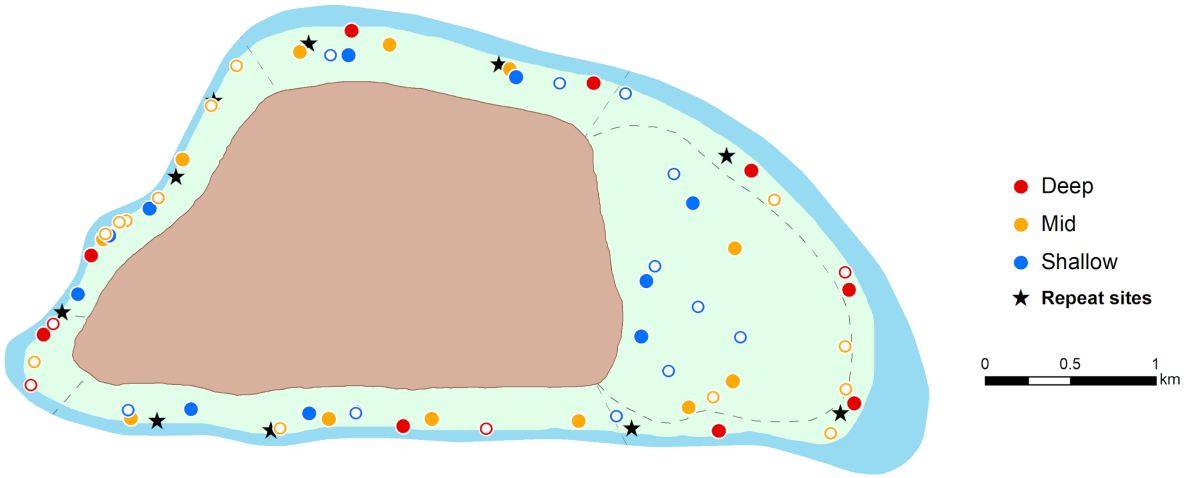

Figure 26. Jarvis Island benthic Rapid Ecological Assessment surveys locations. Repeat sites (stars) were sampled from 2004 through 2012 and stratified-random sampling (StRS) sites were sampled in 2015 and 2017 (blue, yellow, and red circles for shallow [>0–6 m], mid [>6–18 m], and deep [>18–30 m] depth strata). Photoquadrats for assessing benthic communities were collected at all StRS sites (open circle with white fill and solid circles). Coral population surveys were only conducted at sites indicated by solid circles.

Recent State of Benthic Cover

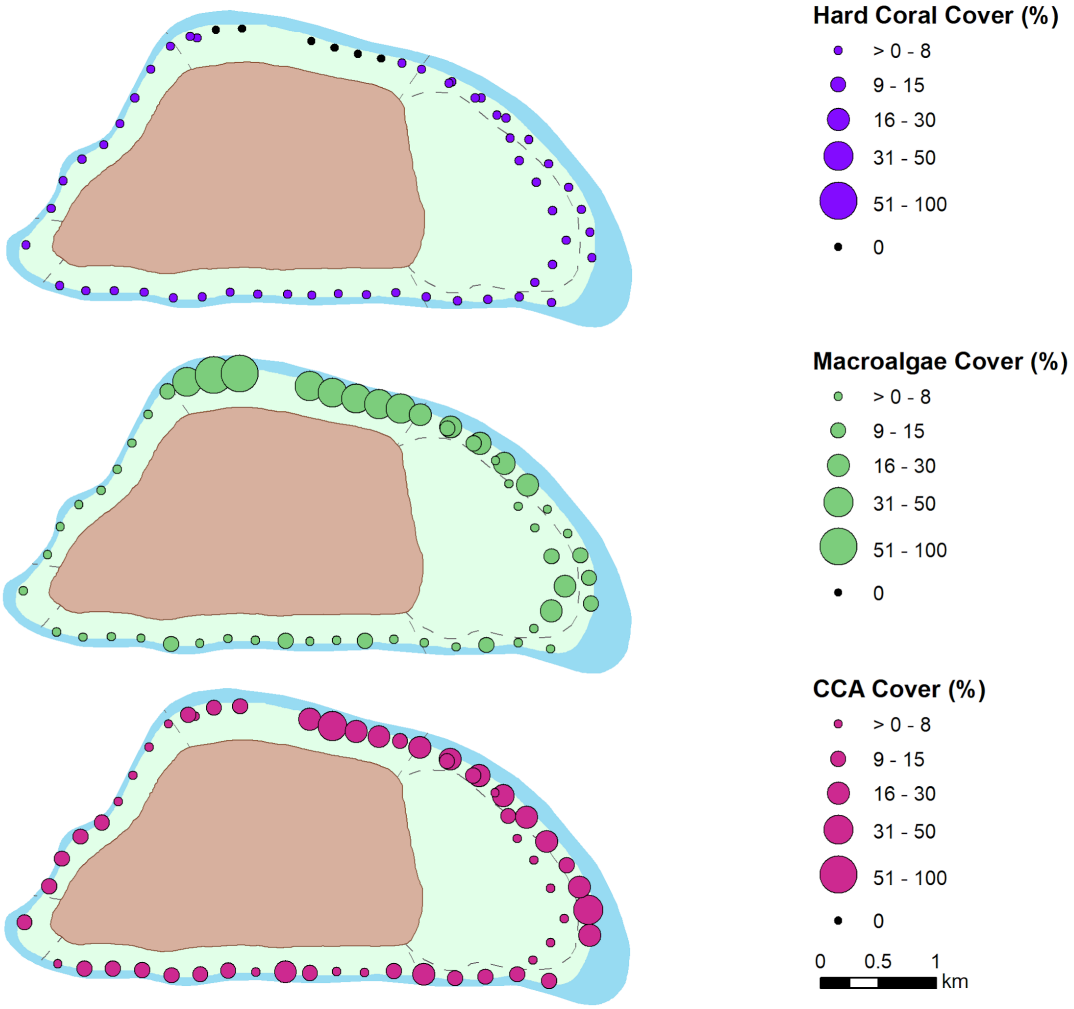

Figure 27. Visual estimates and spatial distribution of mid-depth (>6–18 m) hard coral, macroalgae, and crustose coralline algae (CCA) cover (%) at Jarvis Island from towed-diver surveys in 2017.

As a result of the persistent and anomalously high seawater temperatures during the extreme 2015–2016 El Niño event, the benthic community observed during TDS in 2017 at Jarvis Island was depauperate in hard coral cover (mean = 0.7% ± 0.2 SE) (Figure 27), with no evident signs of recovery post-bleaching. Of the 56 mid-depth segments surveyed, 44 (78%) had hard coral cover ranging between 0% and 1%, and 6 (10%) ranging between 1% and 5%. Presence of macroalgae was variable around the island; 52% of survey segments had macroalgae cover ranging between 0.5% and 7.5%, while the remaining 48% had macroalgal cover ranging between 15% and 35%. Macroalgal cover presented the highest levels along north and northeast facing forereef habitats, with lower macroalgal cover in the South and West georegions. Concomitantly, CCA cover was high as well as variable; values ranged from 2.5% to 35%, with over 70% of segments having CCA cover greater than 15%. Locations where CCA cover was low (0.5% to 7.5%) occurred intermittently around the island, along the Eastern Terrace, the West georegion, as well as discrete portions on the South georegion.

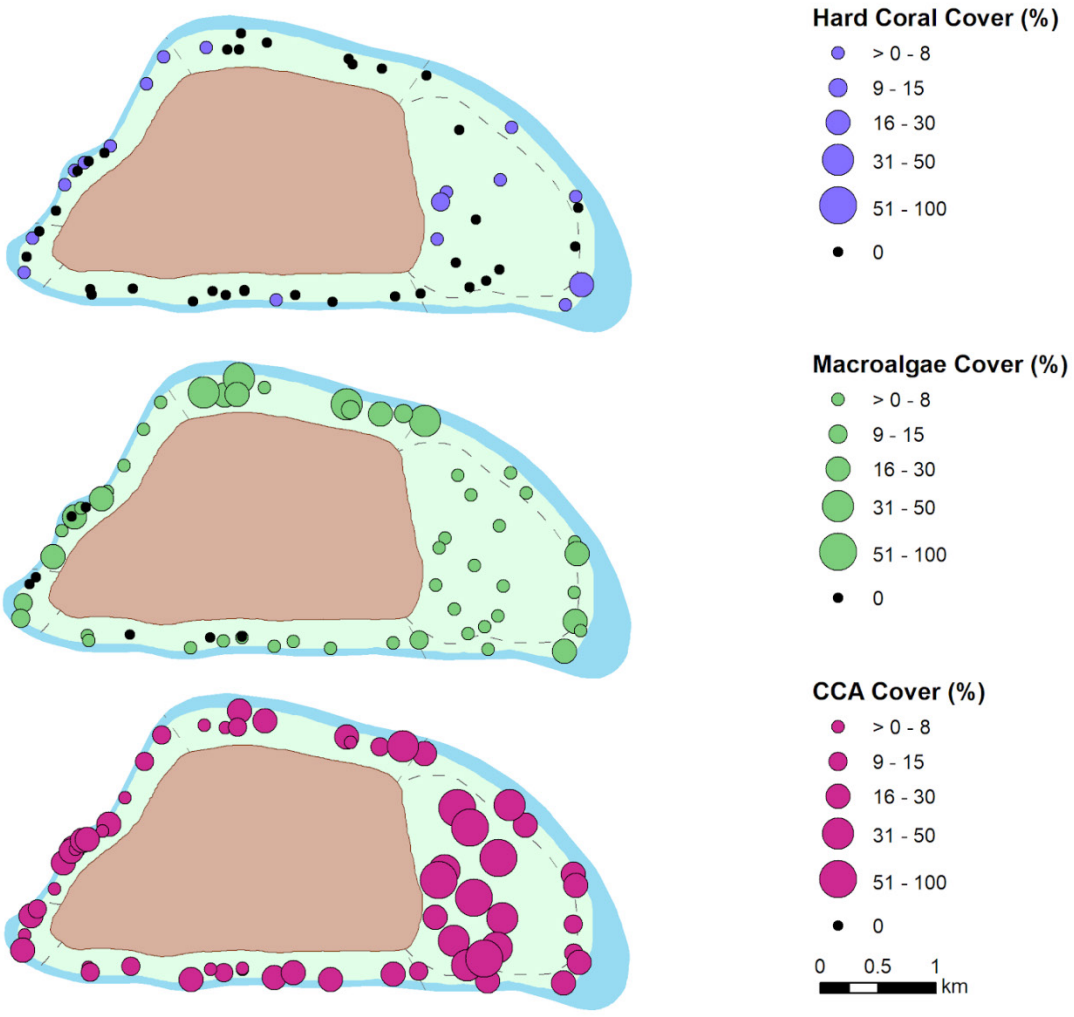

Figure 28. Site level estimates of hard coral, fleshy macroalgae (excluding calcified and encrusting macroalgae), and crustose coralline algae (CCA) cover (%) at Jarvis Island from stratified-random sampling photoquadrat surveys conducted at all depth strata combined (>0–30 m) in 2017.

Benthic cover estimates from StRS photoquadrat surveys in 2017, one year post-bleaching, show comparable spatial patterns to the TDS, whereby hard coral cover remained conspicuously low, followed by spatially variable macroalgal cover, and high but variable cover of CCA (Figure 28). Hard coral was present only in 45% of the StRS sites surveyed in 2017, and ranged from less than 0.3% to 15.7%, but only approximately 20% of sites exhibited hard coral cover greater than 1%. The highest coral cover (15.7%) was reported at a deep site off the Eastern Terrace. Fleshy macroalgal cover (excluding calcified and encrusting macroalgae) was largely variable around the island, with values ranging from 0.3% to 48%. Of the 60 sites surveyed, 71% had macroalgal cover ranging between 0.3% and 15%, and 23% had macroalgal cover greater than 15%. Similar to reports from the TDS, sites with higher macroalgal cover were located in the North and East georegions. CCA cover ranged between 1% and 73% and was reported present at all survey sites. Over 70% of the sites exhibited CCA cover greater than 10%, with the highest levels (>30%)

consistently recorded throughout the Eastern Terrace. Lower benthic CCA cover (<5%) was observed at 13% of sites found mainly in the South and West georegions.

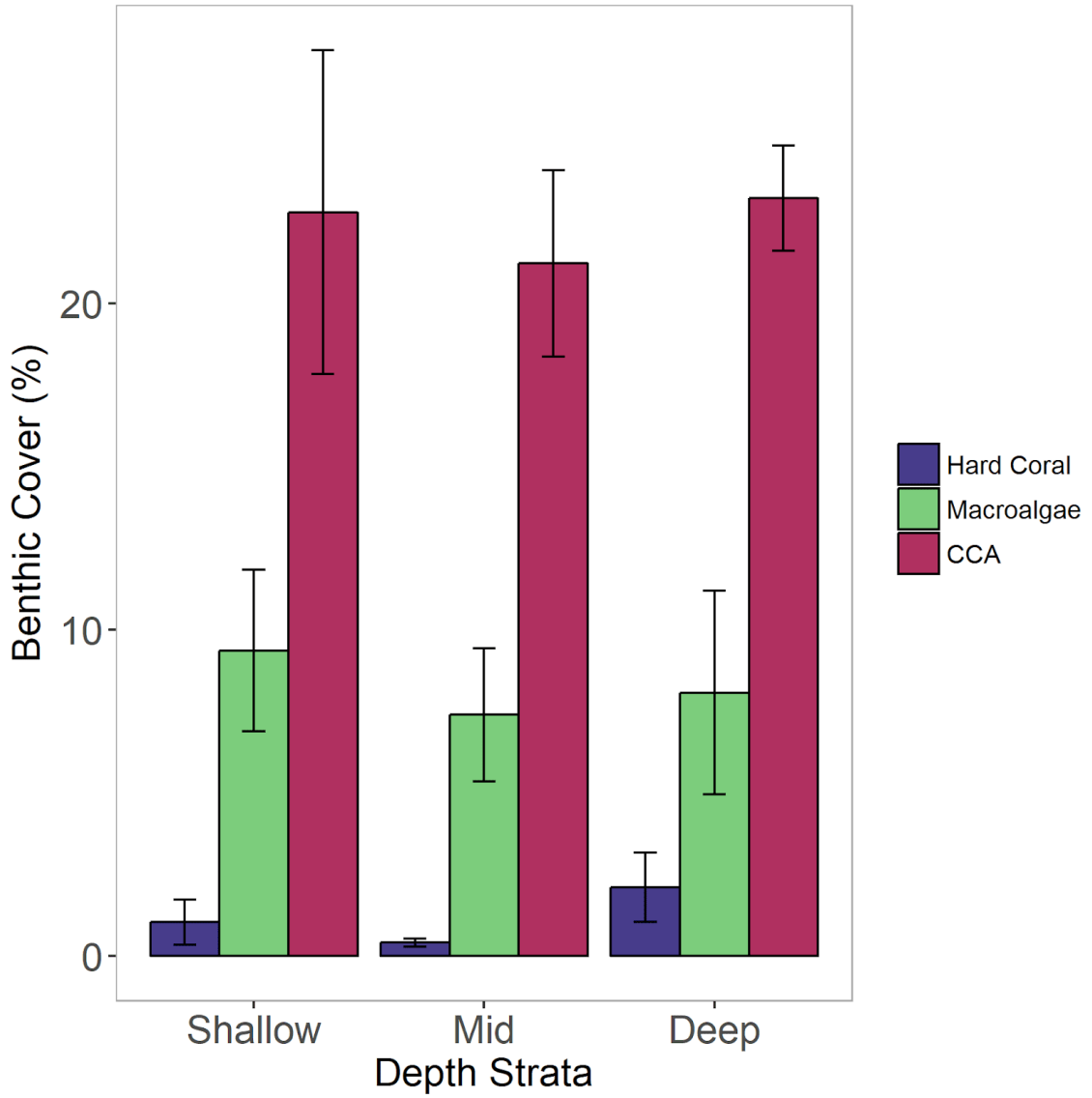

Figure 29. Strata-level mean benthic cover (±1 SE) at Jarvis Island by benthic functional groups of hard coral, fleshy macroalgae (excluding calcified and encrusting macroalgae), and crustose coralline algae (CCA) for shallow (>0–6 m), mid (>6–18 m), and deep (>18–30 m) depth strata from stratified-random sampling photoquadrat surveys conducted in 2017.

The 2017 photoquadrat surveys at Jarvis indicted that of the three main functional groups studied, CCA was the dominant group throughout all depth strata (Figure 29). Mean hard coral cover was the lowest and ranged between 0.4% and 2.1%, with no significant signs of recovery following the extreme 2015–2016 El Niño warming event and the associated mass coral bleaching and mortality observed in 2016 (Brainard et al. 2018). Coral cover at Jarvis was the lowest among the other PRIMNM islands (i.e., Howland, Baker, and Wake) surveyed during 2016 and 2017 StRS surveys in the wake of the El Niño. Comparatively, mean macroalgal cover

was higher and similar among depth strata. Values ranged between 7% and 9%, with marginally higher levels recorded in the shallow and deep strata. Mean CCA cover was high and comparable across strata (~21% to 23%) as well; it consistently amounted to at least ten-fold the cover of hard corals and at least twice the cover of macroalgae at all depths.

Time Series of Benthic Cover

Figure 30 illustrates the island-scale time series of mean benthic cover at mid depths (>6–18 m) for the period between 2001 and 2017 using REA and TDS methods. Both methods suggest that hard coral cover remained moderately high (20% to 25%) and stable throughout the period 2001–2012. In 2015–2016, corals at Jarvis Island experienced mass bleaching and catastrophic mortality, reflected in the greater than 95% drop in hard coral cover between those survey years. Subsequent surveys in 2017 found little to no recovery thus far, regardless of sampling methods (Figure 31).

The transition from LPI at repeat sites to photoquadrats at stratified-random sites in 2015 is marked by an approximately 30% decrease in hard coral cover. This drop is likely attributable to differences in survey designs and sampling methods as this decline was not observed in the TDS data. Surveys using the stratified-random approach starting in 2015 have been conducted at more sites across a range of habitats, whereas the repeat sites method purposefully targeted mid-depth (>6–18 m) sites.

Cover of macroalgae and CCA were variable and dynamic over time. The TDS baseline recorded a reduction in macroalgal cover from approximately 26% to approximately 11% (>50%) between survey years 2001 and 2002, followed by a sustained increase to 41.4% in 2006. This TDS estimate was noticeably higher than the amount of macroalgae recorded during the LPI surveys (25.4%). High macroalgae values were likely due the inclusion of turf algae in TDS estimates of "macroalgae" from 2004 to 2006, in addition to a bloom of the macroalgae *Rhodymenia* that was reported in 2006, mainly affecting sites in the North and South georegions. Both the TDS and the photoquadrat method registered an increase in macroalgal cover following the 2015 mass coral bleaching and mortality event.

Although patterns of CCA cover were variable over time, the REA and TDS methods showed some comparable trends between survey years. The lowest levels were registered in 2008, followed by an increase and stabilizing over the 2010–2015 period, a reduction from 2015 to 2016, and an increase from 2016 to 2017 in the aftermath of the 2015–2016 El Niño-induced bleaching event.

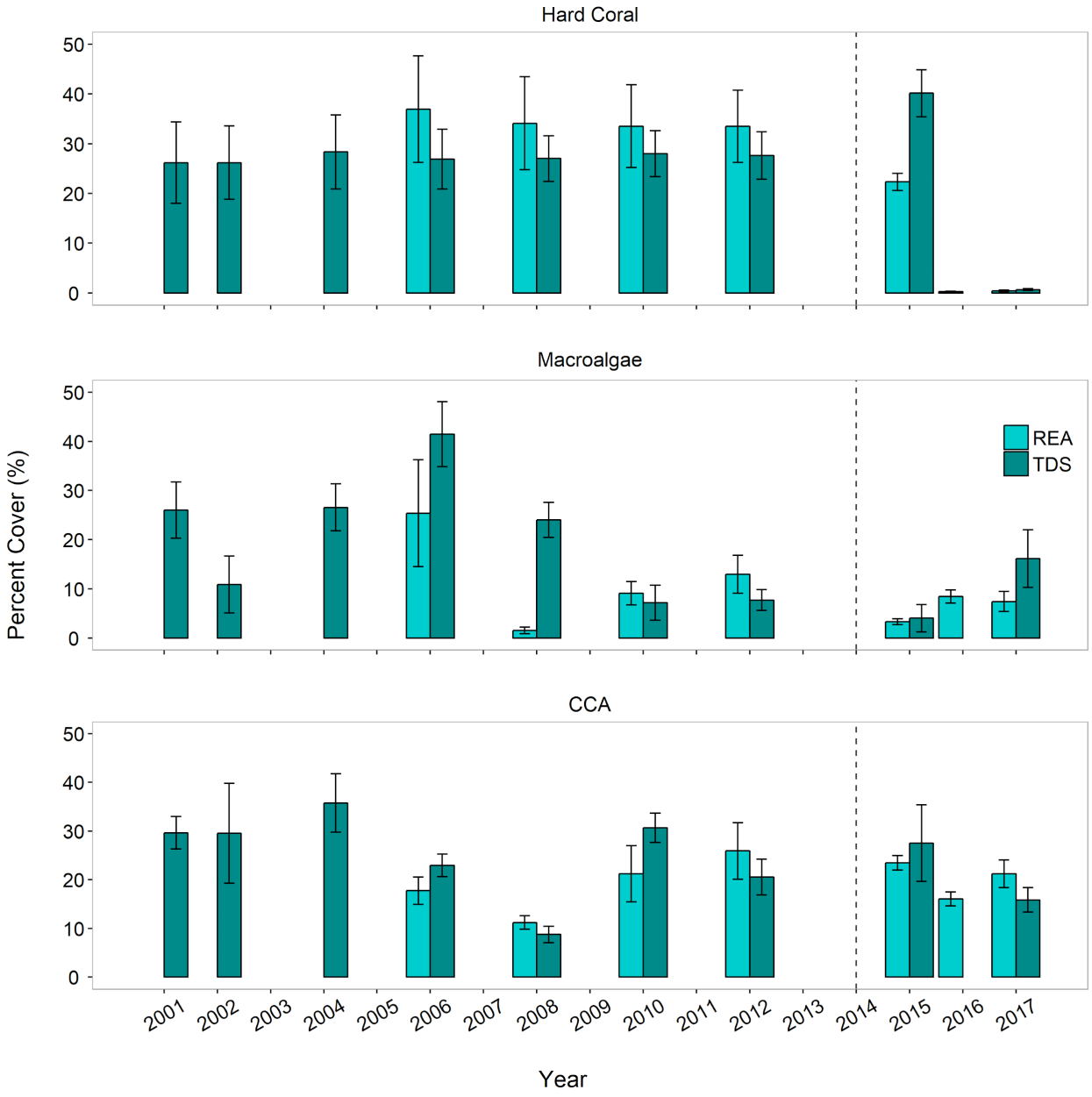

Figure 30. Time series of mean (± 1 SE) hard coral, macroalgae, and crustose coralline algae (CCA) cover (%) at Jarvis Island by survey method (rapid ecological assessment [REA] and towed-diver survey [TDS]) conducted at the mid-depth stratum (>6–18 m) from 2001 through 2017. In 2014 (dashed line), REA survey methodology changed from line-point-intercept at repeat sites to photoquadrat surveys at stratified-random sampling. *Note: TDS macroalgae data include calcified and encrusting macroalgae; the REA macroalgae data exclude it.

To examine temporal trends in coral cover, survey data were averaged across all survey years (2001–2017) and methods. Long-term mean coral cover was highest in the West, Southwest, and South georegions of Jarvis (Figure 31a). Coral cover remained relatively stable in all regions over the period from 2001 through 2015, with slight temporal increases in coral cover along the East and North georegions (Figure 31b). All georegions showed a catastrophic decline in coral cover between the Pacific RAMP surveys in April 2015, just prior to the onset of the extreme

2015–2016 El Niño, and May 2016, just following the return to normal sea surface temperatures (Brainard et al. 2018). Accordingly, the decadal rates of change in coral cover (Figure 31c) were greatest in the georegions that had higher coral cover (i.e., West, South, Southwest) prior to that extreme El Niño event, as well as portions of the East Terrace. The North and East georegions had relatively smaller decadal rates of change in coral cover as they simply had less coral to lose. No indication of recovery in 2017 cover estimates can be seen for any region surveyed.

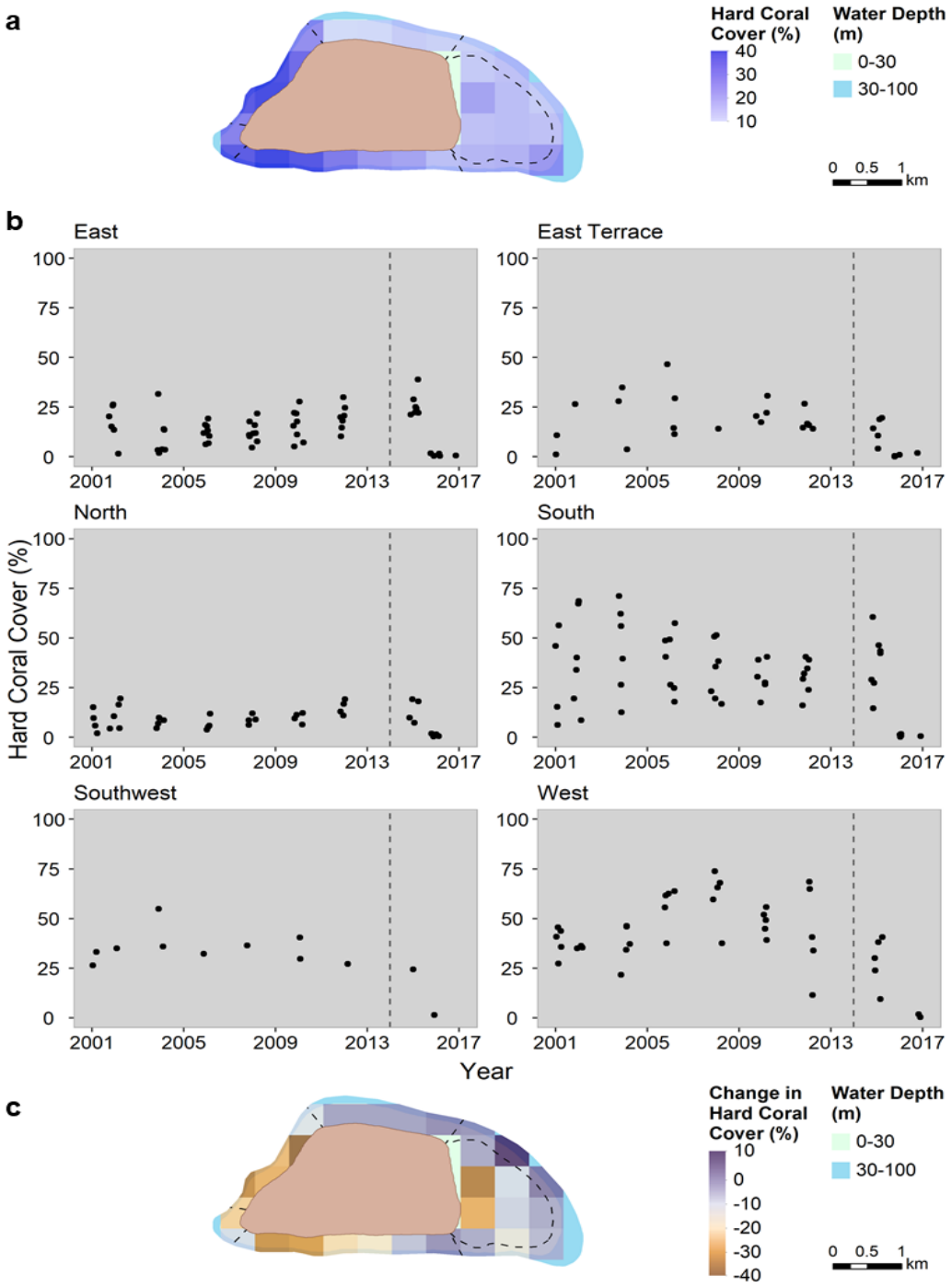

Figure 31. Spatial patterns and temporal trends of gridded (500 × 500 m) mean coral cover at Jarvis Island across survey years (2005–2017) and methods (towed-diver survey, line-point-intercept (LPI), and stratified-random sampling [StRS] benthic and fish photoquadrats). (a) Mean hard coral cover per 500 by 500 m grid cell across all survey years; (b) time series of hard coral cover by georegion; and (c) temporal change in hard coral cover per 500 by 500 m grid cell, only including cells with at least a 10-year span of data and at least 3 observation years. In 2014 (dashed line), Rapid Ecological Assessment survey methodology changed from LPI at repeat sites to photoquadrat surveys at StRS sites. See Survey Methods for Coral Reef Benthic Communities in the Overview chapter for further details.

Time Series of Algal Disease

CCA disease occurrence index is the proportion of the number of disease cases relative to the CCA cover. Values close to or greater than one suggest high disease occurrence; comparatively, numbers close to zero indicate low occurrence. At Jarvis Island, CCA disease occurrence was low and variable over time, with only three types of disease cases registered in three of the seven survey years (Figure 32). In 2006, CCA diseases at Jarvis were conspicuously absent, contrasting with reports of notably high levels of CCA disease at Palmyra, Kingman, and American Samoa during the same survey year (Vargas-Ángel 2010). The coralline fungal disease was observed only in 2008, while the coralline white-band and ring syndromes were detected both in 2012 and in 2015. Overall, however, CCA disease occurrence at Jarvis was markedly low compared to other islands in the PRIMNM during the same period.

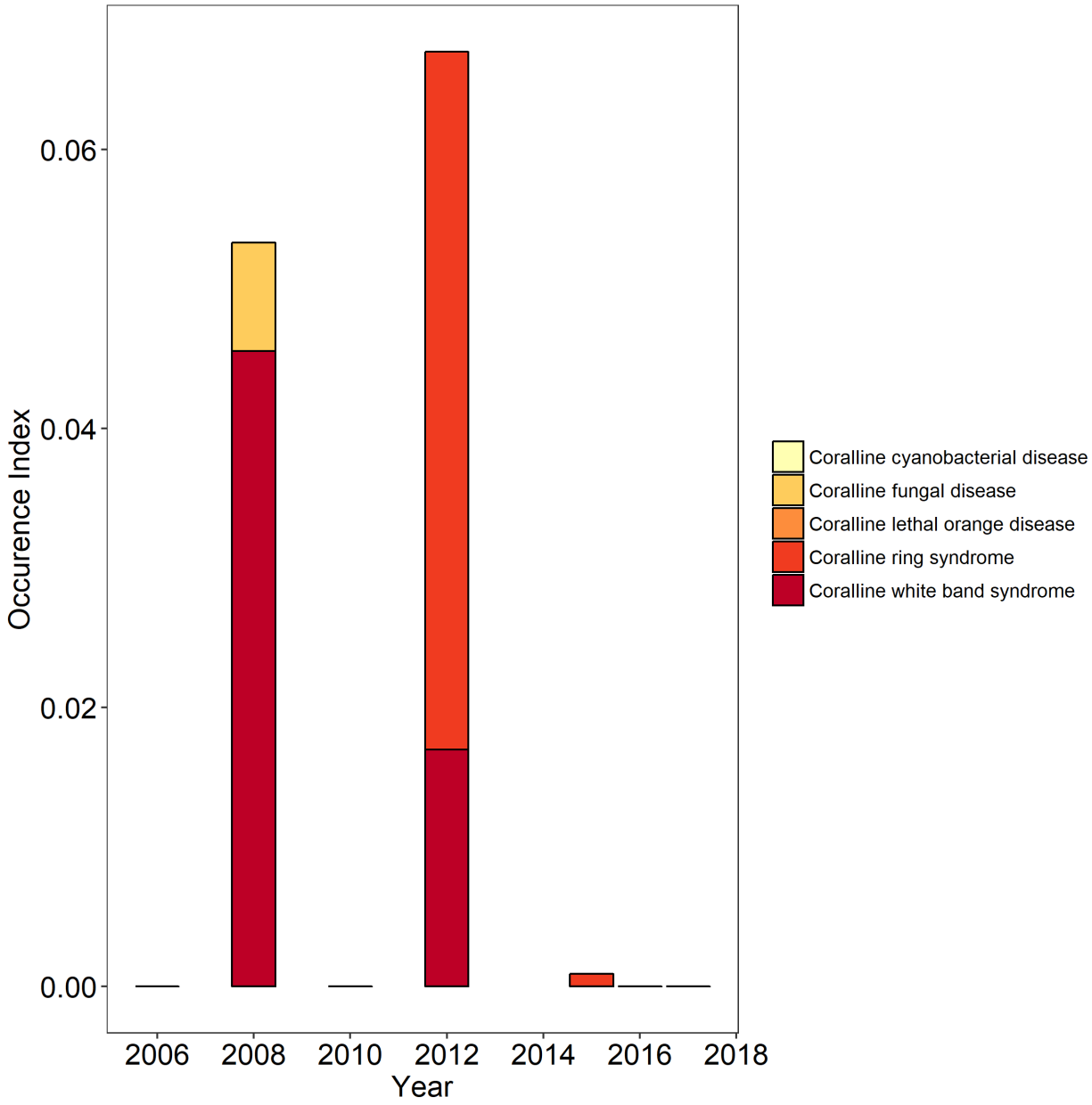

Figure 32. Time series of crustose coralline algae disease occurrences at Jarvis Island for all depth strata combined (>0–30 m) from Rapid Ecological Assessment surveys conducted from 2006 through 2017.

Recent Coral Abundance

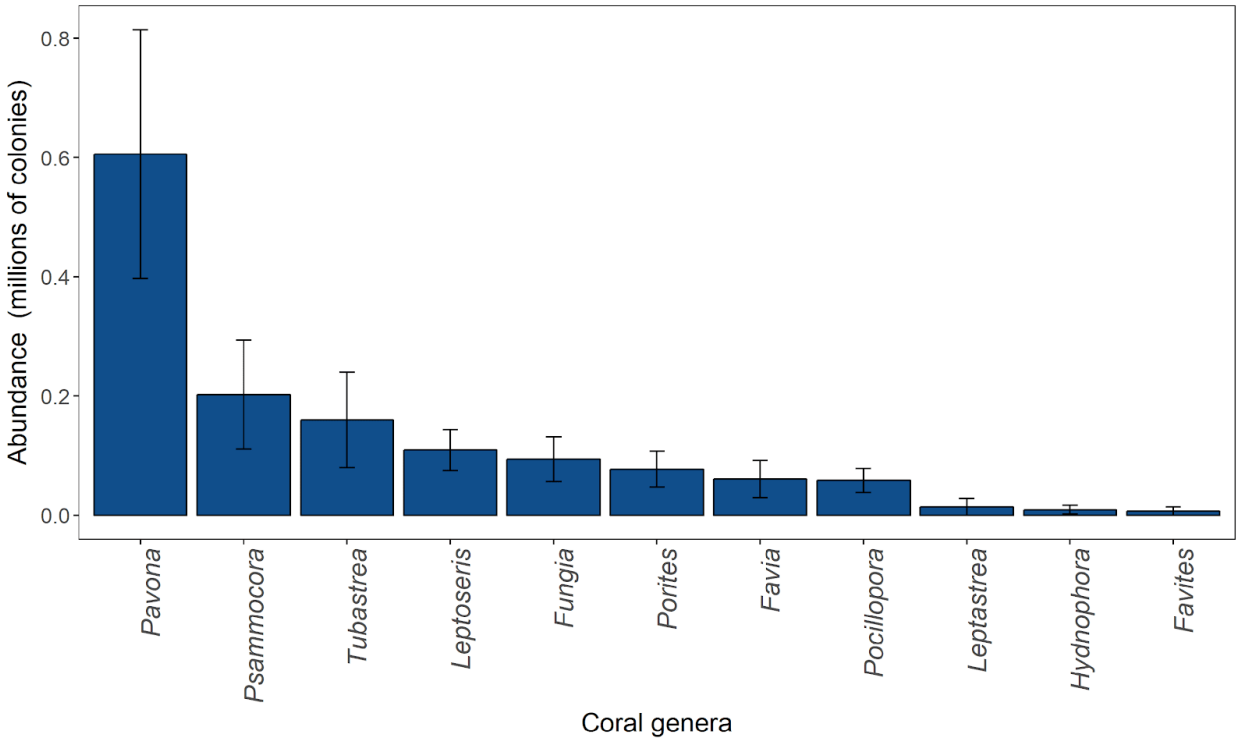

Figure 33. Island-scale abundance (± 1 SE) estimates by coral genera for all depth strata combined (>0–30 m) at Jarvis Island from Rapid Ecological Assessment surveys conducted in 2017.

Island-scale abundance estimates for coral genera were extrapolated from the REA transect colony densities over the area of hard bottom habitat found in the survey strata (0–30 m). In 2017, a total of 11 coral genera were enumerated at Jarvis Island. Of these, *Pavona* was the dominant coral genus; three times more abundant than the next most numerous genus, *Psammocora,* and over 80 times more abundant than *Favites*, the least abundant genus (Figure 33). These observations substantially differ from the abundance patterns recorded prior to the 2015–2016 El Niño-induced mass coral bleaching and mortality event, when *Montipora* and *Pocillopora* together accounted for over 82% of all colonies. Interestingly, following the mass mortality, surveys in 2016 recorded the presence of *Montipora* at extremely low levels (<2% of all colonies enumerated), and in 2017 it was not observed at all.

Remarkably low adult colony densities (<1 colony/m^2) characterized coral reef communities at Jarvis during the 2017 surveys, a year after the 2015–2016 El Niño. Low densities were expected after the 2015–2016 catastrophic mortality, though the presence of juvenile colonies would suggest the beginning stages of a recovery. In 2017, juvenile and adult colonies of the genus *Pavona* represented a significant proportion of the coral populations throughout all depth strata (Figure 34), with adults more abundant in the mid-depth (>6–18 m) and deep (>18–30 m) strata and juvenile colonies more abundant in the shallow (>0–6 m) stratum. Nonetheless, while overall densities of both adults and juvenile colonies were very low, small colonies of *Tubastrea* and *Fungia* were observed, which account for the greater proportion of juvenile total scleractinians observed. For all scleractinians combined, both juvenile and adult abundances were highest in

the deep stratum, suggesting that corals at deeper depths were more likely to have survived the 2015–2016 mortality event compared to their shallower-water counterparts. A table showing total generic richness of hard corals in the PRIMNM can be found in Appendix A of "Chapter 9: PRIMNM in the Pacific-wide Context."

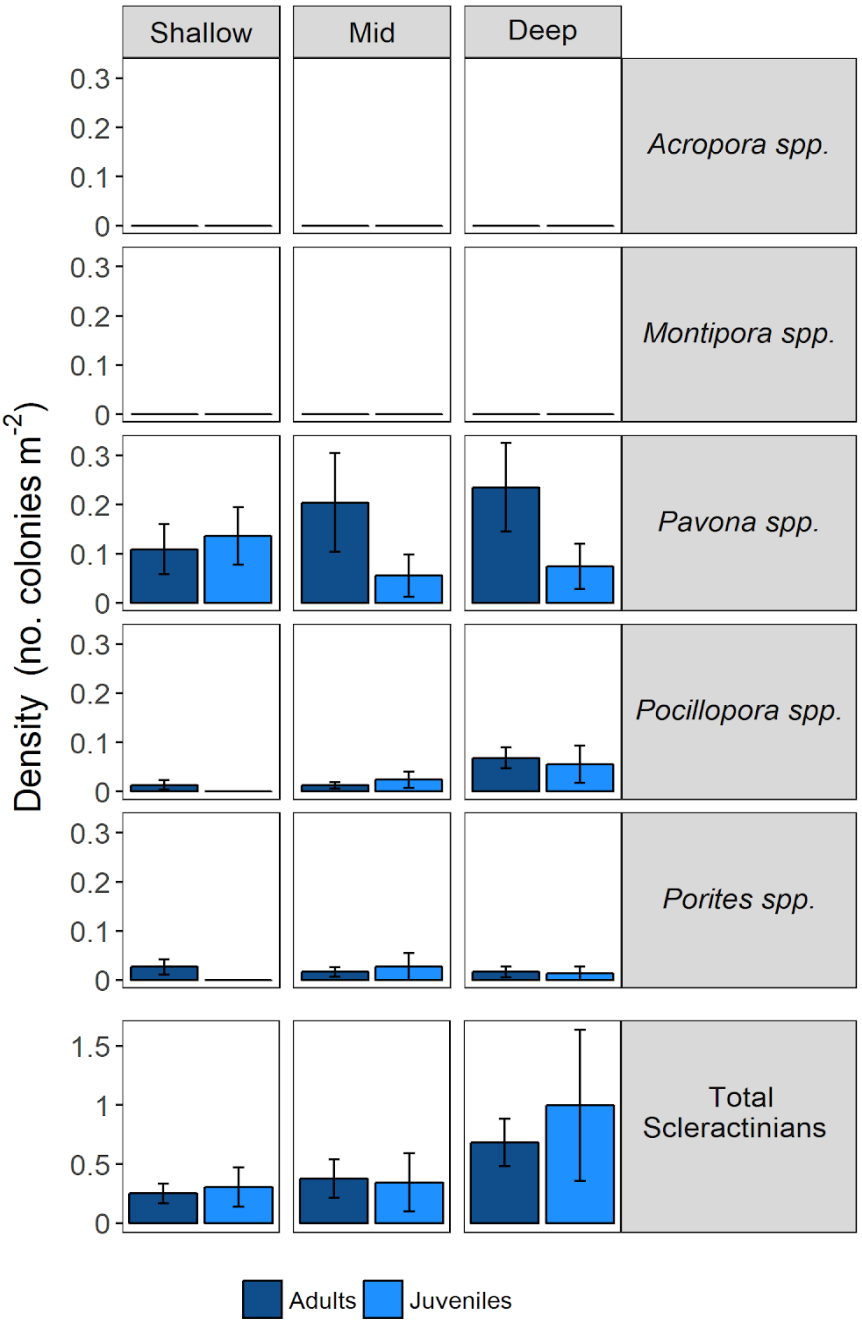

Figure 34. Mean (±1 SE) adult and juvenile colony density from Rapid Ecological Assessment surveys conducted at Jarvis Island in 2017 at shallow (>0–6 m), mid (>6–18 m), and deep (>18–30 m) depth strata for five coral genera generally abundant in the Pacific Remote Islands Marine National Monument (*Acropora* spp., *Montipora* spp., *Pavona* spp., *Pocillopora* spp., and *Porites* spp.) to facilitate comparison among islands.

Time Series of Coral Abundance and Condition

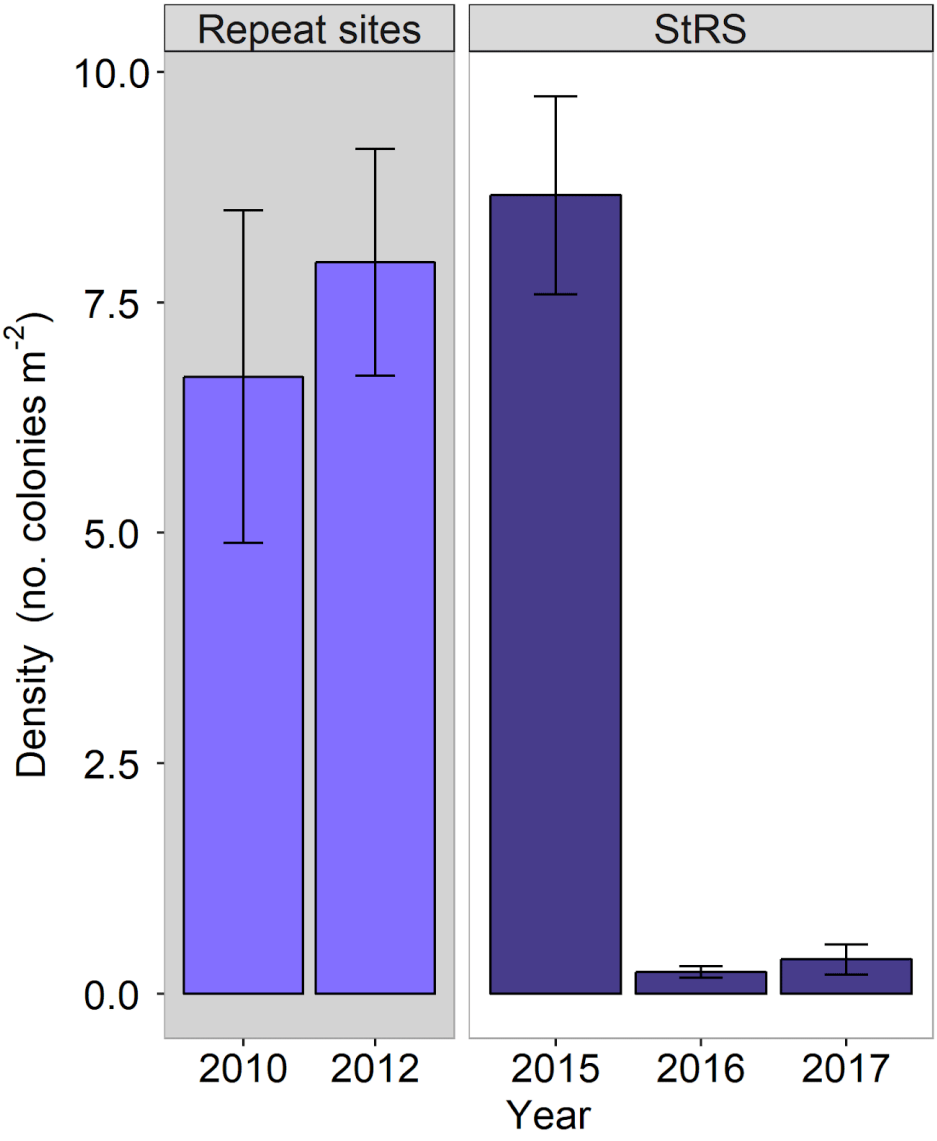

Figure 35. Time series of island-wide mean adult colony density (±1 SE) at Jarvis Island, from mid-depth (>6–18 m) strata Rapid Ecological Assessment surveys by survey design, repeat sites or stratified-random sampling sites (StRS), conducted from 2010 through 2017.

Between 2010 and 2015, island-wide mean coral colony densities at Jarvis Island were dynamic but remained stable overall (Figure 35). The high variance within each year (2010, 2012, and 2015) indicates that colony densities varied widely across space within each sampling year, and a change in survey method between 2012 and 2015 limits the detectability of meaningful changes in colony densities between those two survey years. However, a clear decrease in colony density can be seen in 2016 following the extreme 2015–2016 El Niño-induced mortality event. As with coral cover data (Figure 30 and Figure 31), subsequent surveys in 2017 show little to no recovery of colony density thus far.

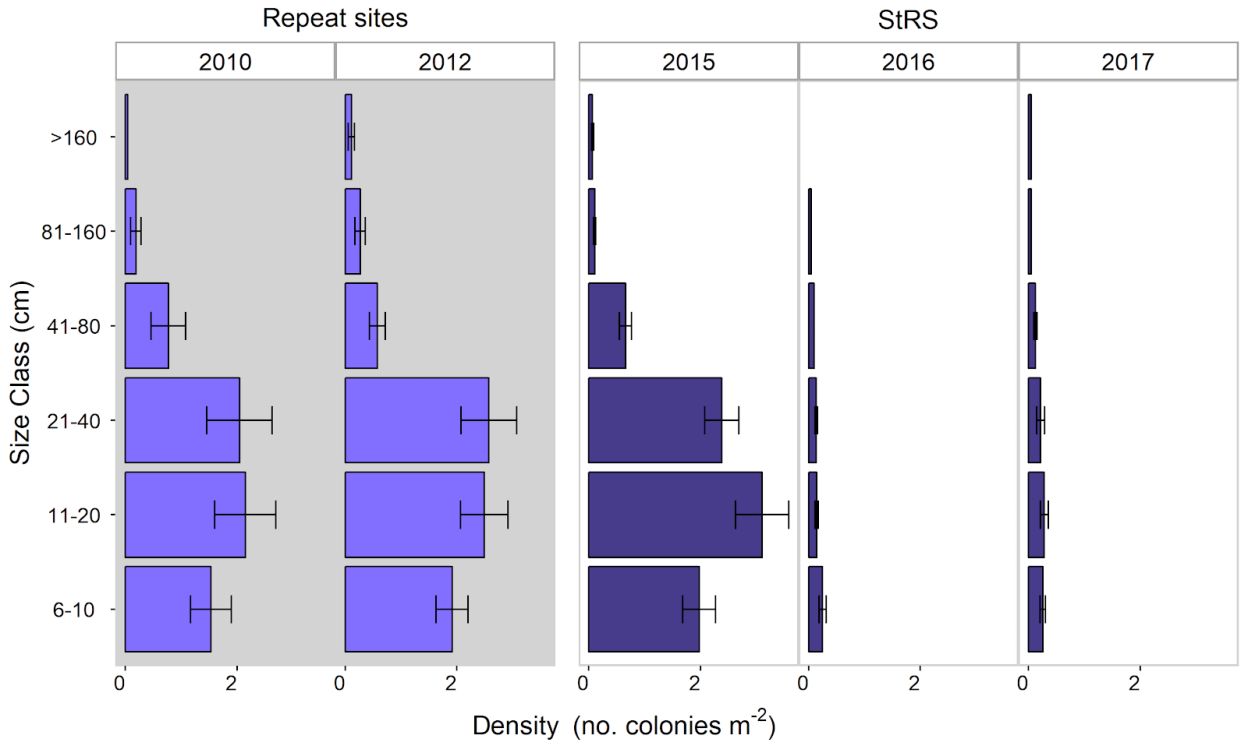

Figure 36. Time series of mean adult coral colony density (±1 SE) at Jarvis Island by size class from mid-depth (>6–18 m) strata Rapid Ecological Assessment surveys by survey design, repeat sites or stratified-random sampling (StRS), conducted from 2010 through 2017.

Several patterns are evident when reviewing the time series of adult colony densities illustrated in Figure 36. Firstly, between 2010 and 2015, size frequency distributions exhibited a unimodal pattern where the majority of the colonies were in the moderate size-classes (11–20 cm and 21–40 cm); smaller (5–10 cm), presumably younger, colonies were present, together with a few large (>81 cm) colonies that have survived many decades. Importantly, coral size-frequency curves holding the above pattern (skewed to moderate and small size classes) are indicative of healthy coral populations. Secondly, the fact that this pattern held consistent between 2010 and 2015 suggests some level of stability in the coral population. Following the catastrophic 2015–2016 mass coral bleaching and mortality event, colony densities in all size classes declined precipitously, and the shape of the size-frequency distribution changed such that the mode, or the most frequent colony size, shifted to a smaller colony size. Both the magnitude in colony density reduction across all size classes, in addition to the change in the shape of the size-class distribution curve, corroborates the severity of the 2015–2016 mass coral mortality event.

Surprisingly, a colony of the species *Acropora retusa* (National Oceanic and Atmospheric Administration 2005)—listed under the Endangered Species Act (ESA) of 1973—was sighted outside the BLTs during the post-bleaching surveys in 2016. It is both encouraging and remarkable that this rare species survived the extreme and prolonged thermal anomalies that accompanied the 2015–2016 El Niño event.

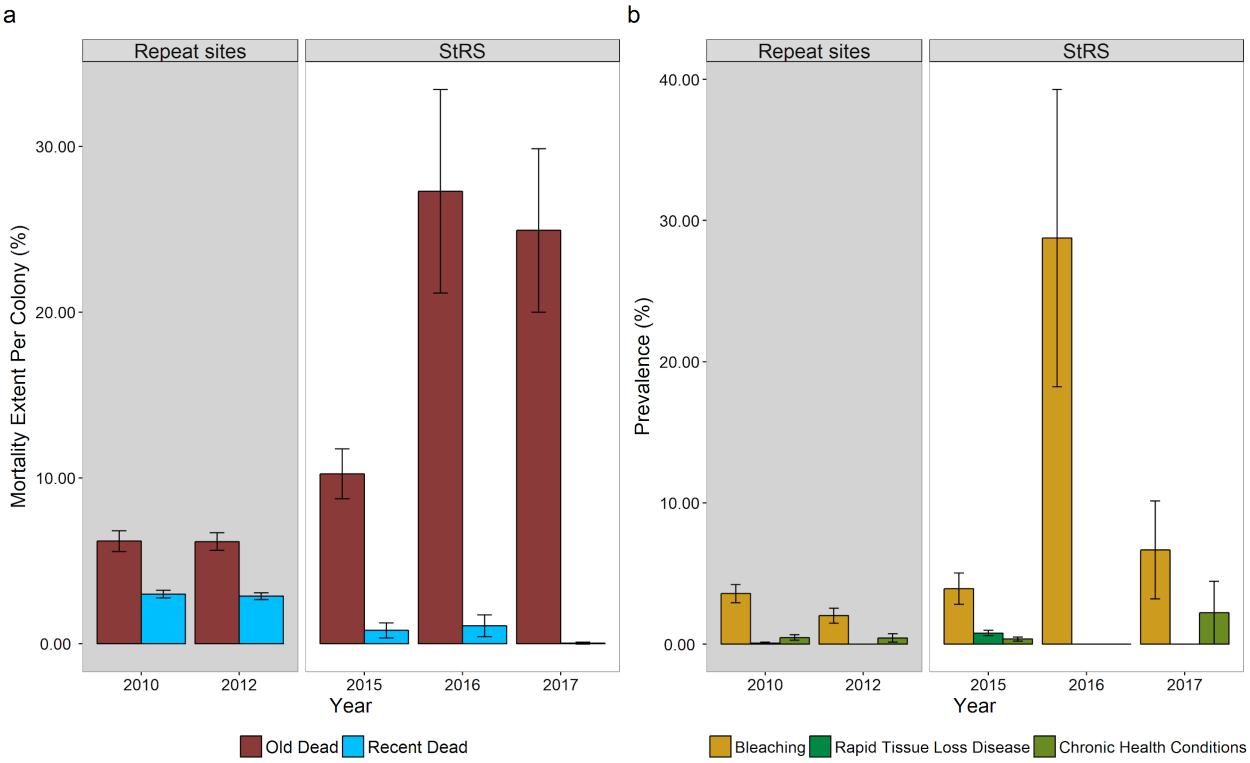

Figure 37. Time series of mean (± 1 SE) (a) percent partial coral mortality and (b) prevalence of bleaching, rapid tissue loss diseases, and chronic health conditions at Jarvis Island based on mid-depth (>6–18 m) strata Rapid Ecological Assessment surveys by survey design, repeat sites or stratified-random sampling (StRS), conducted from 2010 through 2017.

The percentage of old and recent mortality remained stable from 2010 to 2012 (Figure 37a). Contrastingly, the 167% increase in old dead between 2015 and 2016 documents the catastrophic coral mortality that occurred in the aftermath of the extreme 2015–2016 El Niño-induced mass coral bleaching event. Although the 2015 surveys did not capture the peak of the event, where nearly 100% corals bleached, surveys in May 2016 revealed that nearly 30% of the surviving corals remained bleached. In addition, of those few corals that survived into 2017 (0.3% coral cover, Figure 31; mean colony densities ≤0.3 colonies/m^2, Figure 35), bleaching prevalence was still elevated and prevalence of chronic diseases increased (Figure 37b), further impacting colony condition. In 2017, the prevalence of physical colony damage was low (mean = 1.1% ± 1.1 SE); as were the prevalence of predation (mean = 1.1% ± 1.1 SE) and overgrowth (mean = 1.1% ± 1.1 SE). The persistently high levels of old mortality recorded in 2017 illustrate the long-lasting effects of the 2015–2016 mass bleaching.

Benthic Macroinvertebrates

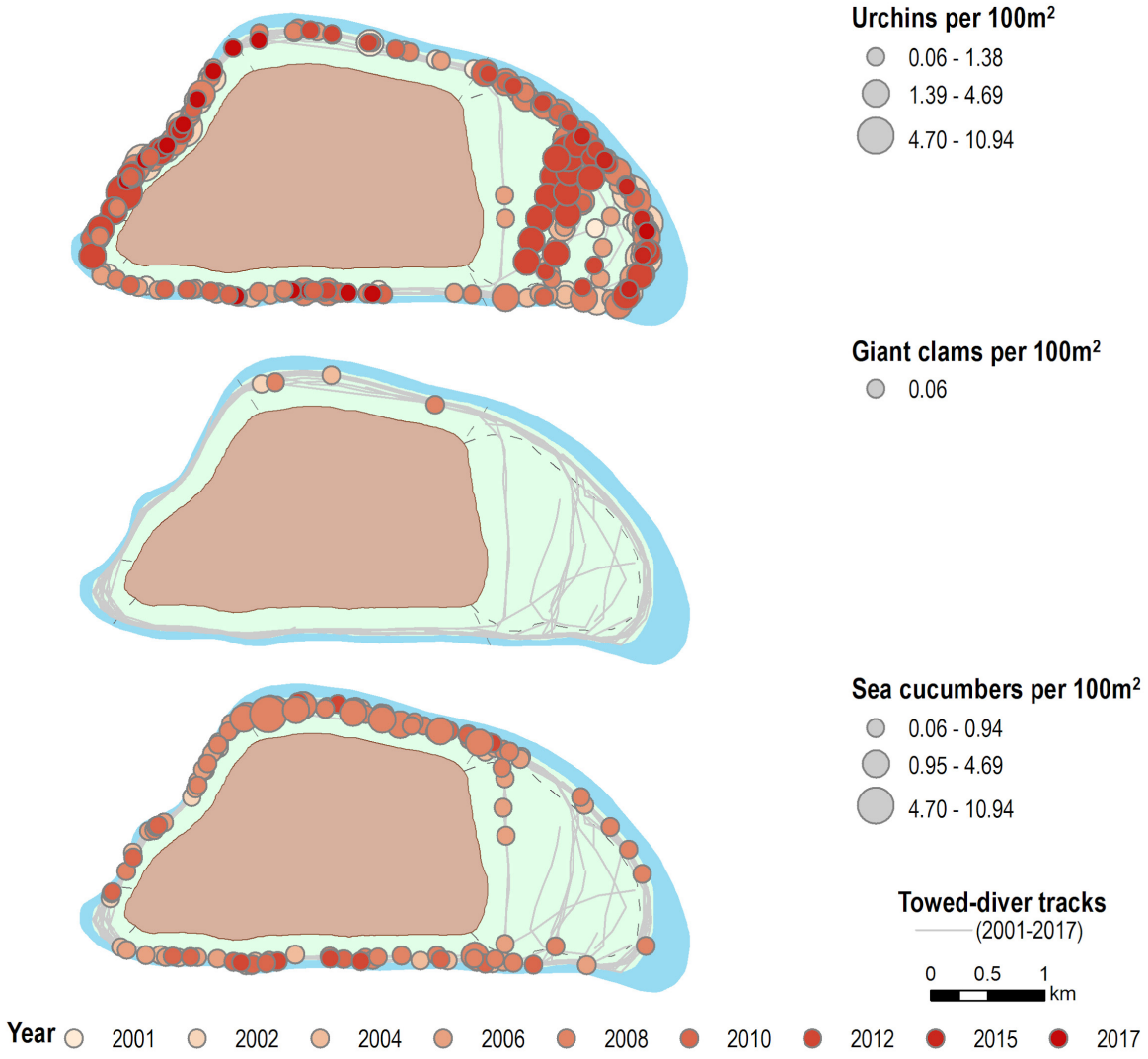

Figure 38. Density of conspicuous ecologically- or economically-important macroinvertebrate (urchins, giant clams, sea cucumbers, and crown-of-thorns sea stars) observed per segment from benthic towed-diver surveys (TDS) conducted throughout all depth strata (>0–30 m) around Jarvis Island from 2001 to 2017. Sea cucumber observations were discontinued from TDS in 2014.

Interestingly, zero sightings of crown-of-thorns sea stars were registered during 770 TDS segments at Jarvis Island over the nine survey efforts from 2001 through 2017, despite consistently high densities at the relatively nearby Kingman Reef and Palmyra Atoll (797 and 733 km away, respectively), which are also located in the Line Islands. Sea urchins exhibited broad spatial coverage over time; they were observed in all survey years and were abundant in all georegions, particularly the West, Southwest, and the Eastern Terrace (Figure 38). Comparatively, giant clams—currently under status review (Federal Register, 2017)—were conspicuously sparse, with only 4 sightings recorded since the inception of the long-term monitoring surveys; one individual in each 2002 and 2004, and two individuals in 2008. Notably, all giant clam sightings occurred in the North georegion. Although sea cucumber observations

were discontinued from TDS in 2014, occurrences were recorded each survey year prior to 2014, except for 2001, when none were reported. The highest sea cucumber densities were recorded in 2008, with the majority of individuals found within the North georegion; individual segment densities peaked at 10.9/100 m^2.

Grey reef shark cruising a biodiverse reef system at Jarvis Island, April 2015.
Photo: Andrew E. Gray, NOAA Fisheries.

Microbiota

4.5 Microbiota

School of Pterocaesio tile swims over the shallow reef flat at Jarvis.
Photo: Andrew E. Gray, NOAA Fisheries.

The reef microbiota facilitates the cycling of essential nutrients by breaking down organic materials released by photosynthetic picoplankton (e.g., Cyanobacteria) and benthic macroorganisms (corals and macroalgae). Habitats dominated by reef-building organisms (i.e., stony corals and calcified algae), such as Jarvis Island, illustrate a functional role that suppresses the energetic losses through microbial catabolism and promotes trophic transfer of energetic resources, carbon and inorganic nutrients, into metazoan food webs. This function is observed through the low microbial standing stocks in the water column and high turnover rates of microbial populations on reefs compared to the surrounding oceanic waters. Reef water samples were collected from all RAMP sites across the U.S. Pacific Islands Region beginning in 2008, with the first PRIMNM samples measured in 2009 (i.e., Wake and Johnston Atolls) and 2010 (i.e., Jarvis, Howland, and Baker Islands, Palmyra Atoll, and Kingman Reef). The assessment and monitoring of the reef microbiota paired with data collected on benthic and pelagic macro-

biota across the entire U.S. Pacific Islands Region allows for characterization of coral reefs from a molecular to an ecosystem scale.

Microbial Composition and Diversity

Microbial communities in reef waters were collected from Pacific RAMP sites across all U.S. Pacific Islands from 2012 to 2014. Reef water samples were processed for molecular identification of microbial populations using metagenomic sequencing. Microbial community composition at Jarvis Island is characterized by higher community diversity (measured using the Shannon Index, a metric of both species richness and evenness) on average compared to other U.S. islands across the Pacific (Figure 39). The community structure of the microbes at Jarvis reflects the complex and nutrient-rich organic material released by coral-dominated ecosystems and the enhanced niche space characteristic of intact reef habitats that promotes biodiversity across macro- and microbiota.

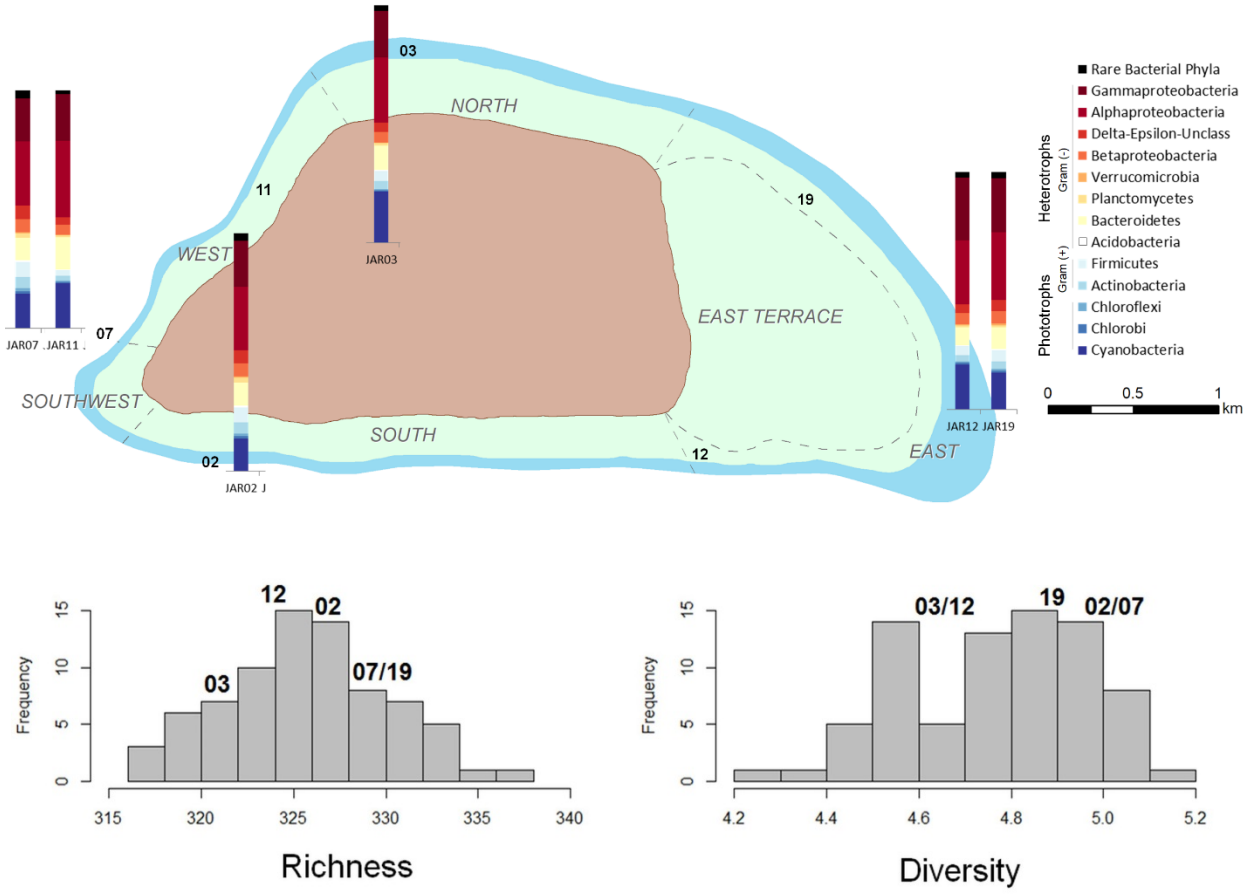

Figure 39. Microbial composition and diversity at Jarvis Island. (a) The microbial taxonomic groups are shown at Phylum Level. Delta-Epsilon-Unclass, Deltaproteobacteria, Epsilonproteobacteria and Unclassified Proteobacteria are all combined. (b) Comparison of microbial diversity at five Jarvis reefs collected in 2012 (Sites 02, 03, 07, 12, and 19) overlaid on a histogram of all Richness and Diversity observations across the U.S. Pacific islands collected between 2012 and 2014 (n=77 reef sites). Community Richness and Diversity were calculated at the Genus Level. H', Shannon Index. R, Rarified Richness.

Microbial Biomass on Reefs

Microbial biomass on Jarvis and other remote equatorial islands that experience equatorial and topographic upwelling (e.g., Howland and Baker Islands) is higher than at the remote islands and atolls that do not experience strong upwelling (Figure 40). Microbial biomass estimates at Jarvis were generally lower in 2015 than 2010, which could reflect seasonal differences based when the data were collected. Reef degradation towards algae-dominated states promotes greater cell biomass and higher proportions of fast growing heterotrophic taxa (as observed on the main Hawaiian Islands), which exhibit up to an order of magnitude more microbial biomass in the overlying reef waters (i.e., Jarvis in 2015 = 18 mg m^{-3} and Oahu in 2008 = 153 mg m^{-3}). The associated changes in microbial community structure and growth strategies when benthic community composition shifts from corals to algae shunts much more of the energy produced by the system towards decomposition pathways with enhanced respiration of organic compounds to carbon dioxide. This phenomenon is referred to as microbialization.

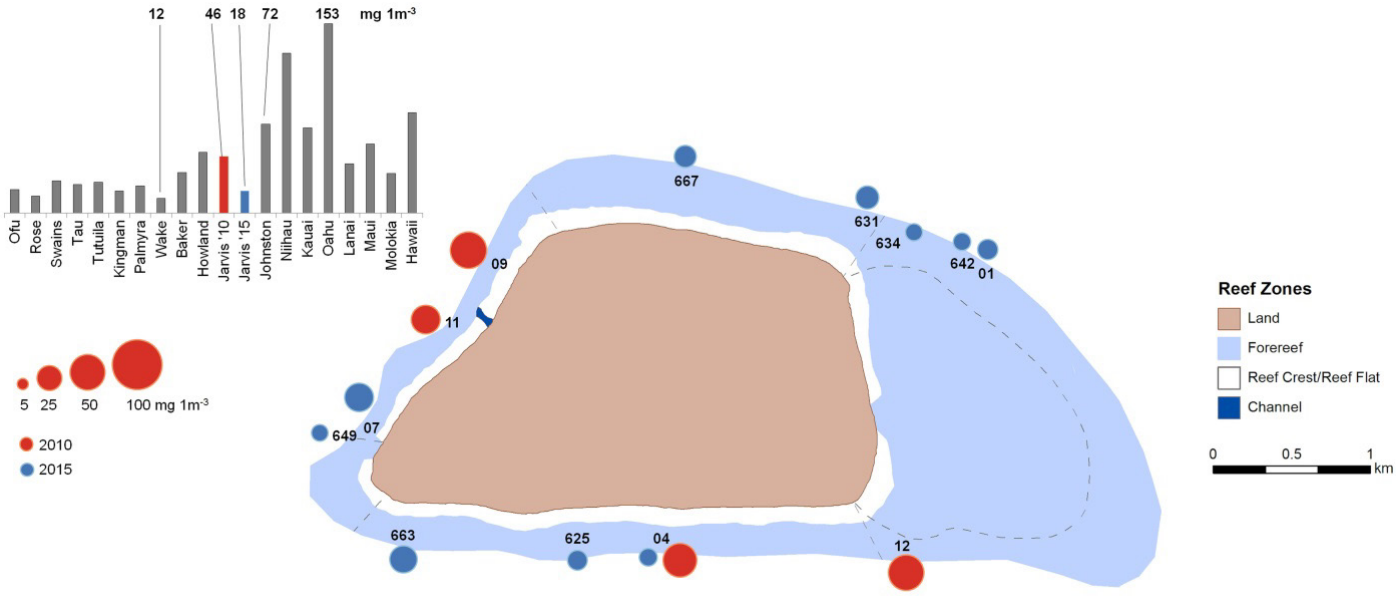

Figure 40. Microbial biomass collected at Jarvis Island in 2010 and 2015 (n = 26). Cell volume is estimated based on measurements of cell length and width and cell abundances enumerated using epi-fluorescent microscopy. Biomass is reported as milligrams per cubic meter (mg m^3). The 2010 data were published in (McDole et al. 2012).

Large school of black fin barracudas (Sphyraena qenie) at Jarvis Island, July 2018.
Photo: Andrew E. Gray, NOAA Fisheries.

Reef Fishes

4.6 Reef Fishes

School of scalloped hammerhead sharks (Sphyrna lewini) at Jarvis Island.
Photo: Paula Ayotte, NOAA Fisheries.

Survey Effort and Site Information

Jarvis Island reef fishes were surveyed on 10 occasions during the period from 2001 through 2017 (Table 4). The 2016 and 2017 surveys were part of an opportunistic supplementary effort conducted outside the normal scope of Pacific RAMP to document impacts and recovery following the extreme 2015–2016 El Niño. Surveys were a mix of comprehensive small-area surveys (belt-transect [BLT] or stationary point count [SPC]), and broad-scale (~2.2 km) towed-diver surveys (TDS), focusing on large-bodied fishes (>50 cm total length).

TDS were conducted during all survey visits to Jarvis, except the opportunistic bleaching response surveys in 2016. On each occasion, TDS were conducted around virtually the entire island perimeter, where large fishes tend to be most abundant, and a smaller number of surveys were conducted in the shallower East Terrace georegion (Figure 44). BLTs, which were utilized between 2001 and 2008, were conducted at haphazardly-located, mostly mid-depth (~10–15 m) outer forereef sites (Figure 41). In 2008, Pacific RAMP initiated the transition from BLT surveys

to the current SPC survey method and at the same time moved to a stratified-random survey design encompassing all hard-bottom habitats in less than 30 m water depths (Figure 41). Since that time, there have also been concerted efforts to increase the number of survey sites per visit, with 28 or more sites being surveyed every visit since and including 2010, compared to 9 or fewer sites prior to 2008 (Table 4). As a result of the shift in survey design, SPC sites have been much more widely spread around the island than were BLT surveys—including good coverage of the East Terrace (Figure 41). Because of a mix of low sample size and some inconsistency in the application of the BLT survey method in the program's earliest years, data collected before 2003 are not used to generate quantitative estimates, such as density. Also, BLT data gathered at the time the data collection method was changed to the stratified-random design in 2008 cannot be meaningfully compared with earlier BLT data gathered at repeat site locations. Thus, the time series shown in this chapter are primarily built from the TDS for the period from 2001 through 2017 and the SPC surveys conducted during the period from 2008 through 2017.

Table 4. Reef fish survey effort at Jarvis Island. Data are number of surveys by year and method. Towed-diver surveys (TDS) are ~2 km long by 10 m wide transects (~20,000 m^2), typically in mid-depth forereef habitats in which divers counted only fishes >50 cm total length (TL). In contrast, during belt-transect (BLT) and stationary point count (SPC) surveys, divers attempted to count all fishes within small areas of reef (~350–600 m^2).

Year	All Fishes		Large Fish (>50 cm TL)
	BLT	SPC	TDS
2001	4	–	2
2002	4	–	2
2004	6	–	8
2006	9	–	11
2008	20	19	13
2010	–	30	9
2012	–	42	6
2015	–	62	6
2016	–	30	–
2017	–	28	5

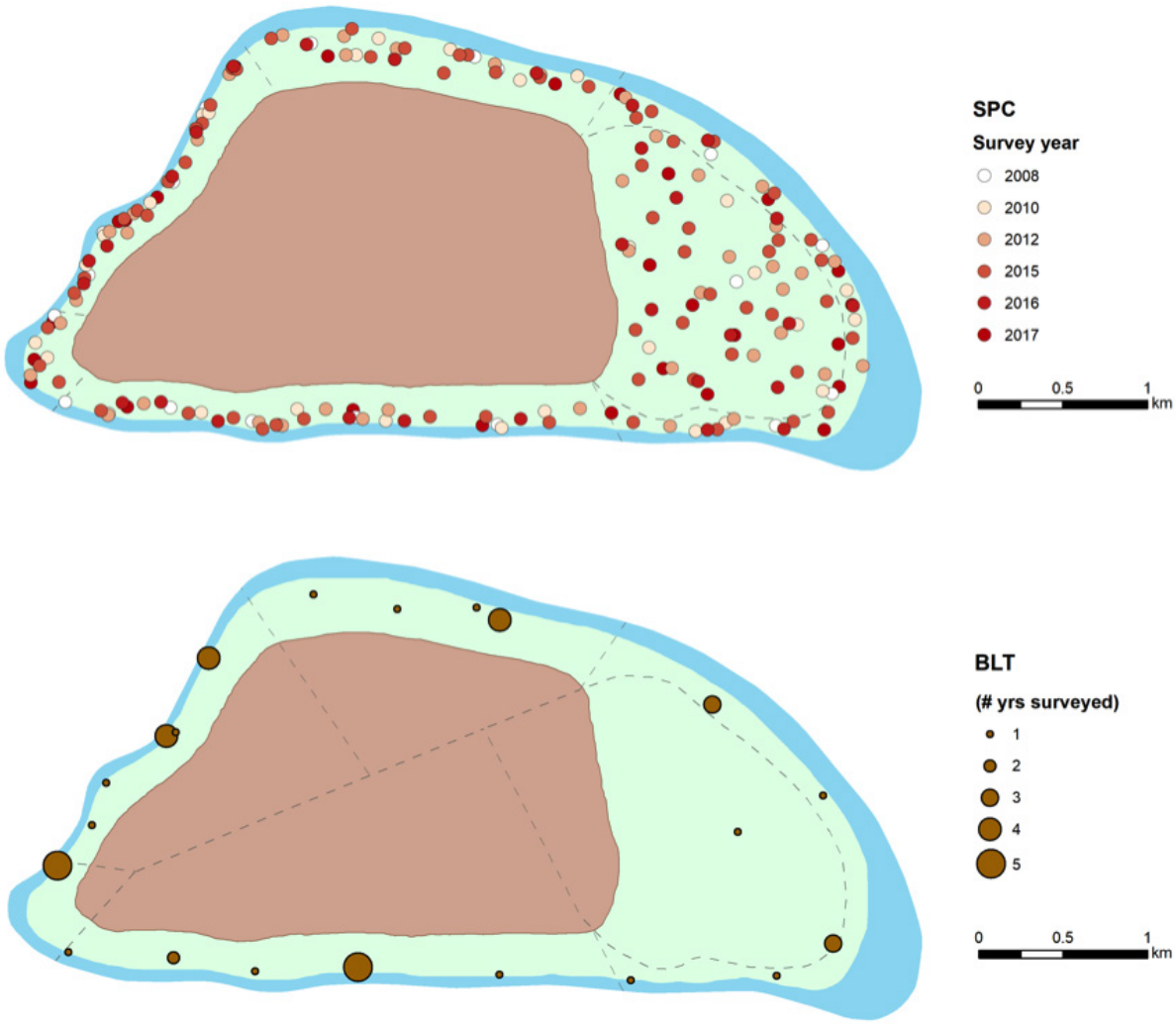

Figure 41. Location of stationary point count (SPC; top) and belt-transect (BLT; bottom) sites at Jarvis Island. SPC sites were not revisited, and the year of SPC survey is distinguished by color. BLT survey sites were generally revisited during multiple survey years. The total number of times each BLT site has been surveyed is indicated by the size of the bubble.

Distribution of Reef Fish Biomass and Abundance

Reef fish biomass was generally highest on outer forereef habitats—highest in the East and Southwest georegions, and somewhat lower in the North and East Terrace georegions (Figure 42). That pattern was largely driven by higher biomass of planktivores and piscivores, particularly reef sharks, in those areas (Figure 42 & Figure 44).

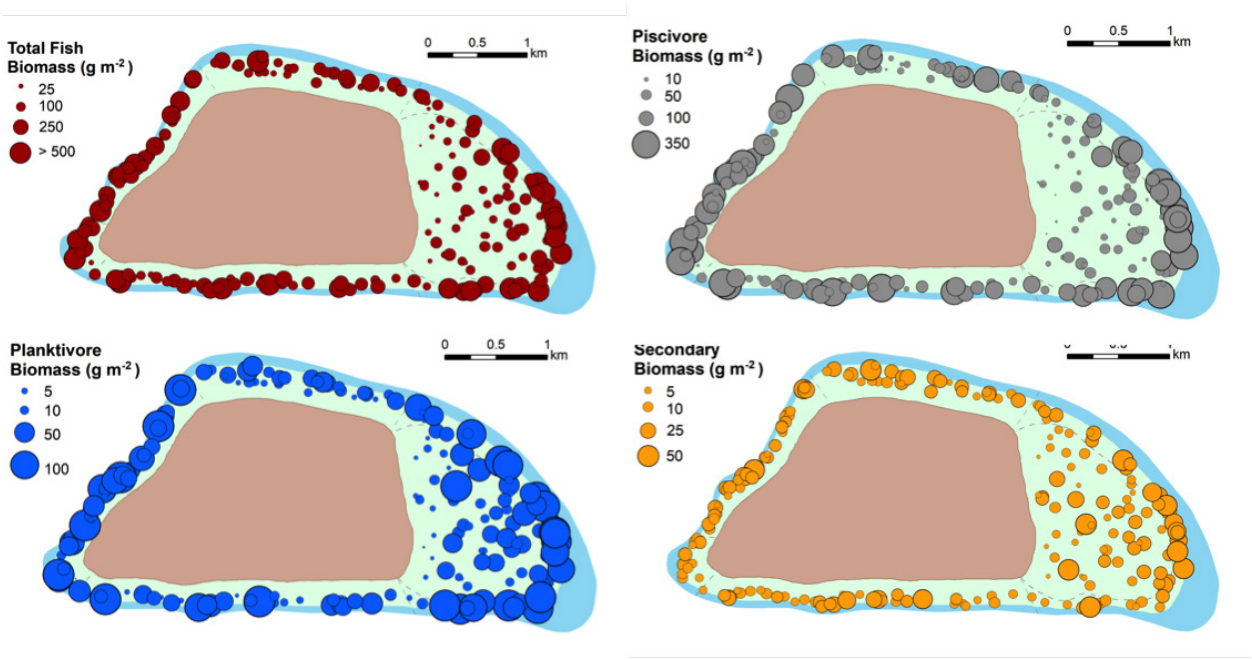

Figure 42. Maps of Total Fish Biomass, Planktivore Biomass, Piscivore Biomass, and Secondary (consumer group) Biomass from stationary point count surveys around Jarvis Island over the period 2008 through 2017. Secondary consumers include corallivores, omnivores, and invertivores, including many abundant and generally small-bodied species, as well as the bumphead parrotfish, *Bolbometopon muricatum*.

Planktivore biomass was high at the majority of outer forereef sites at both the eastern and western ends of the island, but especially high in the East georegion, potentially due to higher vertical oceanographic mixing by exposure to trade wind-driven waves (Figure 42). Dominant planktivorous taxa included the sleek unicornfish, *Naso hexacanthus*, Marr's fusilier *Pterocaesio marri*, and a number of extremely abundant small-bodied anthias, particularly Whitley's splitfin and Bartlett's anthias (*Luzonichthys whitleyi* and *Pseudanthias bartlettorum*). Large schools of small anthias were a conspicuous feature of many outer forereef sites at Jarvis Island.

Herbivore biomass was relatively evenly distributed around Jarvis, although somewhat lower at East Terrace and East georegion sites (Figure 43). That was true for parrotfishes and, to an even greater extent, for surgeonfishes. In all georegions, herbivore biomass was dominated by the whitecheek, lined, and striped-fin surgeonfish (*Acanthurus nigricans, A. lineatus, Ctenochaetus marginatus*) and by the ember and bridled parrotfishes (*Scarus rubroviolaceus, S. frenatus*).

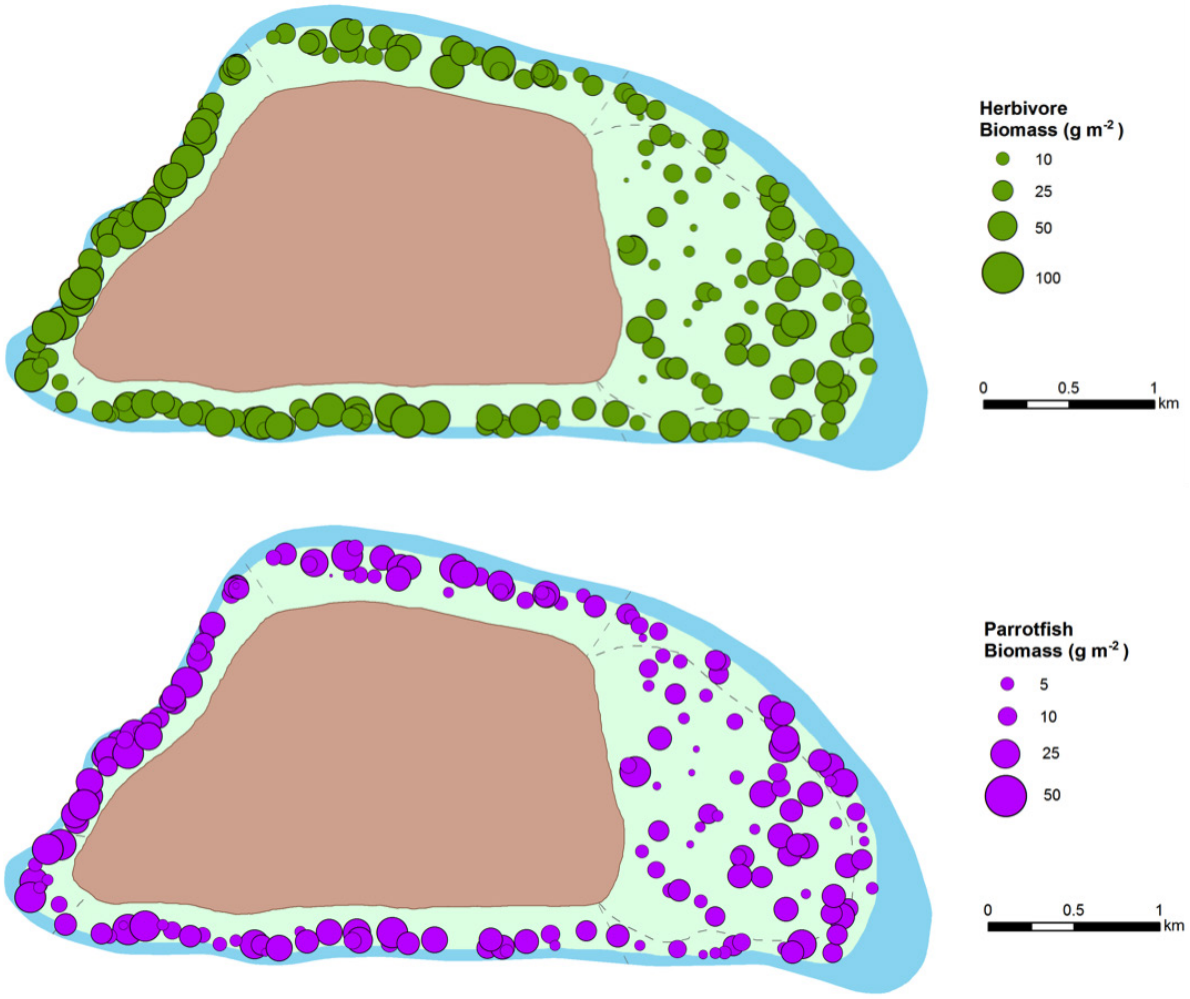

Figure 43. Total Herbivore Biomass and Parrotfish Biomass at Jarvis Island from stationary point count surveys over the period 2008 through 2017.

Gray reef sharks (*Carcharhinus amblyrhynchos*) were the most commonly observed shark species around Jarvis, followed by whitetip reef sharks (*Triaenodon obesus*), seen at, respectively, 60% and 26% of all towed-diver segments (~220 m long sub-units of the survey). Overall, reef sharks were seen on 71% of all towed-diver segments, but encounter rates were lower in the East Terrace (30%, Figure 44), which was the one georegion where a different shark species dominated—the blacktip reef shark (*Carcharhinus melanopterus*). Hammerhead sharks were observed on 3% of towed-diver segments, and the majority of those were identified as scalloped hammerhead (*Sphyrna lewini*), which is listed as threatened under the ESA for the Indo-West Pacific discrete population segment that includes Jarvis. For this species, the highest frequency of encounters was along the slopes of the West and Southwest georegions.

Other common predatory species included the blackjack and bluefin trevally (*Caranx lugubris, C. melampygus*), and the two-spotted red snapper (*Lutjanus bohar*), which was the most

abundant piscivorous snapper. *L. bohar* comprised a large portion of piscivore biomass in the East Terrace georegion, where sharks were much less abundant.

Humphead wrasses (*Cheilinus undulatus*) were infrequently observed during either REA or TDS. All observations were in outer forereefs, mostly in the East georegion (Figure 44). A single bumphead parrotfish (*Bolbometopon muricatum*) was observed during a TDS in 2006, in the Southwest georegion (Figure 44). However, this species has never been recorded by divers conducting BLT or SPC surveys at Jarvis.

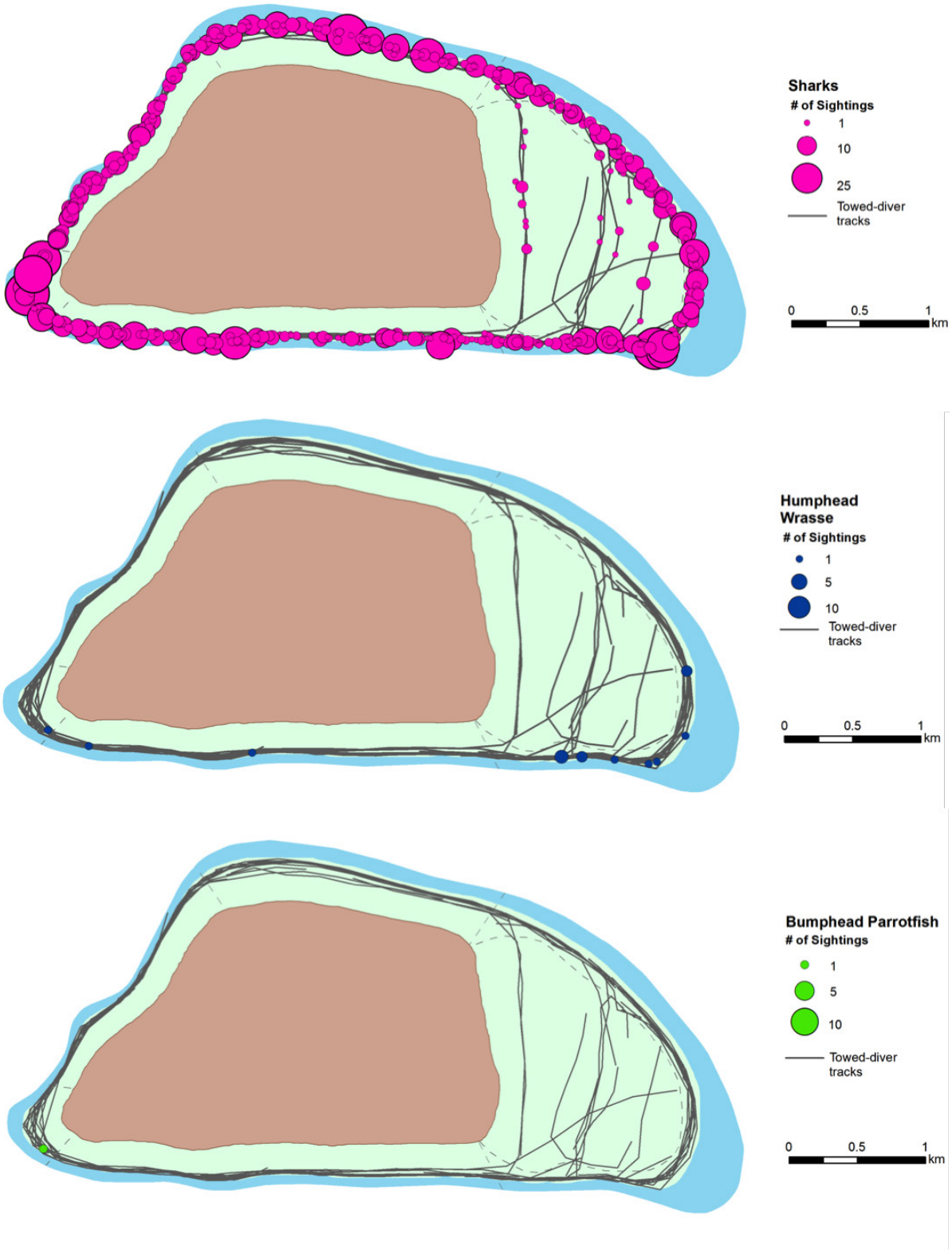

Figure 44. Towed-diver survey sightings of sharks, humphead wrasse, and bumphead parrotfish at Jarvis Island from 2001 through 2017.

Distribution of Other Species of Interest

Manta rays (*Mobula* spp.) have been sighted during Jarvis Island TDS in all georegions of Jarvis, but densities and encounter rates were clearly higher in the East Terrace georegion close to the east end of Jarvis, and in forereef areas along the south shore close to the east end of Jarvis (Figure 45). The clusters of manta ray observations at the east and southeast ends of Jarvis (Figure 45) appear to be associated with soft-bottom substrates located in those areas (Figure 6) or a channel that divers have reported there.

Sea turtles were very commonly observed during the TDS: green sea turtles (*Chelonia mydas*) were recorded during 39% of all TDS segments, and hawksbill sea turtles (*Eretmochelys imbricata*) during 1% of all segments. Both species are ESA-listed. Green sea turtles were common in all georegions, but with clearly lower encounter rates in the East and deeper portions of the East Terrace georegions (Figure 45). It is harder to draw conclusions about the typical distribution of hawksbill sea turtles, as they were only observed on 8 of the 728 segments surveyed (Figure 45).

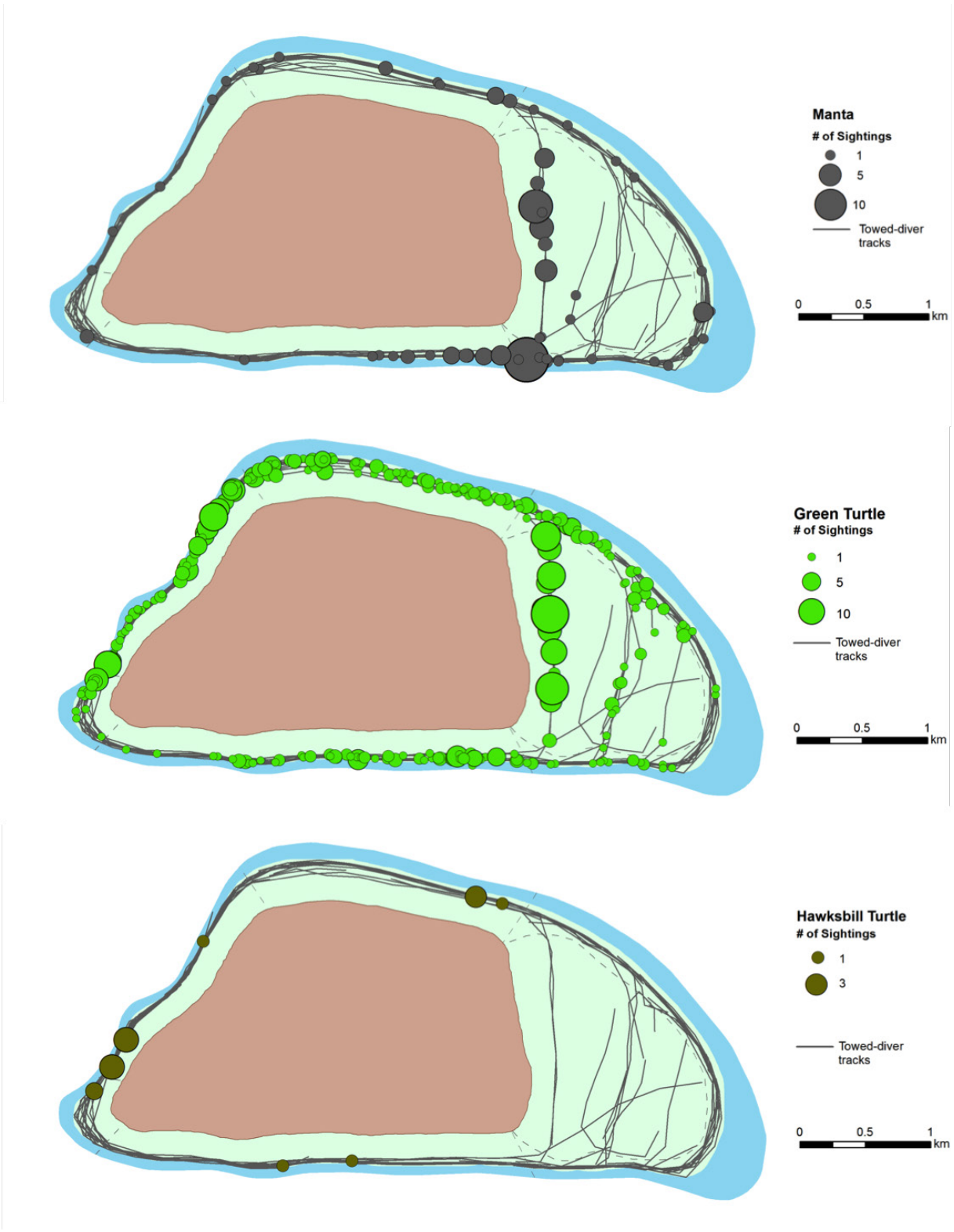

Figure 45. Towed-diver survey sightings of manta rays and sea turtles at Jarvis Island over the period from 2001 through 2017. Green sea turtle sightings shown above include observations recorded as (unspecified) turtle, as the great majority of sea turtles seen at Jarvis were green sea turtles.

Reef Fish Time Series

The time series of biomass of reef fishes over time, incorporating data from both BLT and SPC surveys, is shown in Figure 46. As is evident from the size of the confidence intervals in early years, there were insufficient data from earlier survey periods to identify statistically significant patterns (Figure 46). Based on the SPC data that were collected between 2008 and 2017, there are no clear indications of a long-term trend in total reef fish biomass, but values tended to be higher for several groups of fishes in 2012, and lower for some groups, particularly planktivores and secondary consumers, in 2016 (Figure 46). The increase in total reef fish biomass in 2012 may have been due to increased primary production (as represented by high chl-*a* pigment concentrations) associated with La Niña conditions over the period 2010–2011, and the decrease of planktivores and secondary consumers in 2016 was potentially related to the exceptionally low primary productivity (as represented by low chl-*a* pigment concentrations) during the extreme 2015–2016 El Niño event (Figure 14d).

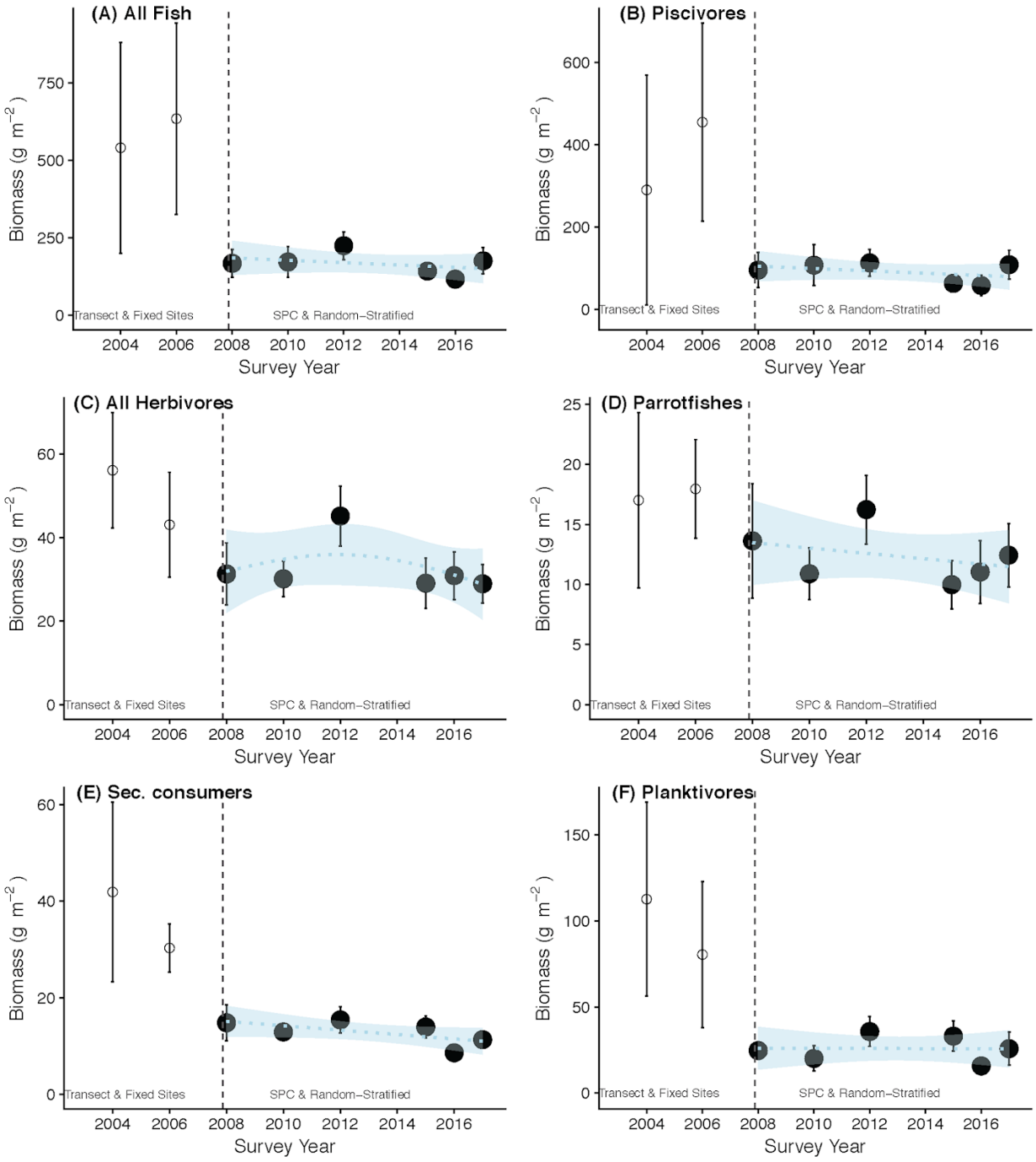

Figure 46.Time series of reef fish biomass at Jarvis Island. Data are shown for belt-transect surveys conducted at a limited number of mid-depth forereef sites in 2004 and 2006, and stationary point count (SPC) surveys conducted at randomly located sites encompassing all hard-bottom forereef in water depths <30 m, over the period from 2008 through 2017. Circles represent mean values, and error bars represent 95% confidence intervals per time period. The light blue dotted trend lines and confidence intervals were derived from generalized additive models of biomass against survey year. Biomass values from the different periods cannot be directly compared due to differences in methods and survey locations.

Although TDS data are extremely useful for identifying species' distributions and for gathering data on otherwise infrequently encountered species, this method is prone to high variability between years (as is shown by the large error bars in Figure 47). That variability is largely due to two factors: (i) overall counts can be heavily influenced by encounters with large schools of some species; and (ii) sample sizes are relatively low. Therefore, it is important not to over-interpret apparent trends within this dataset. Although counts of large-bodied jacks and surgeonfishes have been low in recent years, interannual variation in those families was largely driven by encounters with schools of either the sleek unicornfish, *Naso hexacanthus*, occasionally seen in groups of approximately 50 to 150 individuals, and the bigeye trevally, *Caranx sexfasciatus*, which have been seen in groups of several hundred to over a thousand individuals in some years. Thus, the high variability in recorded abundance in those groups was likely due to inherent natural variability and extreme patchiness of several roving, schooling species (Figure 47).

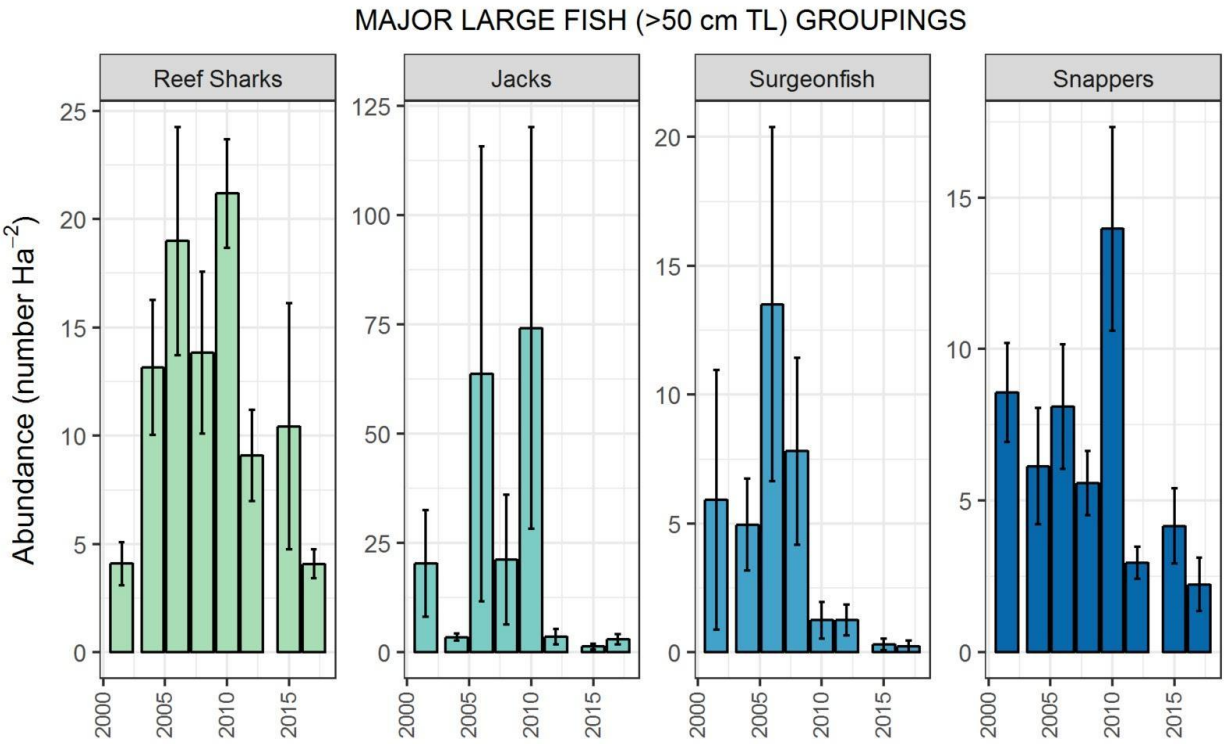

Figure 47. Bar plots by year for reef sharks, jacks, surgeonfishes, and snappers from towed-diver survey (TDS) data at Jarvis Island during the period from 2001 through 2017. Values shown are mean and standard error. Note that 2001 and 2002 data are pooled due to low sample sizes in those years. In order to increase consistency among years, trends were derived only from TDS >500 m in length, which were conducted in forereef habitats between 10 and 20 m deep.

Species Lists, Encounter Rates, and Diversity

Island-wide mean species richness values, which measure the number of species observed per survey independent of their abundance, ranged between around 30 and 36 species per SPC survey at Jarvis Island. Island-wide mean evenness, which measures diversity while taking into account the distribution of abundance of individual species, was at the lower end of values

observed from the islands/atolls of the PRIMNM as part of Pacific RAMP, ranging between 0.45 and 0.61 (Figure 48). Despite some variability among years, there are no clear indications of a trend in fish assemblage diversity at Jarvis over the 2008–2017 period (Figure 48). Interestingly however, richness was lowest, and evenness was highest in both 2010 and 2016, which both followed the 2009–2010 and 2015–2016 El Niño events characterized by warm, low productivity waters.

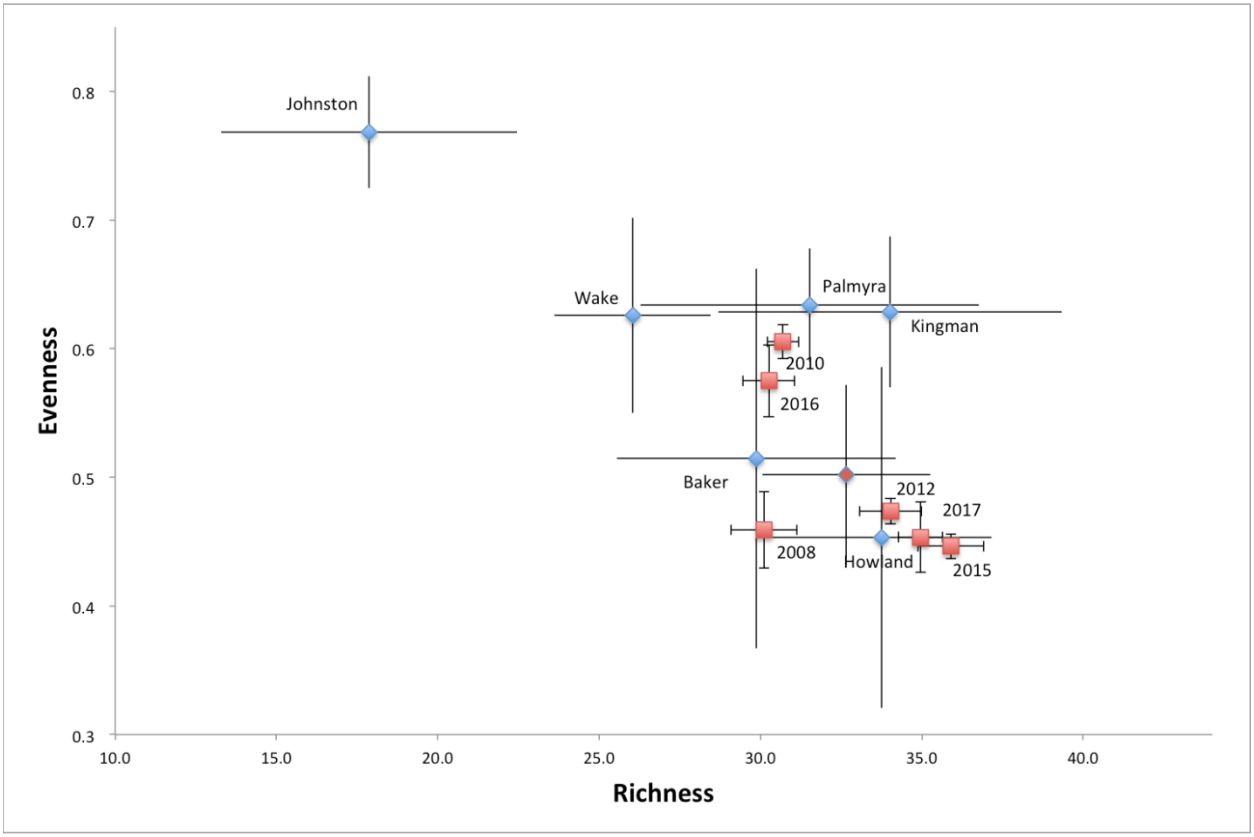

Figure 48. Richness vs evenness for reef fishes at Jarvis Island and other Pacific Remote Islands Marine National Monument (PRIMNM) locations. Red squares are species richness (the number of species encountered) and evenness (how equally abundance was distributed) values at Jarvis by year (± SE). Blue circles represent mean (± SD) richness and evenness values for other islands in the PRIMNM across all years. The single red dot represents the mean (± SE) value at Jarvis across all years. For consistency, only data from forereef sites are included.

ESA-listed species observed at Jarvis include the green and hawksbill sea turtles (*Chelonia mydas, Eretmochelys imbricata*), and the scalloped hammerhead (*Sphyrna lewini*). Although divers have frequently observed manta rays (*Mobula* spp.) at Jarvis, it is not possible for divers to reliably distinguish between the giant manta (*Mobula birostris*), which is ESA-listed, and the reef manta (*Mobula alfredi*), which is not.

Ten species of fish recorded during surveys at Jarvis are listed as endangered, vulnerable, or near threatened by the International Union for Conservation of Nature (IUCN) Red List (IUCN, 2017). Three of these—*Carcharhinus amblyrhynchos*, *C. melanopterus,* and *Mobula* sp. (both species of which are IUCN listed)—were regularly seen by survey divers (on at least 1 in 6 of the SPC surveys over the period they were conducted, from 2008–2017). Two species—*Cheilinus*

undulatus and *Sphyrna lewini*—were seen on approximately 1 in every 15 to 20 surveys. Others were only rarely encountered. For example, the giant grouper, *Epinephelus lanceolatus*, has been recorded in the vicinity of the dive surveys on only three occasions. The remaining four IUCN-listed fish species recorded at Jarvis were observed on only one or two surveys. *Bolbometopon muricatum* and the spotted eagle ray, *Aetobatus narinari,* were both recorded once in 2006. A single observation of a Galapagos shark (*Carcharhinus galapagensis*) in 2004 was likely a misidentification of a gray reef shark, which is very similar in appearance. Finally, divers have twice recorded the presence of yellowfin tuna, *Thunnus albacares,* in the vicinity of survey sites. Those encounters were likely anomalies due to the close proximity to open ocean water around Jarvis. A complete list of all fish species observed is provided in Appendix B of "Chapter 9: PRIMNM in the Pacific-wide Context."

Marine Debris

4.7 Marine Debris

Marine debris was noted sporadically at Jarvis Island during TDS from 2001 through 2015 (Figure 49). Various forms of debris were recorded a total of 26 times during the surveys. This does not encompass all debris found at Jarvis, as debris assessments were not always conducted during TDS. It is possible that the same pieces of debris were noted in different survey years. Fishing line made up the majority of the debris recorded.

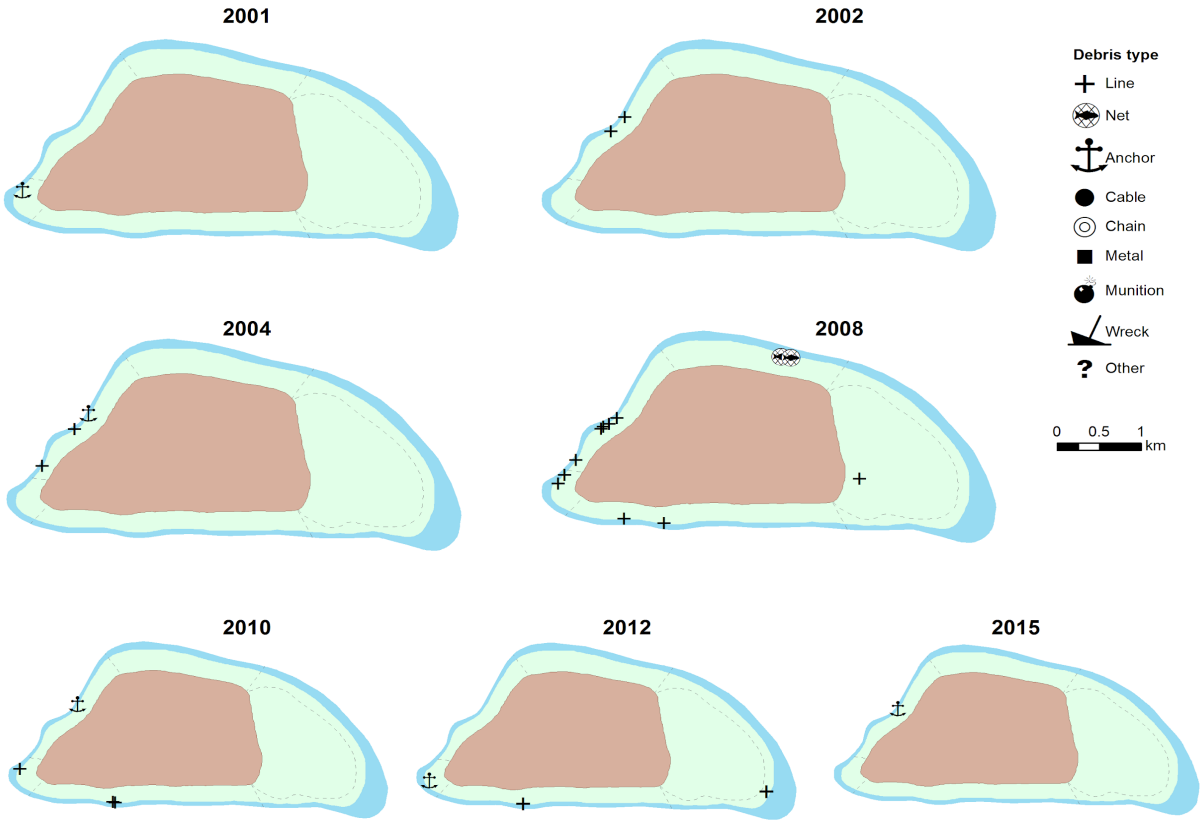

Figure 49. Marine debris sightings, including line, net, and anchor debris, observed around Jarvis Island between 2001 and 2015 during benthic towed-diver surveys.

Two manta rays at Jarvis Island, July 2018.
Photo: Andrew E. Gray, NOAA Fisheries.

Ecosystem Integration

4.8 Ecosystem Integration

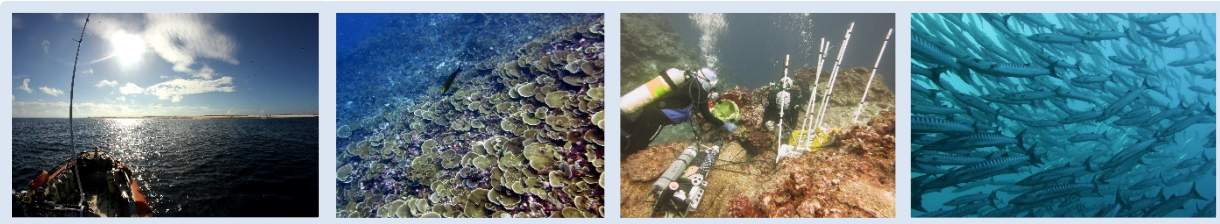

Photos left to right: Jarvis Island from small boat, Photo: NOAA Fisheries; Forereef seascape at Jarvis Island, Photo: Paula Ayotte, NOAA Fisheries; Collecting water samples, Photo: NOAA Fisheries; A school of barracuda swim in the shallows of Jarvis Island, Photo: Andrew E. Gray, NOAA Fisheries.

Oceanic Drivers of Benthic and Fish Populations

As a steep seamount located just south of the equator in the path of both the westward-flowing surface South Equatorial Current and the strong, eastward-flowing subsurface Equatorial Undercurrent (EUC), Jarvis Island is distinctly characterized by intense equatorial and topographic upwelling that strikingly varies in strength and intensity across years with the El Niño Southern Oscillation. During La Niña conditions, enhanced upwelling resulted in anomalously cool, nutrient-rich, and biologically productive surface waters that were also relatively acidic and lower in aragonite saturation state. In contrast, the weakening of upwelling during El Niño events resulted in warmer temperatures and declines in chlorophyll-*a* concentrations as surface waters shifted toward lower productivity. Island-wide measures from 2001 to May 2015 indicated hard coral cover had remained relatively stable. Forereef areas of Jarvis were also characterized by low prevalence of both coral and coralline algal disease, as well as an absence of the corallivorous crown-of-thorns sea star, perhaps due to a lack of planktonic larval dispersal to this remote and isolated island. There was also a lack of a clear trend in reef fish biomass through time, with the exception of an increase in biomass of most fish trophic groups (particularly parrotfishes) in 2012, following a transition in 2010 from nutrient-poor to nutrient-rich waters as conditions shifted from a moderate El Niño event to a strong La Niña event.

The 2015–2016 El Niño event was the most extreme thermal disturbance ever recorded at Jarvis in terms of the magnitude, duration, and severity of impact (Brainard et al. 2018). Severe coral bleaching was evident by November 2015 (Barkley et al. 2018), at which point water temperatures had exceeded the local bleaching threshold for 43 consecutive weeks and reached an accumulated heat stress of 35.8 DHWs (Boyle et al. 2017; Brainard et al. 2018). Immediately following the bleaching event, surveys in May 2016 revealed a catastrophic, island-wide decline in hard coral cover of over 98%, including about a 30% loss in cover of crustose coralline algae, as well as a two-fold increase in encrusting macroalgal cover (particularly *Peyssonnelia*) that represented 40% to 60% of live benthic cover. Coral populations suffered an overall 92% decline in adult colonies and approximately 87% decline in juvenile colonies. Surveys further indicated colonies that survived the bleaching event still experienced sublethal impacts in the form of increases in both chronically-compromised health conditions (0.4% in 2015 to 2.2% in 2017) and

partial colony mortality (10.8% in 2015 to 31.2% in 2016). Concurrent decreases in the biomass of planktivorous and piscivorous fishes were also evident following this particular El Niño event (Brainard et al. 2018), yet it remains unclear if and to what extent these patterns were related to the sustained period of low productivity versus the severe bleaching event and associated shifts in the benthic community and habitat structure.

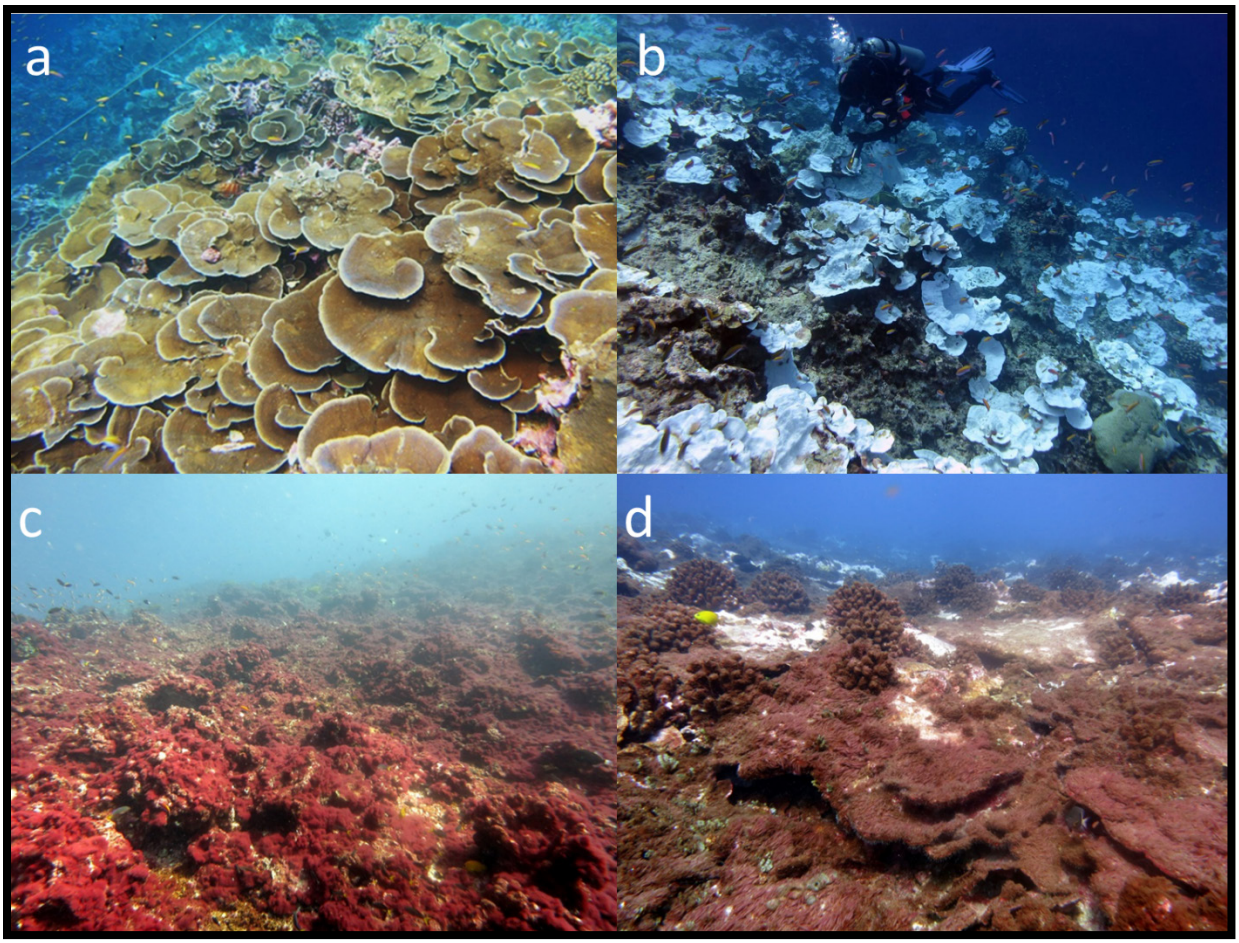

Figure 50. Underwater seascapes illustrating the appearance of the coral reefs at Jarvis Island: (a) before, (b) during, and (c–d) after the 2015–2016 bleaching event. Photos: (a) NOAA Fisheries, (b) Hannah Barkley, NOAA Fisheries, (c–d) Bernardo Vargas-Ángel, NOAA Fisheries.

Spatial Variation within the Island

Localized topographic upwelling was most pronounced along the western side of Jarvis Island as the eastward-flowing EUC encountered the steep western slope, resulting in cool, nutrient-rich surface waters. The greatest cover of corals (40% to 47% at mid-depth) were measured in the West and Southwest georegions, with benthic communities dominated by massive *Porites* and densely-plating *Montipora* along the steep slope. The scalloped hammerhead (*Sphyrna lewini*)—listed under the Endangered Species Act (ESA)—was observed in low abundances around the entire island, with a higher frequency of encounters along the slopes of the West and Southwest georegions, including a single encounter with a large schooling group of over 100 individuals in this region. Similarly, piscivore biomass (primarily grey reef sharks, *Carcharhinus*

amblyrhynchos) was evenly distributed around Jarvis, with greater localized biomass off the western slope and high-current habitats within prominent exposure areas at the southeastern and southwestern ends of the island.

The composition of benthic communities in the West and Southwest georegions of Jarvis were strikingly different from those observed throughout the remaining georegions, likely due to the gradual diffusion of upwelling-driven water conditions from the western to the eastern end of the island. Forereef areas of the North and South georegions were mostly comprised of coral rubble with the lowest values of coral cover (~2% to 15%) measured in the North georegion, which was exposed to the highest wave energy during the winter months. Sea cucumbers were most abundant throughout these two georegions, and sightings of giant clams (4 individuals) all occurred in the North georegion.

Fish biomass remained low inside the Eastern Terrace, a shallow georegion exhibiting warmer water temperatures, habitat structure low in relief and slope, and benthic communities comprised of consolidated pavement interspersed with a variety of branching, table, massive, and encrusting coral taxa. Sightings of the ESA-listed green sea turtle (*Chelonia mydas*) and manta rays (potentially including *Mobula birostris*) suggested clustering of each species in the nearshore areas of the Eastern Terrace, perhaps due to localized soft-bottom habitat features and/or refugia from predators. The ESA-listed hawksbill sea turtle (*Eretmochelys imbricata*) has also been sighted at Jarvis.

Importantly, the variation in the composition and structure of benthic communities described above were characteristic of georegions at Jarvis prior to the extreme 2015–2016 El Niño event; all surveyed forereef areas and depths were substantially impacted by this record-setting thermal disturbance (Brainard et al. 2018). The most recent surveys suggested a general simplification of benthic communities and concomitant loss of three-dimensional structure, with most forereef habitats now composed of coral rubble and macroalgae. In addition, there was no strong evidence that suggested a possible depth refuge for corals during this thermal event; deep (>18–30 m) sites still suffered an estimated 90% loss in coral cover (versus 99% losses for both shallow and mid-depth sites). Though it is possible that some depth refugia existed deeper than 30 m, no observations from those depths currently exist.

4.9 References

Barkley HC, Cohen AL, Mollica NR, Brainard RE, Rivera HE, DeCarlo TM, Lohmann GP, Drenkard EJ, Alpert AE, Young CW, Vargas-Ángel B, Lino KC, Oliver TA, Pietro KR, Luu VH (2018) Repeat bleaching of a central Pacific coral reef over the past six decades (1960–2016). Commun Biol 1:177. doi: 10.1038/s42003-018-0183-7

Boyle S, De Anda V, Koenig K, O'Reilly E, Schafer M, Acoba T, Dillon AK, Heenan A, Oliver T, Swanson D, Vargas-Angel B, Weijerman M, Williams I, Wegley Kelly L, Brainard R (2017) Coral reef ecosystems of the Pacific Remote Islands Marine National Monument: a 2000-2016 overview. Honolulu

Brainard RE, Oliver T, McPhaden MJ, Cohen A, Venegas R, Heenan A, Vargas-Ángel B, Rotjan R, Mangubhai S, Flint E, Hunter SA (2018) Ecological Impacts of the 2015/16 El Niño in the Central Equatorial Pacific. Bull Am Meteorol Soc 99:S21–S26. doi: 10.1175/BAMS-D-17-0128.1

Bryan EHJ (1942) American Polynesia and the Hawaiian Chain, 2nd edn. Tongg Pub. Co., Honolulu, HI

Bryan EHJ (1974) Panala'au Memoirs, 1st edn. Pacific Scientific Information Center, Bernice P. Bishop Museum, Honolulu

Clark SJ, Oliver T Incident Wave Swath: A new approach to quantifying coastal wave exposure in regions with remotely generated waves.

Executive Office of the President (2014) Pacific Remote Islands Marine National Monument Expansion Proclamation 9173. Fed Regist 79:58645–258653.

Jewell HGJ (1961) Preliminary report on the marine mollusca of the Line Islands. Haw Shell News 9:1–7.

Keating B (1992) Insular Geology of the Line Islands. In: Keating BH, Bolton BR (eds) Geology and Offshore Mineral Resources of the Central Pacific Basin, Circum-Pac. Springer, New York, NY, pp 77–99

Maragos J, Miller J, Gove J, De Martini E, Friedlander AM, Godwin S, Musburger C, Timmers M, Tsuda R, Vroom P, Flint E, Lundblad E, Weiss J, Ayotte P, Sala E, Sandin S, McTee S, Wass T, Siciliano D, Brainard R, Obura D, Ferguson S, Mundy B (2008) US Coral Reefs in the Line and Phoenix Islands, Central Pacific Ocean: History, Geology, Oceanography, and Biology. In: Coral Reefs of the USA. Springer Netherlands, Dordrecht, pp 595–641

McDole T, Nulton J, Barott KL, Felts B, Hand C, Hatay M, Lee H, Nadon MO, Nosrat B, Salamon P, Bailey B, Sandin S a., Vargas-Angel B, Youle M, Zgliczynski BJ, Brainard RE, Rohwer F (2012) Assessing Coral Reefs on a Pacific-Wide Scale Using the Microbialization Score. PLoS One 7:e43233. doi: 10.1371/journal.pone.0043233

National Oceanic and Atmospheric Administration (2005) U.S. Distributions of the 15 ESA-

listed Indo-Pacific Coral Species. In: Pacific Islands Reg. Off. https://www.fpir.noaa.gov/Library/PRD/Coral/us_indo-pacific_corals_distribution.pdf.

National Oceanic and Atmospheric Administration (2009) Establishment of the Pacific Remote Islands Marine National Monument. Fed Regist 74:1565–1575.

National Oceanic and Atmospheric Administration (2017) Endangered and Threatened Wildlife; 90-Day Finding on a Petition To List 10 Species of Giant Clams as Threatened or Endangered Under the Endangered Species Act. Fed Regist 82:28946–28977.

Palawski D (2007) Jarvis Island National Wildlife Refuge Draft Comprehensive Conservation Plan and Environmental Assessment. Honolulu

Pandolfi JM, Connolly SR, Marshall DJ, Cohen AL (2011) Projecting Coral Reef Futures Under Global Warming and Ocean Acidification. Science (80-) 333:418–422. doi: 10.1126/science.1204794

Stanton WR (1975) The great United States Exploring Expedition of 1838-1842. University of California Press, Berkeley

Vargas-Ángel B (2010) Crustose coralline algal diseases in the U.S.-Affiliated Pacific Islands. Coral Reefs 29:943–956. doi: 10.1007/s00338-010-0646-x

NOAA

NATIONAL OCEANIC AND ATMOSPHERIC ADMINISTRATION

U.S. DEPARTMENT OF COMMERCE

NOAA FISHERIES